Establishment of *in vivo* bioluminescence imaging models for tumor immunology

Inaugural-Dissertation

Tewfik Miloud

DISSERTATION

Submitted to the

Fakultät für Biowissenschaften of

Ruprecht Karl Universität

Heidelberg

and to the

UFR sciences de la vie of

Université de Bourgogne

Dijon

Presented by

Tewfik Miloud

Born in: Le Creusot, France

Oral-examination: 23rd of November 2007

Establishment of *in vivo* bioluminescence imaging models for tumor immunology

Supervisors:

Prof. Dr. Günter J. Hämmerling

Prof. Johanna Chluba

Reviewers:

Dr. Protzer

Dr. Aprahamian

List of figures:

List of tables:

Publications:

- Remote control of tumour-targeted Salmonella enterica serovar Typhimurium by the use of L-arabinose as inducer of bacterial gene expression in vivo. <u>Cell Microbiol.</u> Feb 2007.
Loessner H, Endmann A, Leschner S, Westphal K, Rohde M, **Miloud T**, Hämmerling G, Neuhaus K, Weiss S.

- Quantitative comparison of Click Beetle and Firefly luciferases for *in vivo* bioluminescence imaging. <u>Journal of biomedical optics.</u> Accepted for publication.
Miloud T, Henrich C, Hämmerling G.

- An efficient and Versatile System for Acute and Chromic Modulation of Renal Tubular Function in Transgenic Mice. <u>Nature medecine</u>. Submitted
M. Traykova, K. Schönig, O. Greiner, **T. Miloud**, A. Jauch, D. W. Felsher, A. B. Glick, D. J. Kwiatkowski, H. Bujard, J. Horst, M. von Knebel Doeberitz, F. Niggli, W. Kriz, H-J. Gröne, R. Koesters.

Summary

In vivo bioluminescence imaging (BLI) technology allows to monitor tumor growth, to track cells or to follow pathogens. As BLI is still in its relative infancy, my work was focused on the choice of an optimal luciferase. Subsequently this optimal luciferase was used for establishment of *vivo* BLI models for tumor immunological studies. Additionally, visualization of tumors with luminescent bacteria was investigated.

First, I have compared the most commonly used luciferase, namely firefly luciferase (Fluc), with the green and red luciferases (CBGr99 and CBRed) from the click beetle which recently became available. For this purpose, cell transfectants were generated expressing equimolar amounts of CBGr99, CBRed or Fluc. Equimolarity was achieved by coexpression of the luciferase with eGFP using a novel bicistronic 2A system, which results in stoichiometric coexpression of the respective proteins. *In vitro* the CBGr99 transfectant exhibited the highest total photon yield. By injecting the transfectants into mice at different locations, the click beetle luciferases (CBLucs) have been shown to be superior over Fluc for BLI. Moreover the comparison of the CBLucs showed that CBGr99 has either a superior or a similar sensitivity *in vivo* as compared to CBRed, depending on the time point of the analysis. In addition, the analysis of CBGr99 transfectants showed that CBGr99 expression correlates with cell number and can be used for monitoring of tumor growth *in vivo.*

Therefore, using a Cre/loxP system an inducible transgenic mouse line that expresses specifically CBGr99 in the liver (ASC line) was generated. These mice were crossed with the AST line generated in the laboratory that has been shown to develop autochthonous hepatocarcinoma growth after injection of adenovirus encoding Cre recombinase. The resulting mice, named ASCT, permit non-invasive monitoring of hepatocarcinoma development in live animals via *in vivo* BLI of CBGr99 expression. The ASCT model permits longitudinal monitoring of tumor onsets, progression and may be used effectively for testing response to therapy.

Another approach for visualization of tumors is to employ bacteria expressing luciferase. Several bacterial strains are known to specially target and survive in tumors after intravenous injection while they are cleared in other tissues. Tumor homing by *Vibrio cholerae* expressing a bacterial luciferase gene (luxCDABE) was visualized by BLI in immunodeficient deficient mice bearing tumors. I have shown that *V.choleare* as well as the *Top10 E.coli* strain could efficiently target subcutaneous tumors in immunocompetent mice which are able to mount an immune response against the bacteria. Moreover, the tumor colonization observed in various

tumors such as AG104A, B16, and RMA was a transient phenomenon. In addition, the ability of bacteria to target tumors in different spontaneous tumor model such as a hepatoma model (Albumin-Tag mice), an insulinoma model (RIP.Tag-5 mice) and a mammary carcinoma model (Her-2/neu mice) was investigated. Vizualisation of bacterial homing by BLI showed that in these models the tumor targeting efficiency is lower than in subcutaneous tumors.

In addition, I envisaged the usage of bacteria as delivery vector for GM-CSF and IL-2 in order to enhance elimination of tumors by the immune system. Secretion of GM-CSF and IL-2 by *Top10.lux* bacteria was achieved by inserting their DNA sequences into a plasmid encoding the Hemolysin A secretory system allowing their secretion in the tumor site. In a therapeutic vaccination study, intravenous injection of *Top10.lux*.GM-CSF in mice bearing subcutaneous tumor did not enhance the delay on tumor growth which was observed with Top10.lux

Finally, to monitor the infiltration of T cells in tumors, a transgenic mouse line (CAG-L2ACh line) that can serves as a source of CBGr99 positive cells was generated. In the CAG-L2ACh mouse line CBGr99 and a red fluorescent protein (mCherry) are co-expressed under the control of a ubiquitous promoter. By BLI, CBGr99 expression was visualized in all tissues. At the single cell level, 100% of the T cells expressed mCherry and thereby CBGr99. Therefore, CAG-L2ACh constitutes a universal donor for cell trafficking studies by BLI.

Zusammenfassung

Die Überwachung des Tumorwachstums bzw. das Verfolgen von Zellen oder Pathogenen kann anhand des bildgebenden Verfahrens der *in vivo* Biolumineszenz (engl. *in vivo* bioluminscence imaging, Abk. BLI) erfolgen. Da die Methode des BLI noch in ihren Anfängen steht, konzentrierte sich diese Arbeit auf die Auswahl der optimalen Luciferase, um diese anschließend zur Etablierung eines *in vivo* BLI-Modells, das Studien der Tumorimmunologie dient, zu nützen. Außerdem sollte anhand von lumineszierenden Bakterien die Visualisierung von Tumoren untersucht werden.

Zuerst wurde daher die meist verwendete Luciferase, die firefly luciferase (Fluc), mit der neu zur Verfügung stehenden grünen sowie roten Luciferase (CBGr99 und CBRed) des Schnellkäfers (engl. click beetle) verglichen. Zu diesem Zweck wurden equimolare Mengen der verschiedenen Proteine, CBGr99, CBRed bzw. Fluc, mit Hilfe von Zelltransfektion exprimiert. Um eine Equimolarität zu erzielen, wurde die jeweilige Luciferase mit eGFP (engl. enhanced green fluorescent protein) koexprimiert. Dies erfolgte durch Anwendung eines neuartigen bicistronischen 2A Systems, das in einer stöchiometrischen Koexpression der entsprechenden Proteine resultiert. Durch *in vitro* Experimente konnte die höchste absolute Photonen Ausbeute bei CBGr99 festgestellt werden. Injektion der Transfektanten an verschiedenen Stellen einer Maus zeigtendass die click beetle Luciferasen (CBLucs) besser gelisnet als Fluc fur die BLI sind. Der Vergleich zwischen den verwendeten CBLucs ergab, dass CBGr99 eine bessere oder ähnliche *in vivo* Sensitivität als CBRed aufwies, die jedoch vom Zeitpunkt der Analyse abhing. Die Analyse der mit CBGr99 transfizierten Zellen zeigte, dass die CBGr99 Expression mit der Zellanzahl korrelierte und somit für das Überwachen des Tumorwachstums *in vivo* verwendet werden konnte.

Dafür wurde eine induzierbare transgene Mauslinie generiert, die mit Hilfe des Cre/loxP Systems CBGr99 spezifisch in Leberzellen (ASC Linie) exprimiert. Diese transgene Mauslinie wurde mit der Linie AST gekreuzt, die nach Injektion eines Cre-recombinase kodierenden Adenoviruses autochthones Hepatokarzinom Wachstum entwickelt. Der Nachwuchs dieser Kreuzung, als ASCT benannt, ermöglichte das nicht-invasive Beobachten der Entwicklung des Hepatokarzinoms in lebenden Tieren durch *in vivo* BLI mittels der Expression von CBGr99. Das in dieser Arbeit entwickelte ASCT-Modell kann daher zur zeitlichen Überwachung des Tumorbeginns und -fortschreitens genützt und effektiv für Analysen zur Wirkug von Therapien verwendet werden.

Ein weiterer Ansatz zur Visualisierung von Tumoren ist die Verwendung von Luciferase-exprimierenden Bakterien. Viele Bakterienstämme visieren nach intravenöser Injektion speziell Tumore an (engl. tumor targeting) und können dort überleben, während sie in Geweben vernichtet werden. BLI-Messungen zeigten, dass transgene *Vibrio cholerae*, die ein bakterielles Luciferase Gen (luxCDABE) exprimieren, Tumore in tumortragenden, immundefizienten Mäusen besiedeln („Tumor homing"). In dieser Arbeit konnte sowohl mit *V. cholerae* als auch mit *Top10 E.coli* ein effizientes „targeting" von subkutanen Tumoren in immunkompetenten Mäusen, die eine Immunantwort gegen Bakterien erzeugen können, erzielt werden. Es konnte vorübergehend beobachtet werden, dass in verschiedenen Tumoren, wie z.B. AG104A, B16 sowie RMA, Tumorkolonisierung stattfand. Zusätzlich wurde die Fähigkeit der Bakterien, Tumore in verschiedenen spontanen Tumormodellen anzuvisieren, untersucht, z.B. in dem Hepatom-Modell (Albumin-Tag Mäuse), dem Insulinom-Modell (RIP.Tag-5 Mäuse) oder den Mammakarzinom-Modell (Her-2/neu Mäuse). Mit Hilfe des BLI konnte das bakterielle „homing" in diese Tiermodellen untersucht werden und zeigte, dass die Effizienz des „tumor targeting" geringer war als in subkutanen Tumoren.

Außerdem konnte nachgewiesen werden, dass Bakterien als Vektoren für GM-CSF und IL-2 genützt werden können, um die Abwehr von Tumoren durch das Immunsystem zu verstärken. Damit eine Sekretion von GM-CSF und IL-2 mit Hilfe des Bakterienstammes *Top10.lux* im Tumorgewebe ermöglicht werden konnte, wurden die entsprechenden DNA-Sequenzen in ein Hemolysin A sekretorisches System kodierendes Plasmid inseriert. Die therapeutische Vakzinierung zeigte, dass Mäuse mit subkutanen Tumoren nach intravenöser Injektion mit *Top10.lux*.GM-CSF keine verstärkte Verzögerung des Tumorwachstums aufweisen, was im Gegensatz dazu bei Injektion mit *Top10.lux* beobachtet wird.

Um die Infiltration von T-Zellen in das Tumorgewebe zu analysieren, wurde zusätzlich eine transgene Mauslinie (CAG-L2ACh) generiert, die CBGr99-positive Zellen liefert. Die CAG-L2ACh Linie koexprimiert CBGr99 und ein rot fluoreszierendes Protein (mCherry) unter der Kontrolle eines ubiquitären Promoters. Anhand des BLI konnte in allen Geweben eine CBGr99 Expression festgestellt werden. Jede einzelne T-Zelle exprimierte mCherry und somit CBGr99. Daher zeichnet sich die CAG-L2ACh Linie als universeller Donor für „cell-trafficking" Studien mit Hilfe der BLI-Methode aus.

A. Introduction

1. Imaging

Tumor imaging in mouse model of cancer

The ability to manipulate the mouse genome has resulted in improved mouse models of human diseases. Transgenic mouse lines were generated in which inactivation of genes or expression of oncogenes leads to the development of autochthonous tumors. These models better recapitulate many futures of human tumorigenesis and facilitate the understanding of cancer development as well as the development of novel tumor therapies. However, the stochastic and often non-visible nature of tumorigenesis has limited their applications. Imaging techniques could be used to obviate these limitations allowing identification of tumor bearing mice and monitoring the tumor responses to therapy. The imaging modalities commonly used in cancer patients have been adapted for use in small animals, including magnetic resonance imaging (MRI), computed tomography (CT), positron emission tomography (PET), single photon emission computed tomography (SPECT) and ultrasound (US). Several features should be taken into account when selecting an imaging modality for use in the laboratory as each of these approaches has its advantages and limitations (Table1).

MRI

MRI uses strong magnetic fields to align the spin of hydrogen nuclei in tissues. A pulse of radiowaves is applied, which "flips" the spin of the hydrogen nuclei into an exitated state. The relaxation of the spin of the hydrogen atom to realign with the principal magnetic field emits pulse of radiowaves that are detected and quantified. Contrast agents modulate the properties of the tissues and can enhance the signal. There is no loss of resolution due to the changes in tissue depth (Massoud and Gambhir, 2003). MRI allows a much higher spatial resolution than optical techniques. It is also safer than techniques that use ionizing radiation. In small animals, MRI has shown promise in stem cell and lymphocyte trafficking studies (Rudin et al., 1999). The major drawbacks are the relative long time required for imaging (sometimes several hours). Moreover the use of contrast agents may be toxic and the sensitivity is relatively poor, thus requiring accumulation of large amounts of a molecular probe at a target site.

CT

CT imaging is most commonly method used for identification of anatomical structures. Images are obtained from the differential absorption of the X-rays through the various tissues. The resolution achievable is 50 μm, and there is no limit on the depth of penetration. CT refers to the method of obtaining serial images and volumetric data from the source and detector around the specimen. Unlike MRI, there are little natural contrasts between different soft tissues. CT has limited potential as a molecular imaging tool owing to the difficulty in designing contrast agents and probes for this modality.

US

Ultrasound pictures are obtained by using high-frequency sound waves that are transmitted through tissues and are then reflected back and detected. Diagnostic ultrasound using 7.5-15 MHz frequencies has a spatial resolution of 300-500 μm, while ultrahigh frequency (40 MHz) systems have been developed for mouse imaging than can obtain resolution of 40-60 μm (Foster et al., 2002). Typically, US is used to observe perfusion and anatomical characteristics.

PET and SPECT

PET is used to detect decaying nuclides such as ^{11}C, ^{18}F, ^{15}O, ^{124}I. PET images the distribution *in vivo* of trace quantities of positron-emitting molecular probe. Positrons emitted from the probe travel few millimeters in the tissue before being annihilated by collision with an electron resulting in a pair of high-energy photons. These photon pairs are detected by the PET scanner and are then used to reconstruct volumetric images of the positron emitting probe (Reader and Zweit, 2001). This technique can be applied in studies of gene therapy and gene expression in transgenic mice.

SPECT acquires information on the concentration of gamma emitting radionuclides, such as ^{111}IN, ^{123}I, ^{201}TI introduced into the organism. These radionuclides emit a single photon. SPECT imaging involves the rotation of a photon detector array around the body to track the position and concentration of radionuclide distribution from multiple angles. SPECT has been used to image cell-surface-expressed receptors and transporters (Zinn et al., 2001).

Optical imaging

Additional modalities based on genetically engineered proteins are also available including optical imaging technologies that detect fluorescence or luminescence. Optical imaging holds several advantages over the other imaging modalities. Imaging times are shorter and multiple animals can be imaged simultaneously. Operation of a CCD camera is typically easier than that of other modalities, permitting the use by a non-specialist. Optical imaging also permits quantification of metabolically active cells and permits the visualization of gene expression (Rice et al., 2001). For the purpose of our studies, bioluminescence imaging is superior to other optical methods, such as fluorescence. A key advantage of BLI is that no light is produced or detectable until the substrate/enzyme interaction of luciferase and luciferin occurs. Consequently, there are very low background luminescence levels in mice. In contrast, the light used for excitation in fluorescence imaging can also excite other fluorescent molecules within tissues, and often results in high levels of background autofluorescence that sometimes hinders detection of the reporter proteins. Moreover, in fluorescence imaging the tagged cells within an animal need to be illuminated with an external light source in order to fluoresce, essentially doubling the path length for the light during which it can be scattered or absorbed in the tissue before it is detected.

Table 1 summarizes the main features of the various imaging systems.

	MRI	CT	PET	SPECT	BLI	US
Equipment size	Large	Small	Small	Small	Small	Small
Resolution	High	High	Low	Low	Low	High
Session time	Hours	Minutes	Hours	Hours	Minutes	Minutes
Provides functional information	Not usually*	No	Yes	Yes	Yes	Not usually
Staffing/training requirements	High	Intermediate	Intermediate	Intermediate	Low	Intermediate

Table 1 : Comparison of tumor imaging modalities for use with small animals. (Adapted from Olive and Tuveson; 2006)

*advance applications incorporate magnetic particles or other contrast agent to provide functional information.

Bioluminescence imaging

Bioluminescence

Bioluminescence exists in nature in a variety of forms. A number of organisms emits visible light, ranging from the firefly to marine bacteria. Organisms exhibit bioluminescence for a variety of reasons: courtship and mating signaling, luring prey, defense, camouflage, and in response to stress (Greer and Szalay, 2002). This natural phenomenon has been harnessed for use in research as an optical reporter tool. Bioluminescence results from interaction of the luciferase enzyme with the substrate luciferin in presence of oxygen. A wide range of luciferase enzymes exists, each of which catalyze the oxidation of luciferin with corresponding release of photons of light. Luciferases have been cloned and their chemical properties characterized to a point where they can be used routinely in the laboratory.

Principle of Bioluminescence imaging

Bioluminescence imaging (BLI) of tissues requires that the gene encoding the bioluminescent reporter protein has been transferred to tissues of interest. This can be accomplished using any number of standard gene transfer method such as virus infection, bacteria or cell injection and also constitutive or inducible expression of luciferase genes in transgenic mice [Fig. 1A and B]. For BLI, the animals are anesthetized and placed in a light-tight box equipped with a CCD camera [Fig. 1C]. A grayscale reference image is acquired under weak illumination thereafter in complete darkness the photons emitted from luciferases in the body of the animals are detected externally using a range of integration times from 1 s to 5 min. The data are transferred to a computer equipped with an image acquisition and analysis software for quantification [Fig. 1D]. To display the anatomical origin of photon emission, a pseudocolor image representing light intensity is generated and superimposed over the grayscale reference image. The observation and the quantification of the photons emitted by the reporter expressed in these cells that pass through the host tissue reveals the spatial and temporal distribution of the labeled cells in the living animal.
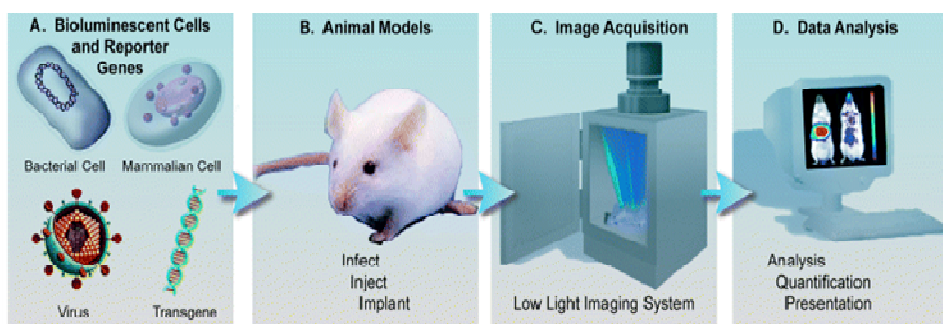
Figure 1 : Schematic of bioluminescence imaging.

(A) Cells, infectious agents or genes can be bioluminescently labeled. (B) Live mice harboring labeled cells or genes are imaged with (C) a CDD camera mounted on a black box. (D) Acquired data can be quantified with imaging software.   Adapted from Doyle et al 2004 (Doyle et al., 2004).

Luciferases

Firefly luciferase

The firefly (*Photinus pyralis*) is one of the most familiar bioluminescent organisms. The luciferase from this organism is a single polypeptide related to the CoA ligase family proteins (Conti et al., 1996). It uses luciferin substrate together with ATP and oxygen for generation of light through the following reaction (Gould and Subramani, 1988).

$$\text{Luciferase} + \text{Luciferin} + \text{ATP} + O_2 \xrightarrow{Mg^{++}} \text{Luciferase-Luciferin} + \text{AMP} + \text{PPi} \quad (1)$$

$$\text{Luciferase-Luciferin} + \text{AMP} + O_2 \longrightarrow \text{Oxyluciferin*} + CO_2 + \text{AMP} \quad (2)$$

$$\text{Oxyluciferin*} \longrightarrow \text{Oxyluciferin} + \text{light} \quad (3)$$

In the presence of oxygen, magnesium, and ATP, the reaction of the luciferase enzyme with the substrate luciferin yields an electronically excited oxyluciferin. The return of oxyluciferin to its ground state is accompanied by the release of a single photon (Nguyen et al., 1988). Thus, in the presence of excess luciferin, oxygen, and ATP, the number of photons emitted is proportional to the number of molecules of luciferase present (Brasier et al., 1989). The gene encoding firefly luciferase (Fluc) has been cloned, and the coding sequence has been optimized for mammalian expression (de Wet et al., 1987). Cells expressing this enzyme, when provided with luciferin, will emit a yellow-green light with an emission peak at ~ 560 nm using cellular ATP as the energy source. Recently, green (CBGr68; CBGr99) and red (CBRed) luciferases from yellow click beetle (*Pyrophorus plagiophthalamus*) have been cloned and optimized for mammalian expression. They also use luciferin as a substrate and have been reported to exhibit a spectral peak at 543 and 618 nm, respectively.

Renilla luciferase

Bioluminescence is common in the marine *Cnidaria*. The luciferase from the sea pansy *Renilla* has been cloned and sequenced (Lorenz et al., 1991). This enzyme uses coelenterazine as a substrate. Unlike the firefly luciferase, it does not require a cellular energy source; the coelenterazine substrate itself provides the necessary energy (Cormier et al., 1989). Light emission from the enzymatic reaction peaks at ~ 475 nm.

$$\text{Coelenterazine} \longrightarrow \text{Coelenteramide} + CO_2 + \text{light}$$

Renilla luciferase catalyzes the oxidative decarboxilation of coelenterazine in the presence of dissolved oxygen to yield coelenteramide, CO_2, and blue light.

Bacterial luciferase (lux operon)

Several bacteria use a dimeric luciferase to generate light using as substrate long-chain fatty aldehydes (e.g. decanal), reduced flavin mononucleotide ($FMNH_2$) and oxygen to produce a blue-green light (emission peak at 490 nm).

$$FMH2 + O_2 \longrightarrow FMN + RCOOH + H_2O + \text{light}$$

For all the bacterial luciferases characterized to date, the gene *lux* that encodes the luciferase enzyme (Lux) and biosynthetic enzyme for synthesis of the substrate are present in a single operon (the lux operon). There are 5 genes called *luxA-luxE*, with luxA and B encoding the alpha and beta subunits of the heterodimeric luciferase and lux CDE encoding proteins for aldehyde production (Meighen, 1993). The lux operon from *P.luminescens* is ideally suited for the study of pathogens in mammalian animal models as the enzyme retains significant activity at 37°C (Meighen and Dunlap, 1993; Szittner and Meighen, 1990).

Light transmission through mammalian tissue

The signal intensity at the animal surface is dependent on the optical properties (absorption and scattering) of the tissues through which the photons pass. Blue and green light (wavelengths shorter than 600 nm) are largely absorbed by tissues, and red light (wavelengths longer than 600 nm) is less affected. The pigment hemoglobin is the primary absorber in the body with strong absorption peaks in blue-green wavelengths. Melanin in the skin is also a significant contributor to absorption if the animal is pigmented. Therefore it is preferable to use a red light emitting luciferase as a source of light for a higher sensitivity (Zhao et al., 2005) . Rluc, for example, hardly emits light above 590 nm. Thus light produced by Rluc

would not be expected to transmit through deep tissues. In contrast about 30% of the emission spectrum of Fluc is above 600 nm, which is probably the region of the emission spectrum which is detected when used an *in vivo* reporter [Fig. 2] (Rice et al., 2001).
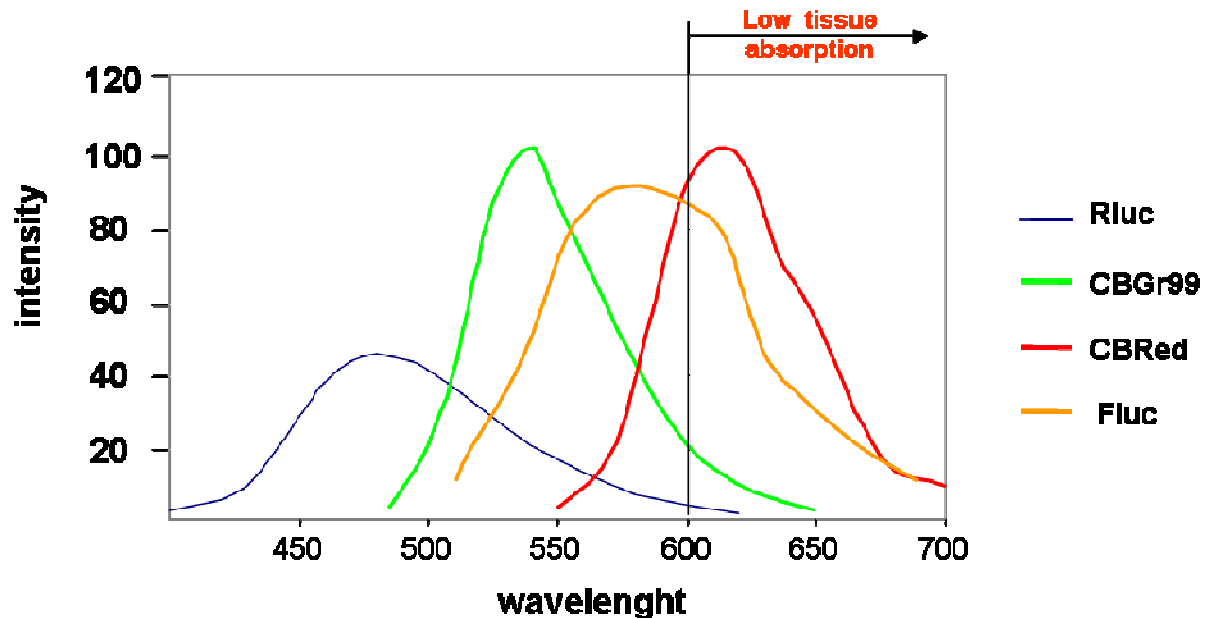
<u>**Figure 2 :**</u> **Comparison of luciferases emission spectrum**

Use of BLI in monitoring biological processes

Many small animal models of human biology and disease have been investigated successfully using BLI. This modality was first demonstrated using bacteria, *Salmonella typhimurium*, that were engineered to express the lux operon (Contag et al., 1995). In infected mice the labeled bacteria were detectable in various organs. Since this initial demonstration many bacterial strains have been engineered similarly and used in different models of infectious disease (Burns et al., 2001). BLI can be used to either track the course of an infection or monitor the efficacy of antimicrobial therapies. Similarly, other classes of pathogens such as fungi and viruses have been engineered to express luciferase or deliver luciferase genes to host cells (Cook and Griffin, 2003; Luker et al., 2002).

An essential step towards being able to monitor host response to infection was to label mammalian cells and assess cell numbers and gene expression patterns *in vivo* (Contag et al., 1997). This was most easily demonstrated in tumor models where cells can be engineered in culture and transferred to animal models (Mandl et al., 2002; Sweeney et al., 1999). This has proven to be a powerful approach to study tumor biology as signals originating in body tissues can be detected thereby allowing measurements of tumor growth. Patterns of gene

expression have also been imaged in animal models using transgenes composed of the luciferase linked to specific promoters (Contag et al., 1997).

BLI has also lent itself to extending some of the innovative tools developed for the study of molecular events in cells and cell lysates into similar studies in live animals. Tools such as the yeast two-hybrid screen to identify protein–protein interactions have been modified for use in living rodents (Ray et al., 2002), as has the suppression of gene expression by RNA interference using small RNA molecules (McCaffrey et al., 2002; McCaffrey et al., 2003) with bioluminescence as the reporter. As such, these approaches can be validated in the more complex milieu that exists in the animal that is absent in cultured cells.

2.   Animal models for tumor immunology

Animal models have played and still play a critical role in establishing basic paradigms of tumor immunology because they provide an *in vivo* milieu that cannot be reproduced *in vitro*. Animal models are also often important for the development of novel immunotherapies and for preclinical testing. Therefore, much effort has been invested into the establishment of murine models that closely mimic pathological and biochemical features of cancer in humans. Historically, investigators have used transplantable tumor models, in which inbred animals are inoculated with tumor cells. The transplantation tumors were initially derived from spontaneous occurring malignancies or induced by chemicals or irradiation, and maintained either by *in vivo* or *in vitro* passage. Unfortunately, many of these tumor models are not good predictors for human clinical trials, as numerous therapies that look promising in experimental animals have turned out to be ineffective in patients. Therefore, efforts have been directed towards the development of transgenic mouse models in which tumors develop spontaneously and thereby mimic the complex set of interactions occuring in human tumor development.

Transplantable tumor models

Experiments with transplantable mouse tumors are usually performed with well characterized tumor lines that are maintained *in vitro*. This allows the execution of experiments under well standardized conditions concerning the minimal lethal dose, the latency and the growth characteristics in syngeneic recipients, or immunodeficient nu/nu mice, as in the case of xenotransplanted human tumors. Although transplantable tumors have long been integral to tumor immunology research, their applicability to human disease is limited which, therefore,

renders them less optimal for predicting immunotherapy efficacy in patients. First, transplanted tumors are typically inoculated subcutaneously (s.c.) or intravenously (i.v.) and therefore do not grow in the anatomical appropriate site. As a result the animal model does not mimic the organ-specific physiological characteristics of the tumor. Hence, the positive responses of such tumors to certain therapies have been questioned. In some cases it has been shown that orthopically transplanted tumors do not necessarily recapitulate the "encouraging" responses of their ectopically grown counterparts (Wilmanns et al., 1992). Second, transplantable tumors generally grow very rapidly following inoculation, whereas spontaneous human tumors tend to develop more slowly through a gradual series of cellular changes from pre-malignant to malignant stages. Therefore, the immune system of patients may gradually accept the tumor, whereas in transplanted mice the immune system is abruptly exposed to the foreign tumor antigens. Third, vaccination against "artificial" tumor antigens only expressed by transplanted tumor may be totally foreign for the mouse. In this case, the induction of a protective immunity against the transplanted tumor does not have to overcome tolerance. Most human cancer antigens are normal, non-mutated differentiation molecules or non-mutated proteins found only in tumor germ cells. Therefore, the human immune system is often tolerant of these tumor antigens, either completely or partially. Despite these short comings, transplantable tumor models are still useful for many aspects of tumor immunological studies, but it is clear that models are required that mimic the clinical situation.

Autochthonous tumor models

Autochthonous tumors, e.g. spontaneously occurring tumors and chemically, virally, or carcinogen-induced tumors are believed to model human tumors more closely than transplanted tumors. Advantages of autochthonous tumors include orthotopic growth, tumor histology devoid of transplantation introduced changes, and metastasis via lymphatic and vascular vessels surrounding and within primary tumor. Despite the significance of spontaneous and environmentally induced tumor model to biomedical research, the long latency of most of these models make them impractical for most preclinical studies of tumor modulation.

In the last decades of the 20th century, mammalian genetics has been revolutionized by the development of methods for modifying the mouse germ line. Efforts have been directed towards developing transgenic mouse models in which tumors develop spontaneously and progress through the pre-malignant and malignant stages; defined antigens are expressed so

that the host is tolerized to tumor-encoded molecules. In the initial models viral and cellular oncogenes were overexpressed (Brinster et al., 1984). Subsequent studies used genes targeted to mouse embryonic stem cells, providing oncogene-bearing transgenic mice (knockin) or loss of function (knockout mice). In addition, to the use of transgene overexpression models, conditional strategies have been developed that allow controlled gene expression in both a tissue- and temporal-specific manner. Therefore, tumors arise when the host has a mature immune system as they do in humans.

SV40-driven transgenic models

Numerous transgenic mice have been generated by placing the transforming genes of SV40 or polyoma virus early regions under the control of a tissue or cell specific promoter. These mice spontaneously develop tumors in the targeted tissue. These models are useful because the mice develop organ-localized tumors and in some cases metastatic lesions (Masumori et al., 2001). The early region of simian virus 40 (SV40) encodes a large T antigen protein (Tag), which is a multifunctional regulatory protein responsible for the alterations of cellular processes required for viral infection (Dobbelstein et al., 1992). SV40 Tag forms complexes with and inactivates the key cell cycle regulatory proteins, such as p53 and retinoblastoma (Rb) tumor suppressor gene product (DeCaprio et al., 1988; Dobbelstein et al., 1992). Loss of these functional tumor suppressor gene products is often associated with human's cancers. SV40 Tag has been used to generate a variety of transgenic models for cancers such as bone sarcoma (Marton et al., 2000), hepatoma (Paul et al., 1988), prostate cancer (Greenberg et al., 1995), ovarian cancer (Connolly et al., 2003), pancreatic cancer (Hanahan, 1985), and melanoma (Bradl et al., 1991).

However, most of these models share a major limitation. Unlike human malignancies, which typically develop after birth, the transgenes in these mouse models are often expressed during embryonic development. Therefore disease onset is much earlier than in humans and the kinetics of tumor progression do not parallel those of human malignancies.

Inducible gene expression systems

A number of inducible systems that can be used effectively to switch genes on and off *in vivo* have been developed. These include interferon (Bachiller and Ruther, 1990), tetracycline (Furth et al., 1994), Ru-486 (Morgan et al., 1999) controlled gene expression. These systems permit both reversible expression and tuning level of expression. Although there is a growing number of reports in which regulatable systems have been shown to work reliably *in vivo* in

mice, it is still not routine methodology to produce such mice. A number of variables, such as the promoter used, the site of transgene insertion can profoundly influence the expression and regulation characteristics. Extensive characterization of resultant transgenic lines is therefore inevitable and often a significant number has to be screened before the suitable line is obtained. In this class of approaches, the most widely used and characterized is the Cre recombination system that allows conditional gain or loss of gene expression.

Cre/LoxP system

Site-specific DNA recombinase technology provides a means to delete, insert, invert or exchange chromosomal DNA with high fidelity. The Cre recombinase (<u>c</u>auses <u>re</u>combination), a protein from bacteriophage P1, recognizes a 34 bp long sequence called loxP (locus of crossing-over). This sequence consists of an 8 bp long asymmetric core sequence, which is flanked by two 13 bp inverted sequences [Fig. 3A] (Sadowski, 1993). Three different combinations can be used, inversion (head-to-head), excision (head-to-tail) or translocation (different strands).

The most powerful application is conditional gene inactivation, which allows analysis of the later functions of an essential gene (Lobe and Nagy, 1998; Lomeli et al., 2000; Sauer, 1998). The region to be deleted is flanked by loxP sites in such a way that does not disrupt expression of the wild type gene. The recombinase can be introduced via intercrosses with transgenic mice that express Cre in a cell or tissue specific manner. Thus, by controlling the expression of Cre it is possible to control where the knockout is produced [Fig. 3B]. For example, mice nullizigous for either Brca1 or Brca2 die early in embryogenesis, and heterozygous mice are not predisposed to tumorigenesis as are humans harboring a mutation of either gene. However, conditional mutation of either gene in the mammary epithelium promotes mammary tumorigenesis (Xu et al., 1999). Because a larger number of characterized promoters are now available, it is possible to express Cre in a variety of tissues and cells in the mouse, making modeling of cancer simple and efficient (Sauer, 1998). It is also possible to use viral systems or inducible systems to deliver Cre to specific regions of tissues or to more finely control Cre expression (Shibata et al., 1997; Xu et al., 1999).

Another way to make use of the Cre/loxP system is to induce gene activation. The promoter and the coding region for the gene of interest can be separated by a loxP-flanked STOP region, which does not allow transcription iniated from the promoter to be read through. When the STOP region is removed by Cre-mediated excision, the gene can be expressed [Fig. 3C]. Because targeted gene expression as well as Cre recombinase expression can be

modified through a tissue specific promotor, this system provides various combination possibilities (Sauer, 1998). The first demonstration of this idea was a lens-specific activation of Tag through Cre mediated excision (Lakso et al., 1992). Additional models have been developed that use recombination to limit the activation of K-ras oncogene to specific cells (Jackson et al., 2001; Meuwissen et al., 2001). Removal of the STOP element and activation of K-ras was accomplished by recombinant Cre adenovirus delivered to the lung, resulting in tumors.
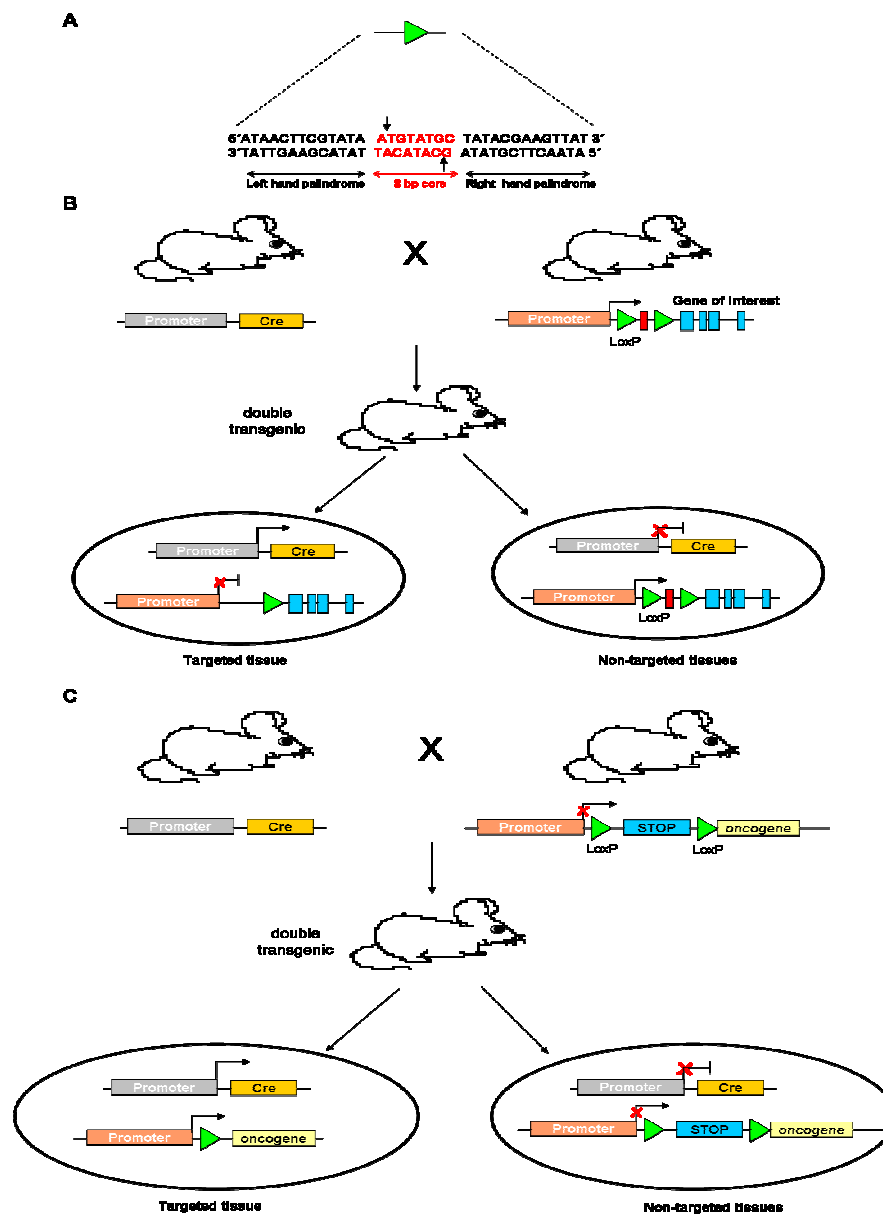
Figure 3 : **The Cre/loxP system.**

(A) DNA sequence of loxP site. The 13 bp inverted repeats (palindromes) flank an 8 bp asymmetric core sequence where the recombination exchange takes place. Strand cleavage positions are after the first, and before the last base of the 8 bp core. (B) Recombitional gene inactivation. Cre transgenic mice are mated with transgenic mice harboring a lox-flanked exon of the gene to inactivate. In the resulting transgenic mouse, excision of the exon leads to inactivation of this gene in the targeted cell type. (C) Recombitional activation of gene expression. Mice carrying the dormant gene are mated with Cre transgenic to generate a doubly transgenic mouse in which Cre has evicted the STOP sequence to activate the dormant gene. Restriction of expression of the transgene to a particular tissue can be achieved by a suitable choice of promoter for both the reporter and the cre gene. Thin arrows indicate transcription.

14

Conditional liver tumor model

To develop an inducible tumor model for autochthonous liver tumors, an Albumin-floxstop-Tag (AST) transgenic mouse was generated in our laboratory (T. Sacher; PhD thesis). The albumin promotor/enhancer and the Tag oncogene are separated by a STOP cassette flanked by loxP sites. After excision of the STOP cassette by Cre Recombinase, Tag oncogene expression is initiated. Mating of AST mice with Cre deleter mice, which express Cre recombinase ubiquitously (Schwenk et al., 1995) leads to double transgenic mice that have been shown to express Tag already two days after birth. Tag expression results in the development of liver dysplasia at the age of four weeks, proceeding over nodular carcinoma into multinodular hepatocellular carcinoma (HCC) accompanied by a dramatically decreased life span of about 12 weeks. Tumor formation is observed exclusively in the liver whereas AST single transgenic show no signs of tumor growth in the liver or other organs at the age of 12 months as examined by histology.

To obtain temporal control over Tag expression, a recombinant adenoviral vector encoding *cre* was generated. Intravenous injection of the adenovirus vector into AST mice mediates recombination *in vivo* mainly in the liver due to the tropism of the adenovirus. Within three months, injected mice develop liver tumors in a dose dependant manner. Low dose adenovirus injection leads to formation of dysplasia and small nodular adenoma or carcinoma while high dose inoculation results in multinodular HCC. [Summary of AST transgenic characterization done by S.Stahl, PhD thesis].

3. Bacteria and anticancer therapies

Bacteria and tumor colonization

Live bacteria were first actively used in the treatment of cancer nearly 150 years ago. The first cancer patient to be purposefully infected with bacteria was probably treated by the German physician W. Busch in 1868. Busch induced a bacterial infection in a woman with an inoperable sarcoma by cauterizing the tumor and placing her in bedding previously occupy by a patient with "erysipelas" (*Streptococcus pyogenes*). Busch reported that within a week the primary tumor had shrunk by half that lymph nodes in the neck had also shrunk in size. Almost 30 years later, William B. Coley encountered a patient with cancer who seemed to be cured by a severe erysipelas infection (Coley, 1991). This observation led Coley to deliberately infect patient with *S.pyrogenes*. Unknown from Coley, similar studies had already started in 1883. The German surgeon, Friedrich Fehleisen, had successfully identified

S.pyrogenes as the cause of erysipelas and had treated cancer patients with live bacteria. However, all these studies are anecdotal. Moreover, they clearly would not conform with our standards for clinical trials. Since these early studies, many bacteria have been shown to infiltrate, replicate and preferentially accumulate in tumors (Table 2). These observations have renewed the interest in the use of bacteria as gene delivery vehicles for tumors.

Organism	Ref	Model	Length	Strategy	Results
Clostridium tetani*	(Malmgren and Flanigan, 1955)	Carcinoma, hepatoma	2 days	Localization of obligatory anaerobic *C.tetani* to hypoxic and necrotic regions in tumors	Rapid death of tumor bearing mice
Clostridium butyricum (M-55)*	(Moese and Moese, 1964)	Ehrlich carcinomas	Short-until death	Identification of the most effective of 14 different clostridium species	Regression but eventual animal death
*Clostridium beijerinckii**	(Lemmon et al., 1997)	EMT6		*Clostridium* delivery of nitroreductase to activate prodrug CB 1954	Nitroreductase activity detected in tumor lysate
Bifidobacterium infantis *	(Kohwi et al., 1978)	Meth-A sarcoma	30 days	Targeted immunomodulation	Tumor regression
*Bifidobacterium bifidum**	(Kimura et al., 1980)	Fibrosarcoma	90 days	*B.bifidum* to identify tumors	*B.bifidum* localize to tumors and its non toxic
*Bifidobacterium longum**	(Yazawa et al., 2000)	B16-F10 melanoma	7 days	Gene delivery using engineered *Bifidobacterium*	Engineered bacteria found only in tumors
Salmonella typhymurium	(Low et al., 1999)	B16-F10 melanoma	40 days	Attenuated toxicity of *Salmonella* and tumor targeting	Significant delay in tumor growth
Salmonella typhymurium	(Clairmont et al., 2000)	B16-F10 melanoma	30 days	Attenuated *Salmonella* target tumor over other organs	Accumulate in tumor >1,000 fold
Vibrio cholerae	(Yu et al., 2004)	C6 glioma	6 days	*V.cholerae* expressing lux.operon to visualize tumor by BLI	Tumor colonization observed until day 6
E.coli (DH5α)	(Yu et al., 2004)	C6 glioma	6 days	*DH5α* expressing lux.operon to visualize tumor	Tumor colonization observed until day 6

Table 2 : **Examples of bacteria therapy of tumors in mice. (Adapted from Jain and Forbes; 2001).**

All organism marked with * are obligatory anaerobic whereas the other are facultative anaerobic

Why do bacteria colonize tumors?

Early observations that strains of *Clostridia* preferentially proliferate in necrotic centers of tumors (Moese and Moese, 1964) lead to hypothesis that, unlike normal tissues, the hypoxic environment in tumors provides anaerobic growth conditions (Dang et al., 2001; Lemmon et al., 1997), as it may do for the growth of anaerobic *Bifibacterium longum* (Yazawa et al., 2000). If the anaerobic/necrotic environment is a pre-requisite for accumulation of anaerobic bacteria it may limit the use of bacteria in the treatment of cancer. However, it was demonstrated that the vast majority of human tumors contain large necrotic regions. Of 20 randomly selected liver metastasis (>1cm³) all contained relatively large (25-75%) avascular regions (Dang et al., 2001). One major advantage that facultative anaerobes have over obligatory anaerobes is that their entry and accumulation in the tumor is not dependent upon tumor size, as small bladder (~10 mm³) and large glioma and breast (100-400 mm³) tumor

were colonized equally well, as well as micrometastases (Lee et al., 2005; Luo et al., 2001). Interestingly, auxotroph mutants of *S.typhimurium* have been shown to multiply in tumors in mice (Pawelek et al., 1997; Sznol et al., 2000). Therefore, anaerobicity in the necrotic center of tumor alone is not the factor that determines bacteria accumulation in the tumor.

It is also believed that the tumor microenvironment is an immunological sanctuary, where bacterial clearance mechanisms are less active. Light-emitting bacteria have identified three sites of bacterial accumulation after initial infection (incision wound, primary tumor and metastatic tumors) (Yu et al., 2004; Yu et al., 2003). This suggests that elimination of bacteria from the primary tumor may not occur due its impaired lymphatic system and poor vasculature network. Therefore the degree of vascularization and the state of the lymphatic system seem to be determining factors for colonization. Thus an established tumor can protect bacteria from immune clearance. However, the majority of malignant tumors contain a mixed array of cell types, including infiltrating leukocytes whose most-prominent component is macrophages (Murdoch et al., 2004). These phagocytic scavenger cells are found in both the well vascularized stromal tissue and the avascular, hypoxic/necrotic areas, where they are closely associated with tumor cells. However once macrophages have migrated into the hypoxic/necrotic regions of the tumor, it appears that their production of reactive oxygen and nitrogen species is lost (Siegert et al., 1999) and their ability to make ATP is decreased (Leeper-Woodford and Mills, 1992) rendering them non-phagocytic. The activities of other immune cell types (T lymphocytes and polymorphonuclear neutrophilic granulocytes) are also inhibited under hypoxic conditions (Bjerknes et al., 1990; Robbins et al., 2005). Therefore in many respects the tumor microenvironment appears to provide an immune privileged site.

Bacteria as a vaccine vehicle

Based on the observations that bacteria preferentially localize and proliferate in tumors, the use of bacteria as a tumor-targeting vector for the delivery of therapeutic agent was investigated. Indeed, bacteria present several advantages of being use as a vector (i) they are non toxic to the host; (ii) they are only able to replicate within tumor; (iii) they are slowly and completely eliminate from the host (iv) they can express multiple therapeutic transgene due to their large genome size. Several therapeutic options have been already investigated like the delivery of eukaryotic antigen expression vectors into professional antigen presenting cells of the vaccinated host (Dietrich et al., 1998) or the delivery of therapeutic genes encoding angiogenic inhibitors or prodrug-converting enzymes (King et al., 2002; Lee et al., 2004; Yazawa et al., 2000; Zheng et al., 2000).

4. Aims of the study

The main goal of my PhD thesis was the establishment of *in vivo* BLI tools for tumor immunology studies. For this purpose, this thesis is organized in four interrelated parts:

- Determination of the most appropriate luciferase for *in vivo* BLI.

- Generation of a conditional hepatocarcinoma model for BLI.

- BLI of tumor targeting by bacteria and their usage in tumor therapy.

- Generation of a transgenic mouse line that can be used as source of luciferase positive cells for transplantation and cell tracking studies *in vivo* by BLI.

B. Material and methods

1.   Material

1.1   Chemicals

All reagents used in this study were of molecular biology grade and obtained from commercial sources: Sigma (Deisenhofen), Serva (Heidelberg), Merck (Darmstadt), Roche (Mannheim), Gibco-BRL (Eggenstein), and Roth (Karlsruhe). Restriction/modifying enzymes and molecular biological reagents were obtained from Fermentas Life Sciences (St. Leon-Rot) or New England Biolabs (Frankfurt). Plasmid isolation, gel extraction and PCR purification kits used in this study were obtained from Qiagen (Hilden).

1.2   Basic equipment

Plastic articles for cell culture and for molecular biological works were purchased from Eppendorf (Hamburg), Gilson (Villiers le Bel), Greiner (Frickenhausen), Falcon (Heidelberg), Nalgene (Rochester, USA), Nunc (Wiesbaden), Hybaid (Heidelberg), and Renner (Darmstadt).

1.3   Kits

Qiaquick Gel extraction Kit (Qiagen): Purification of DNA fragments from agarose gels via columns.

Reflotron™ GPT (ALT): Measurement of Alanine aminotransferase activity.

1.4   Technical devices

Name	Company
Centrifuge Minifuge	Heraeus Christ (Osterode)
Centrifuge Sorvall RC5C Plus	Kendro (Hanau)
Centrifuge TJ-6	Beckmann (Palo Alto, USA)
Desk centrifuge Biofuge pico	Heraeus (Osterode)
Electrophoresis chamber Easy Cast	MWG Biotech GmbH (Ebersberg)
FACSAria Cell-sorting System	Becton Dickinson (Heidelberg)
FACSDiva Cell-sorting System	Becton Dickinson (Heidelberg)
FACScan/FACS-Calibur	Becton Dickinson (Heidelberg)
Fridges-freezers	Bosh, Liebherr
Ice machine Wessamat	Zugck (Leimen)
Incubator 3029	Forma Scientific (Egelsbach)
IVIS® imaging system 100	Xenogen (Alameda, USA)
Lumi-Imager	Boehringer Mannheim (Mannheim)
Magnetic stirrer	Heidolph (Schwabach)
Microscope	Olympus (Hamburg)
Millex-Gs, syringes and filters	Millipore (Bedford, MA, USA)
PCR block Peltier Thermal Cycler 200	MJ research Inc. (Watertown, USA)
pH-meter 761 Calimetric	Knick
Photometer Ultraspec 2000	Pharmacia Biotech (Freiburg)
Pipetman-pipets	Gilson
Sterile bank Biogard Hood	Baker Company Inc. (Maine, USA)
Thermomixer Compact	Eppendorf (Hamburg)
Reflovet™ plus (ALT measurement)	Roche
Waterbath (shaking)	Köttermann (Hänigsen)

1.5 Buffers and solutions

For the preparation of buffers and solutions double distilled and autoclaved water was used. The concentration factor for stock solutions is listed in brackets. Autoclaved solutions (121°C, 25 min) are marked with *. The storage of solutions at temperatures other than room temperature the degrees are listed in brackets. Percentages are referred to as weight per volume (w/v).

Buffers : Molecular biology	
dNTP mix (10x) for Taq polymerase (-20°C) 10 mM dATP 10 mM dTTP 10 mM dCTP 10 mM dGTP	**ligation buffer (10x) (-20°C)** 500 mM Tris/HCl pH 7.5 100 mM $MgCl_2$ 20 mM DTT 20 mM spermidine
O^+ (10x) (-20°C) **(reaction buffer for restriction enzymes)** 500 mM Tris/HCl pH 7.5 100 mM $MgCl_2$ 1 M NaCl 1 mg/ml BSA	**G^+ (10x) (-20°C)** **(reaction buffer for restriction enzymes)** 100 mM Tris/HCl pH 7.5 100 mM $MgCl_2$ 500 mM NaCl 1 mg/ml BSA
Y^+/Tango (2x) (-20°C) **(reaction buffer for restriction enzymes)** 66 mM Tris acetate pH 7.9 20 mM Mg acetate 132 mM KOAc 0.2 mg/ml BSA	**R^+ (10x) (-20°C)** **(reaction buffer for restriction enzymes)** 100 mM Tris/HCl pH 8.5 100 mM $MgCl_2$ 1 M KCl 1 mg/ml BSA
CIAP buffer (10x) (-20°C) 100 mM Tris/HCl pH 7.5 100 mM $MgCl_2$	**KOAc/HCOOH** 3 M KOAc 5% HCOOH (v/v)
B^+ (10x) (-20°C) **(reaction buffer for restriction enzymes)** 100 mM Tris/HCl pH 7.5 100 mM $MgCl_2$; 1 mg/ml BSA	**PCR buffer (10x) (-20°C)** 100 mM Tris pH 8.3 500 mM KCl 25 mM $MgCl_2 \cdot 6H_2O$
Pre-lysis buffer 50 mM glucose 25 mM Tris/HCl pH 8.0 10 mM EDTA	**TAE (10x)** 400 mM Tris/HAc pH 7.4 50 mM NaOAc 10 mM EDTA

Lysis buffer (NaOH/SDS)	Glycerol/CaCl$_2$
200 mM NaOH	10% glycerol (v/v)
1% SDS	100 mM CaCl$_2$
Loading dye	**Tail buffer**
0.1% bromphenol blue	100 mM Tris
0.1% xylen cyanol FF	5 mM EDTA
15% glycerol	0.2% SDS
	200 mM NaCl
TE (10x)	**Injection Buffer**
100 mM Tris/HCl pH 8.0	10 mM Tris/HCl pH 7,5
100 mM EDTA	0.1 mM EDTA
	100 mM NaCl

Buffers : Southern blot	
Prehybridization buffer (4°C)	**Hybridization buffer**
5x Denhardt´s	5x Denhardt´s
4x SSPE	4x SSPE
1% SDS	1% SDS
100 μg/ml salmon sperm DNA	100 μg/ml salmon sperm DNA
	1% Blocking reagent
Neutralization buffer	**Denaturation buffer**
500 mM Tris/HCl	500 mM NaOH
3 M NaCl	1 M NaCl
pH 7.4	
Wash buffer	**Dig buffer 1**
0.3x SSC	100 mM Tris-HCl pH 7,5
0.1% SDS	150 mM NaCl
Dig buffer 3	**SSC(20x)**
100 mM Tris-HCl pH 9,5	3 M NaCl
100 mM NaCl	300 mM Natrium citrate
	pH 7.0
Denhardt´s (-20°C)*	**SSPE (20x)**
1% Ficoll	3.6 M NaCl
1% BSA	200 mM NaH$_2$PO$_4$
1% Polyvinylpyrrolidon	20 mM EDTA
	pH7.4

Buffers : Cell biology	
Trypan blue dye 0.16% (w/v) trypan blue 150 mM NaCl	**PBS (1x)*** 130 mM NaCl 5 mM Na_2HPO_4 2 mM KH_2PO_4; pH 7.4
2X SDS-PAGE loading dye (-20°C) 10mM Tris-HCl 8% SDS 25% glycerol 0.02% Bromophenol blue 4% ß-mercaptoethanol	**6X SDS-PAGE loading dye (-20°C)** 150mM Tris-HCl 12% SDS 30% glycerol, 0.0015% Bromophenol blue 5% ß-mercaptoethanol
1x Lysis buffer (cell lysate) 1% NP-40, 1 protease inhibitor tablet in 50 ml 1x TBS	**Anode buffer** 25mM Tris base in H_2O 20% methanol pH 10.4
Cathode buffer 25mM Tris base in H_2O (pH 9.4), 40mM 6-aminocaproic acid	**Concentrated anode buffer** 300mM Tris base in H_2O 20% methanol pH 10.4
Z-buffer PBS pH 7.6, 9 mM $MgCl_2$, 0.15 mM CRPG, 100 mM ß-mercaptoethanol 0.125 % NP-40	**DPBS (Dulbecco`s Modified PBS)*** 8 g/l NaCl 200 mg/l KCl 100 mg/l $MgCl_2 \cdot 6H_2O$; 100 mg/l $CaCl_2$; 1.47 g/l $Na_2HPO_4 \cdot 2H_2O$; 200 mg/l KH_2PO_4 pH 7.2
1x TBS* 50mM Tris 150mM NaCl 5mM $MgCl_2$	

1.6   Media

Media and additives for cell and bacteria culture were purchased from Gibco BRL (Eggenstein), Difco (Detroit), Sigma (Munich), Merck (Darmstadt), and Boehringer Mannheim (Mannheim).

1.6.1 Media for bacterial culture

LB medium: 10 g/l tryptone

5 g/l yeast extract

10 g/l NaCl

Antibiotic stock solution: Amp^{50} (50 mg/ml Ampicillin (sodium salt) in H_2O)

$Chlr^{35}$ (35 mg/ml Chloramphenicol in ethanol)

Zeo^{100} (100mg/ml, Zeocin, Invitrogen)

Kan^{50} (50 mg/ml Kanamycin in H_2O)

LB medium for bacteria culture was prepared with distilled water, the pH was adjusted to 7.5, and the medium was autoclaved for 25 min at 121°C at 1 bar. For pouring plates 1.5% agar was added to the medium before autoclaving. After cooling down to approximately 56°C the mixture was filled into 10 cm Petri dishes under a hood and left there until the agar becomes solid. For selective agar the respective antibiotic was added after cooling down the agar to 56°C (final concentration 50 µg/ml). Plates can be stored at 4°C for three months.

1.6.2 Media for cell culture

Standard media are completed with additives from 100x stock solutions. FCS is heated to 56°C for 45 min before use to inactivate complement factors. L-glutamin is unstable and therefore has to be added to the medium after 2 weeks again.

DMEM standard medium (Dulbecco`s Modified Eagle Medium):

Additives	Final concentration
FCS, heat inactivated	10%
L-glutamin (200 mM)	2 mM
penicillin/streptomycin (10000 U/ml)	100 U/ml

1.7 Bacterial strains

Name	Origin	Source
DH5α	Invitrogen	Woodcock *et al.*, 1989
MM294	Provided by Dr.Stewart (EMBL, Heidelberg)	Buchholz *et al*, 1996
EL250	Provided by K.Schönig (ZMBH, Heidelberg)	Lee *et al.*, 2000
V.cholerae.lux	Provided by Pr.Szalay (Genelux Corp.; San Diego, USA)	Yu et al., 2004
Top10-lux	Provided by Dr. Loessner, (GBF; Braunschweig, Germany)	Loessner *et al.*, 2007

1.8 Mammalian cell lines

- MO4: OVA transfectant of B16 melanoma cells from C57BL/6 mice (kindly provided by S. Schnell; Memorial Sloan-Kettering Cancer Center, New York, USA).

- AG104A: Spontaneous fibrosarcoma from C3H mice (kindly provided by Dr. H. Schreiber; University of Chicago, USA).

- AG104A-Tag: Tag transfectant of AG104A cells.(generated in our lab and kindly provided by Dr. Ruth Ganss)

1.9 Mouse lines

Strain	Origin
C57Bl/6	Charles River, Sulzfeld, Germany
C3H/HEN	Charles River, Sulzfeld, Germany
Cre deleter mice	Provided by Pr. Schütz, DKFZ. (Schwenk et al., 1995).
Her2/neu mice (neu-N)	Provided by Dr. Forni, University of Turin (Guy et al., 1992)
Albumin-Tag (Alb-Tag)	Established in the laboratory (Ryschich et al., 2006).
Albumin-Floxstop-Tag (AST)	Established in the laboratory (T.Sacher); unpublished

All mice were kept under specific pathogen-free conditions at the central animal facilities of the German Cancer Research Center (Heidelberg, Germany).

1.10 Antibodies

Antibody	Origin	Specificity	Isotype	Source
GM-CSF (MP1-22E9)	Rat	Monoclonal	IgG	BD PharMingen
eGFP (Clone 7.1 and 13.1)	Mouse	Mixture of 2 monoclonal	IgG	Roche applied science
CD3-FITC (145-2C11)	Hamster	Monoclonal	IgG	BD PharMingen
IL2 (JES6-1A12)	Rat	Monoclonal	IgG	Biozol

1.11 Plasmids

Name	Gene of interest	Resistance	Size (bp)	Origin
pGMCSF2a	Mouse GM-CSF	Amp^r	3841	Dr. S. Weiss
pIHL-1	Hemolysin A secretory system	Amp^r	13157	Dr. S. Weiss
pCMV-Cre	Flp ampicillin cassette	Amp^r	4668	G. Küblbeck
pAST	Fstop cassette	Amp^r	10504	G. Küblbeck
RP23-14C7	Mouse BAC containing the Albumin gene	Chlr^r	237093	CHORI
pEGFP-N3	eGFP	Amp^r	4729	Clontech
pRSET-BmCherry	mCherry	Amp^r	3600	Pr. Tsien
pßactin-16-pl	ß-actin promoter	Amp^r	6147	Dr. C. Probst
pDrive-CAG	CMV/chicken ß-actin promoter	Zeo^r	6353	InvivoGen
pCBRed-basic	Click beetle red luciferase (CBRed)	Amp^r	4796	Promega
pGL3	Firefly luciferase (Fluc)	Amp^r	4818	Promega
pCBGr99-basic	Click beetle green luciferase (CBGr99)	Amp^r	4793	Promega
pDTR-l-eGFP-l-CBGr99	eGFP-linker-CBGr99	Amp^r	6500	G. Küblbeck

1.12 PCR primers

All primers used in this study were obtained from the DKFZ core facility and stock solutions were prepared at a concentration of 100 pmol/μl.

Name	Sequence 5´→ 3´	Annealing T°C
β_2m-1	CAC CGG AGA ATG GGA AGC CGA A	60°C
β_2m-2	TCCACACAGATGGAGCGTCCAG	60°C
Tag-1	GGACAAACCACAACTAGAATGCAGTG	60°C
Tag-2	CAG AGC AGA ATT GTG GAG TGG	60°C
eGFP-F	GTG TGA AAG CTT GCC ACC ATG GTG AGC AAG G	50°C
eGFP-P.2A-R	CTG CTT GCT TTA ACA GAG AGA AGT TCG TGG CTC CGG AAC CGT TGT ACA GCT CGT CCA T	50°C
P.2A-CBG99-F	GCC ACG AAC TTC TCT CTG TTA AAG CAA GCA GGA GAC GTG GAA GAA AAC CCC GGT CCC ATG GTG AAG CGT GAG AAA AAT GT	59°C
CBG 99-bam-R	CGC CCA GGA TCC CTA ACC GCC GGC CTT CTC C	59°C
F-Bsp-2A-Fluc	GTG TGT CCG AGC CAC GA ACT TCT CTC TGT TAA AGC AAG CAG GAG ACG TGG AAG AAA ACC CCG GTC CCA TGG AAG ACG CCA AAA ACA TAA AG	57°C
R-Fluc	TAA AGA AGA CAG TCA TAA GTG CG	57°C
F-2A-mCherry	GTG TGT CCG AGC CAC GA ACT TCT CTC TGT TAA AGC AAG CAG GAG ACG TGG AAG AAA ACC CCG GTC CCA TGG TGA GCA AGG GCG AGG A	59°C
R-BclI-mCherry	GTG TGT GAT CAT TAC TTG TAC AGC TCG TCC ATG	59°C
F-bfrBI-GM-CSF	GTG TGA TGC ATG GCT GCA GAA TTT ACT TTT CCT	62°C
2.R-PacI-GMCSF	GCT GAT TTC ATT AAT TAA TGG ATT AAG ATC ACC CTG ACT TCC ATA GGC TAA TTT TTG CTT GGT TTT TTG CAT TC	59°C
F-Alb2	CAG ATC ACC TTT CCT ATC AAC CCC ACT AGC CTC TGG CAAA AAT AAC TTC GTA TAG CAT ACA TTA TAC	56°C
R-Alb2	CGG AGA CGA AGA GGA GGA GGA GAA AGG TTA CCC ACT CA TGG TCG ACT AGC CGT AAA TTA	56°C
F-RI-HlyA-IL2	GTC GTG AAT TCA TGC ATC ATA CAG CAT GCA GCT CGC ATC	60°C
R-RI-PacI-IL2	TTT CAG AAT TCT TAA TTA ATG GAT TAA GAT CAC CCT GAC TTC CAT AGG CTA ATT GAG GGC TTG TTG AGA TGA	60°C
F-XmaI-linker-Fluc	CGT GGC CCC GGG GGC GGT GGA TCA GGT GGA GGT GGA TCC ATG GAA GAC GCC AAA AAC AT	62°C
R-Fluc	GGG CAT CGG TCG ACG ATC C	62°C
Bac-zeo-loxP511-L	CGG TTG AGT AAT AAA TGG ATG CCC TGC GTA AGC GGG GCA CAT CGA CGA GGG TGT GGA AAG T	55°C
Bac-zeo-loxP511-R	GTC AGC TCC TTC CGG TGG GCG CGG GGC ATG ACT ATT GGC GCT CAG ACA TGA TAA GAT ACA TTG AT	55°C

2. Methods

2.1 Molecular biology

Bacterial culture

DH5α was the bacterial strain used for classical molecular cloning. It was grown in LB (Luria Bertani) medium and maintained on LB agar plates supplemented with suitable antibiotics wherever necessary. All bacteria were grown at 37°C (with shaking at 220 rpm for liquid cultures). For routine storage, plates were maintained at 4°C.

EL250 Bacteria were used for Bacterial Artificial Chromosome Cloning. They were used in the same way than DH5α at the exception of a growth temperature at 32°C.

Preparation of CaCl$_2$ competent (heat competent) *E. coli* bacteria

A single colony of DH5α cells is grown in 20 ml LB medium over night at 37°C with shaking. 1 ml of this pre-culture is added to 200 ml LB medium in a 2 l flask. Bacteria are grown to an OD$_{600}$ of 0.6. 400 ml of prewarmed LB medium are added, and cells are grown for another 20 min. They are then centrifuged for 5 min at 2500 rpm at 0°C. The supernatant is decanted, traces of liquid are removed, and the pellet is resuspended in 250 ml of ice cold 100 mM CaCl$_2$. The suspension is placed on ice for 1 h. After centrifugation (5 min, 6000 rpm, 0°C) the supernatant is again decanted, traces of liquid are removed carefully, and the pellet is resuspended in 5 ml of ice cold glycerol/CaCl$_2$. Aliquots of 100 µl are frozen in liquid nitrogen, and cells are stored at -70°C.

A test transformation with 1 ng of double stranded circular plasmid DNA in 100 µl of competent cells should yield more than 3×10^3 colonies.

Bacteria storage

Bacteria are plated on agar plates, incubated for 24 h at 37°C and stored at 4°C (maximum two months). For longer storage 0.880 ml of an over night culture are mixed with 0.120 ml glycerol (86%) (long term storage at -70°C). With a sterile scalpel small pieces of the frozen bacteria suspension can be cut off for new cultures.

Transformation of heat (CaCl$_2$) competent E. coli bacteria

A 100 µl aliquot of deep frozen competent cells is thawn on ice for 10 min and mixed with 5-10 µl of a ligation assay. After incubation for 30 min on ice the mix is exposed to 42°C for 60 sec and transferred to ice for another 2 min. Bacteria are then plated out on an agar plate.

DNA minipreparation (alkaline lysis)

The lid of a 1.5 ml Eppendorf tube is pierced with a needle and filled with 1 ml of selective LB medium. The medium is inoculated with one bacterial colony and then incubated at 37°C over night, with shaking. Bacteria are centrifuged (3 min, 13000 rpm), and the pellet is resuspended in 150 µl of pre-lysis buffer. 300 µl of NaOH/SDS are added, the suspension is vortexed and incubated for 5 min on ice for cell lysis. 225 µl of KOAc/HCOOH are added to neutralize the solution; the assay is vortexed and placed on ice for 15 min to precipitate genomic DNA and proteins. The solution is centrifuged (3 min, 13000 rpm), the supernatant is transferred to a new tube and the included DNA is precipitated with 400 µl isopropanol (5 min, room temperature (RT)). After centrifugation (3 min, 13000 rpm) the supernatant is removed while the DNA containing pellet is dried at 37°C for 10 min and finally dissolved in 50 µl TE. 5 µl of DNA are needed for a restriction digest.

DNA midipreparation (alkaline lysis)

For larger amount of pure DNA, large scale purification is performed:

50-200 ml of selective LB medium are inoculated with a bacterial culture and incubated at 37°C over night, with shaking. The suspension is centrifuged at 5000 rpm for 5 min at 4°C. The supernatant is discarded; rests of liquid are removed with a pipette. The pellet is resuspended in 4.5 ml of pre-lysis buffer. 10 ml of NaOH/SDS are added for lysis of bacteria. After mixing cells are placed on ice for 5 min. 7.5 ml of cooled neutralizing KAc/HCOOH are added for genomic DNA/protein precipitation. After mixing, and 15 min of incubation on ice, centrifugation (5 min, 5000 rpm, 4°C) follows. The supernatant is filtered through funnel and glass wool into a new Falcon. The DNA in the supernatant is precipitated with 0.6 volumes of 2-propanol (5 min, RT) and centrifuged (5 min, 5000 rpm, 4°C). The supernatant is taken away while the pellet is resuspended in 2 ml of TE. For further purification 2 ml 4 M LiCl are added and incubated on ice for 5 min. Centrifugation (5 min, 5000 rpm, 4°C) follows. The supernatant is transferred to a new Falcon where the DNA is precipitated with 10 ml 100% ethanol at -20°C for at least 15 min. Centrifugation (5 min, 5000 rpm, 4°C) follows to pellet the precipitate. The pellet is washed with 5 ml 70% ethanol and is then dissolved in 400-600 µl of TE and transferred to a 1.5 ml Eppendorf tube. 5 µl RNase (10 mg/ml) are added for digestion of RNA (30 min, 37°C). After addition of 8 µl 4 M NaAc pH 5.6 per 100 µl DNA solution the plasmid DNA is extracted with phenol/chloroform/isoamylalcohol (50:49:1) three times and two times with chloroform/isoamylalcohol (49:1). It is then precipitated with 0.6 volumes of isopropanol (5 min, RT), and after centrifugation (3 min, 13000 rpm) the pellet is

washed with 1 ml of 70% ethanol. The pellet has to be dried at 37°C for 15 min and can then be dissolved in 100-1000 µl of TE. The concentration of DNA is determined by comparing 1 µg of digested DNA to the DNA marker in an agarose gel.

Restriction digestion

For an analytical digest 3 µg of miniprep DNA or 1 µg of midiprep DNA are incubated with 1 µl of restriction enzyme (4 U), 2 µl of 10x buffer and H_2O ad 20 µl for at least 1 h at 37°C. Digestions with enzymes cutting at temperatures other than 37°C are incubated at the respective ones. According to the enzymes demands concerning buffers the assays are performed with different buffers (B^+, R^+, G^+, Y^+ etc.)

For preparation of fragments for further ligation a 40 µl reaction is prepared with 5 µg DNA, 4 µl 10x buffer, 2 µl enzyme and the respective amount of H_2O.

Dephosphorylation of DNA ends (e.d. in vectors for ligation)

To avoid self-ligation of cut vectors the 5´ phosphate groups at the DNA ends are removed by treatment with alkaline phosphatase (CIAP).

After the preparative restriction digest in a 40 µl assay 1 µl of CIAP is added and incubated at 37°C for 30 min. Removal of CIAP is unnecessary if gel purification of the digest is performed. The enzyme can also be inactivated by heating the assay to 70°C for 20 min.

Electrophoretic separation of DNA fragments in agarose gels

DNA fragments in the range of 0.1-20 kb are separated in differently concentrated agarose gels (0.6-2%) depending on their lengths. Gel preparation is performed by boiling agarose dissolved in 100 ml of 1x TAE buffer. After cooling down it is poured into a gel chamber with combs for slots. When a solid gel has formed the combs can be removed for loading. The samples are mixed with 1/6 of 6x loading dye containing the reference dyes, which promote sinking of the DNA into the slots. Electrophoresis is performed in the voltage range of 20-90 volts. For estimation of the fragments sizes a length marker (GenerRuler™ 1 kb DNA ladder) is separated next to the samples for comparison. After electrophoresis, DNA is stained by placing the gel into a dish with 500 ml of ethidium bromide solution (1x TAE, 0.5 µg/ml Ethidium Bromide) for 15 min. The DNA bands are made visible by a UV transilluminator at 254 nm and are photographed with a videocamera for documentation.

Isolation of DNA fragments from agarose gels with Qiaquick Gel extraction kit

The isolation of the respective fragment is performed according to the manufacturer`s instruction. Briefly, the band is cut out from the gel at 366 nm under the UV transilluminator, weighted and dissolved in 300 µl QG buffer per 100 mg of gel (50°C, with 700 rpm shaking). 750 µl of the assay are placed onto a Qiaquick spin column with collection tube (max. 400 mg per column) and centrifuged (13000 rpm, 30 sec). This step is repeated in case the Qiaquick Gel mix exceeds the volume of 750 µl. The column is washed with 750 µl of PE buffer (13000 rpm, 30 sec) and dried through a second centrifugation step (13000 rpm, 1 min). The column is placed onto a new collection tube. 50 µl EB buffer are placed onto the middle of the filter and incubated for at least 1 min at RT and DNA is eluted by centrifugation (13000 rpm, 1 min).

Ligation of DNA fragments and vectors

A 10 µl ligation assay is prepared using 1 µl of T4 DNA ligase, 1 µl of 10x T4 DNA ligase buffer, 7 µg of the gel purified DNA fragment and 1 µg of vector DNA. After over night incubation at room temperature, 5 µl are used to transform competent cells.

PCR (Polymerase Chain Reaction)

This method allows specific amplification of defined regions on a DNA molecule *in vitro*.
PCR is carried out in three different steps that are repeated in 20-40 cycles. In the first step the piece of DNA to be detected (template) is denatured by heating it to 95°C. Subsequent cooling to 45-70°C allows short single stranded oligonucleotides sequence (primers) specific hybridisation to the template (annealing). In the third step elongation of 3´ ends of the annealed primer along the template DNA takes place with the help of the heat stable Taq polymerase. Since the primers are chosen so that the newly produced DNA strands of both template strands are partly complementary to each other the doubling of DNA molecules per cycle is achieved through the cyclic progression of the three steps.

Analytical PCR

Analytical PCR is performed to verify the presence of a transgene in the mouse genome using tail DNA (see 2.2.3: "Isolation of tail DNA") as a template. For this PCR two pairs of primers were used, one to check the presence of the transgene, the other one to check the DNA preparation by amplifying a house keeping gene. It is done as follow:

PCR mix (25 µl):		PCR Program :		
10x PCR reaction buffer	2.5 µl	1. Denaturation	95°C	5min
Primer forward (10 µM)	2.5 µl	2. Denaturation	95°C	30s
Primer reverse(10 µM)	2.5 µl	3. Annealing	60°C	30s
Primer house keeping 1 (10 µM)	2.5 µl	4. Elongation	72°C	1min/1kbp
Primer house keeping 2 (10 µM)	2.5 µl	5. Back to step 2	39 times	
dNTPs 10 mM	1 µl	6. Final extension	72°C	10min
Taq polymerase (2 U/µl)	0.5 µl			
Tail DNA	5 µl			
H_2O	6 µl			

Preparative PCR

It is performed to amplify specific cDNA sequences that are used for cloning. In this case, primers have additional restriction enzymatic sites that were used to insert the PCR product in a plasmid. In order to obtain an exact copy of the DNA template a specific DNA polymerase (AccuPrime™ *pfx* DNA polymerase, Invitrogen) that minimizes the chances of mistakes was used. The PCR was performed as follow in 200 µl tubes:

PCR mix (50 µl):		PCR Program :		
10x PCR buffer (with dNTP)	5 µl	1. Denaturation	95°C	1min
Primer forward (10 µM)	2 µl	2. Denaturation	95°C	15s
Primer reverse(10 µM)	2µl	3. Annealing	x °C	30s
AccuPrime *Pfx* (2 U/µl)	0.5 µl	4. Elongation	68°C	1min/1kbp
cDNA (1ng/ul)	1 µl	5. Back to step 2	24 times	
H_2O	39.5 µl	6. Final extension	68°C	10min

DNA sequencing

The DNA sequencing was done by MWG Biotech, Ebersberg, Germany using the dideoxy method. 1µg DNA was precipitated in ethanol and air dried. The DNA was further dissolved in 10 µl of HPLC purified water and sent for sequencing.

Preparation of DNA microinjection

For microinjection experiments, the DNA fragment was isolated by restriction cutting from the vector and was isolated through an agarose gel. The DNA was taken up to microinjection buffer and adjusted to a concentration of 1-2 ng/µl.

Preparation of BAC DNA for transgenic mice production
Preparation of electrocompetent cells and generation of recombinants

In order to generate BAC recombinants, homologue recombination is induced between a linear DNA and BAC DNA which is carried by EL 250 bacteria. Indeed, EL 250 bacteria are stably transformed with a defective prophage that carries the *PL* operon. *PL* operon encoding *gam*, *exo* and *bet* genes is under the control of the temperature sensitive λ repressor (allele c*I*857). Recombination functions can thus be transiently supplied by shifting the culture to 42°C for 15 min. Gam inhibits the *E.coli* RecBCD nuclease from attacking the electroporated linear DNA, while Exo and Beta generate recombination activity.

For BAC modification, overnight cultures containing the BAC were grown from single colonies, diluted 50-fold in LB medium, and grown to an OD_{600} = 0.5-0.7. 50 ml cultures were then induced for Beta, Exo, and Gam expression by shifting the cells to 42°C for 15 min followed by chilling on ice for 20 min. Cells were then centrifuged for 5 min at 5000 rpm at 4°C and washed with 1.5 ml of ice-cold sterile water three times. Cells were resuspended in 300 µl of ice-cold sterile water and electroporated. For BAC transformation, the induction step was omitted.

Cell transformation was performed by electroporation of 100-300 ng DNA into 50 µl of ice-cold competent cells in cuvettes (0.1 cm) using a Bio-Rad gene pulser set at 2.3 kV, 25µF with a pulse controller set at 200 ohms. 1 mL of LB medium was added after electroporation. Cells were incubated at 32°C for 1.5 h with shaking and spread either on agar media with Chloramphenicol resistance for BAC transformation or on agar media with Chloramphenicol and Ampicillin resistance for BAC modification.

Transformation and modification of RCPI23-14C7

First, the Albumin BAC was electroporated into EL 250 cells. 10 Chloramphenicol colonies were obtained from 1 x 10^8 electroporated cells. Digestion BAC DNA from the Chloramphenicol resistant colonies with *Bam HI* showed a similar digestion pattern than the original DNA [Fig. 4A, lane A and B]. To replace the first *loxP* site contained in the BAC vector backbone, EL250 cells were shifted to 42°C for 15 min to induce Exo, Beta, and Gam expression and the cells were then electroporated with 300 ng of the amplified Zeocin cassette. Approximately, 5000 $Chlr^R/Zeo^R$ colonies were obtained from 1 x 10^8 electroporated cells (No colonies were obtained from uninduced cells). *Bam HI* digestion of DNA from 10 of these colonies showed the expected shift of a band from 8803 bp to 9777 bp in the digestion pattern [Fig. 4A, lane C]. This indicated that all were correctly targeted.

Using the same procedure the amplified Fstop-CBGr99-FlpAmp cassette was inserted in frame with albumin start codon. 37 $Chlr^R/Zeo^R/Amp^R$ colonies were obtained from 1 x 10^8 electroporated cells. *Bam HI* digestion of DNA from 4 out of 12 of these colonies showed the expected shift of a band from 17218 bp to 12815 bp in the digestion pattern and the appearance of a band at 6360 bp [Fig 4A, lane D]. Next, the Amp selectable marker was removed to prevent its possible interference with the luciferase expression. Overnight culture from single $Chlr^R/Zeo^R/Amp^R$ colony was diluted 50 fold in LB medium and grown till OD_{600} nm = 0.5. *flpe* expression from EL 250 was then induced by incubating the culture with 0.1% L-arabinose. The bacteria cells were spread on $Chlr^R$ plates and the next day colonies were picked, and replated on Amp^R plates to test for loss of Ampicillin resistance which was observed in 100% of colonies. In order to check the appropriate insertion and the sequence of the Fstop-CBGr99 cassette, ligation of the *EcoR I* fragment containing the Fstop-CBGr99 cassette was subcloned in a pBluescript vector (Fermentas). Sequencing showed expected insertion of the cassette as well as a correct sequence (data not shown).

Finally, the last *loxP* site contained in the BAC vector backbone was removed by a final round of gene targeting. Ampicillin cassette flanked by homologous region was used to replace the *loxP* site. 3000 $Chlr^R/Zeo^R/Amp^R$ colonies were obtained from 1 x 10^8 electroporated cells. *Not I* digestion of DNA from 3 of these colonies showed the expected shift of a band from 9833 bp to 10867 bp in the digestion pattern [Fig. 4B]. The albumin BAC was then purified for microinjection.
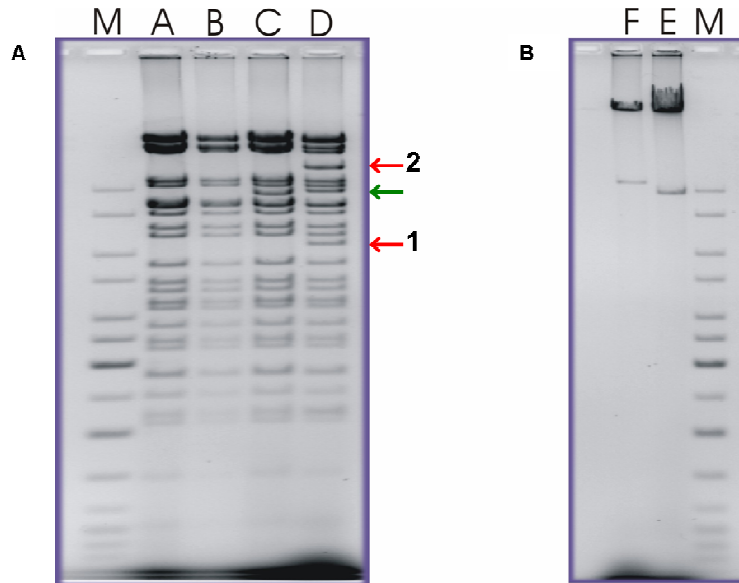
<u>**Figure 4 :**</u> **Transformation and modification of albumin BAC.**

(A) Restriction pattern of RCPI23-14C7 BAC DNA with Bam HI before (lane A) and after transformation in EL250 bacteria (lane B) shows that BAC DNA is fully expressed in the host. Replacement of one loxP site present in the BAC vector by a Zeocin cassette leads to a shift from 8803bp to 9777bp (green arrow) of a band in the Bam HI restriction pattern (laneC). Apparition of one band at 6360bp (red arrow 1) and shift of a band from 17218bp and 12815bp (red arrow2) after insertion of the Stop-CBGr99-FlpAmp cassette (lane D).

(B) Replacement of the second loxP present in the BAC vector leads to a shift from 9833bp to 10867bp (lane F). Lane M: DNA ladder mix.

Purification of BAC DNA for microinjection

The modified BAC DNA (30 µg-50 µg) was digested with *NotI* in reaction buffer including 2.5 mM spermidine (Sigma). Digested BAC DNA mixed with gel loading buffer was run through the sepharose CL-4B (Pharmacia) column, which was equilibrated with 30 ml of the injection buffer. Fractions of 500 µl were collected and a small volume of every fractions was identified on a 1% agarose pulsed field gel. The appropriate fractions with intact BAC DNA and no vector bands were adjusted appropriate DNA concentration (1µg/ml).

2.2   Mouse work

2.2.1 Production of transgenic mice

2.2.1.1 Layout of a microinjection instrument

An inverse stereomicroscope (5-200 x magnification) is equipped with two micromanipulators to operate the capillaries used for securing cells and injecting them with fluid. The capillaries are connected with paraffin oil filled tubes to the paraffin oil reservoir. Knurled screw and pistons at the end of the tubes are used to apply suction or pressure on the capillary. Applying slight negative pressure allows the fixation of a single oocyte to the capillary. The stage is designed for the use of Petri dishes with a diameter of 6 cm.

2.2.1.2 Preparation of glass capillary needles

Injection syringe: the glass capillary is fixed in a micropipette puller and drawn after heating. The capillary is then broken at the end of the needle to an inner diameter of around 15 μm. This is followed by grinding the tip in an angle of 50°. The tip is additionally bended 30°.

Syringe for securing cells: The glass capillary is also fixed in a micropipette puller and drawn after heating. The capillary is then broken at the inner diameter of around 90 -100 μm and the end of the needle is melted down to an inner diameter of around 15 -20 μm.

2.2.1.3 Preparation of zygotes from pregnant mice

To have sufficient high number of fertilized ovules, female mice are super ovulated. 10 (C57BL/6) F_1-females are used as donors of zygotes. Three days prior the preparation 5-10 U Gonadotropin in 500 μl PBS are administered i.p. to induce oogenesis. One day prior preparation 5-10 U Chorionic-Gonadotropin in 500 μl PBS are administered i.p. to trigger ovulation. Subsequently, the females will be mated with F_1-males (C57BL/6). The next day, the females are checked for vaginal plugs, whereas positive females are killed with CO_2, opened up, and their oviducts along with a part of the uterus are removed. Fat tissue and mesometrium are stripped off and the uterus is cut between the forceps and the oviduct directly at the ovary. The oviducts are placed in M_2-medium, supplemented with hyaluronidase (300 μg/μl). The zygotes are found in the ampoule of the oviduct and are dissected under a binocular. For the dissection, the ampoule is pinched off with tweezers and ripped open with a second pair of tweezers. The ovules are collected with a glass capillary and washed twice with M_2-medium. Until the injection of the DNA into the pronucleus, the ovules are kept in a drop culture in M_{16}-medium at 37°C.

2.2.1.4 Microinjection of the transgene cassettes

The linearised transgene cassettes are injected in the pronucleus of the zygotes at a concentration of 2-6 ng/µl. The transgene cassettes are injected by piercing the pronucleus of the oocyte with the injection syringe and activating the special injection pump. If the injection into the pronucleus is correctly conducted, the swelling of the pronucleus can be observed under the stereomicroscope.

2.2.1.5 Transfer of embryos into oviduct

Injected embryos at the one-cell stage (the day of injection) or two-cell stage (1 day after injection) were transferred into the infidibulum of the oviduct of the pseudopregnant recipient (foster mother). To this end, 10-20 female recipient (NMRI) mice have been mated to vasectomized males 3 days before the preparation of the eggs.

2.2.2 Typing of transgenic mice

2.2.2.1 Isolation of tail DNA

0.5-1 cm of the tail is cut off and placed into an Eppendorf tube with 700 µl of tail buffer and 10 µl of proteinase K (10 mg/ml). The tail is digested over night at 56°C. The next day the sample is centrifuged (5 min at 13000 rpm), and the supernatant is transferred into a new Eppendorf tube. The DNA is precipitated with 0.6 volumes of isopropanol (420 µl) by shaking the tube until a DNA string becomes visible. It is fished with a closed glass capillary and washed first in 70% ethanol, then in 100% ethanol by dipping the capillary into the alcohol. The DNA on the capillary is dried at RT for 30 min. After that the capillary end with the DNA is broken off into an Eppendorf tube with 100-500 µl of TE (depending on the amount of DNA) for dissolving the DNA at 68°C with shaking.

2.2.2.2 Mouse genotyping by non-radioactive Southern blot analysis

20 µl of tail DNA were digested with restriction enzymes and separated on a 1% agarose gel in 1x TAE buffer at 80 V. DNA bands were visualised under UV light after staining with ethidium bromide (0.5 µg/ml in 1 X TAE). After visualisation, the agarose gel was submerged into denaturation buffer for 30 min and to neutralisation buffer for 2 times 15 min with agitation. After setting up the capillary blot, the DNA was transferred onto a nitrocellulose membrane overnight in 20x SSC. The DNA was fixed to the membrane by baking at 80°C for 2 hours. After fixation, the membrane was prehybridised with prehybridization buffer for 1 hour at 65°C. For hybridisation, the Dig-labelled probe (10 ng/ml in hybridization buffer),

which was boiled for 10 min, was added on the membrane and hybridisation was carried out at 65°C overnight. To prepare Dig-labelled probe, a PCR product (100 ng to 2 µg) was denatured and immediately cooled down on ice and finally labelled as per directions in Dig-labelling manual. After hybridisation, the membrane was washed 3 times for 5 min each in wash buffer at 65°C. After this step, all the subsequent incubations and washing were done at room temperature. After washing, the membrane was rinsed with Dig-buffer I and blocked in 2% blocking buffer for 2 min. α-Dig-AP conjugate (1ul antibody/5ml of Dig-buffer I, Boehringer) was added to fresh Dig buffer 1 solution and incubated on the membrane for 30 min. After washing 2 x 15 min in Dig buffer 1 solution, the membrane was first equilibrated in Dig-buffer III and then incubated for 10 min. Then, 20 ml of Dig-buffer III containing substrate (90 µl NBT and 70 µl BCIP solution) was added onto the membrane and incubated 3-4 h before signal detection.

2.2.3 Lymphocyte preparation from blood and genotyping by FACS

Blood taken from the tail vein of mice was mixed in D-PBS/Heparin solution in order to prevent blood coagulation. These samples were transferred into centrifuge tubes filled with Ficoll solution (Lymphoprep™) to carry out a density gradient centrifugation at 1800 rpm (Beckman, TJ-6) for 20 minutes. Lymphocytes accumulating in the interphase were harvested and placed into new Eppendorf tubes.

2.2.4 Splenocyte preparation

Mice were sacrificed by CO_2 inhalation. After disinfection with ethanol, the peritoneal cavity was opened using sterile forceps and scissors. Spleen was removed, separated from fatty and connective tissue and placed into a 6 well plate containing D-PBS on ice. The spleens were mashed through a cell strainer using the plunger of a 1 mL syringe, rinsed twice with D-PBS and then centrifuged at 1200 rpm, 4ºC, 5 min. Cells were counted in a Neubauer Heamatocytometer using trypan blue to exclude the dead cells and then washed once more with D-PBS before being resuspended and adjusted to the desired cell concentration in FACS buffer (3% FCS in D-PBS).

2.2.5 Tumor inoculation

To establish subcutaneous tumors from cancer cell lines, 5×10^6 cells were resuspended in 1 ml D-PBS. 100 μl (equal to 5×10^5) of suspension was inoculated subcutaneously in the flank using a 1 ml syringe equipped with 27G needle in the belly of each animal. After tumor inoculation, the growth rate of tumor was monitored by measuring the size using a caliper. To establish experimental metastasis 100 μl of the same cell preparation was injected intravenously in the tail vein and tumor development was monitored by Bioluminescence imaging (BLI).

2.2.6 Bioluminescence imaging of mice

Mice were imaged at indicated time points using the IVIS® imaging system 100 (Xenogen). D-luciferin (Synchem, Felsberg/Altenburg, Germany) dissolved in PBS was injected intraperitoneally at a dose of 150 mg/kg before measurement of luminescence. General anesthesia was induced with 5% isoflurane and continued during the procedure with 2.5% isoflurane introduced via a nose cone.

After acquiring photographic images of each mouse, luminescent images were acquired with various (1 s - 300 s) exposure times. The resulting grayscale photographic and pseudo-color luminescent images were automatically superimposed by the IVIS Living Image Software (Xenogen) to facilitate the matching of the observed luciferase signal with its location within the mouse. Region of interest (ROI) were manually drawn around the signal to assess the signal intensity emitted. Luminescence was integrated over these ROIs and it is expressed as relative light units (RLU). To avoid light absorption and scattering, fur was removed from black mice in the region of interest by shaving prior to the start of the experiment.

2.2.7 Measurement of alanine aminotransferase activity in mouse plasma

Alanine aminotransferase (ALT) belongs to the group of transaminases which catalyse the conversion of amino acids to the corresponding α-keto acids. Increased serum activity of ALT is largely specific for liver parenchymal disease although it can indicate other organ damage. Measurement of high ALT level in the serum could therefore be used as an indication of hepatocarcinoma in AST mice previously injected with adenovirus expressing Cre.

Blood was collected from the tail vein using capillary pipette filled with heparin. Blood is applied to a test strip (Reflotron™) which is immediately placed in the Reflotron instrument. The instrument will display 140 s later the enzyme activity in U/l. The test strip contains α-ketoglutarate and alanine which are converted in glutamate and pyruvate in presence of ALT.

In a second reaction step, catalyzed by the pyruvate oxidase, the resulting pyruvate is cleaved into acetyl phosphate, carbon dioxide and hydrogen peroxide. In the presence of POD the hydrogen peroxide converts an indicator into its oxidized blue form. The formation of the dye is measured at 567 nm as a measure of the enzyme activity of ALT.

2.3   Cell culture

The given cell lines were maintained in monolayer cultures in defined medium (RPMI-1640 or DMEM) supplemented with 10% inactivated foetal serum (FCS) with 2 mM L-glutamine. The cells were grown in a humidified atmosphere with 7% CO_2.

2.3.1 Long term storage

Growing cells were trypsinized, pelleted and washed thoroughly with D-PBS to remove traces of trypsin and medium. Cells were then resuspended in freezing buffer (70% DMEM, 20% FCS, 10 % DMSO), at a density of 2-3 million cells/ml, and aliquoted into cryovial tubes. Vials were placed in a cell freezing box (Nalgene™) and left at -80°C overnight for gradual freezing. Frozen vials were then transferred to liquid nitrogen for long term storage.

Repropagation was performed by placing the vial at 37°C and gradually thawing the cells by the addition of complete medium. The cell suspension was transferred to a 15 ml Falcon tube pelleted and washed with complete medium for removal of DMSO. After resuspension, the cells were added to 20 ml complete medium in a 75 cm² tissue culture flask.

2.3.2 Cell transfection

The adherent cells were transfected with DNA using Lipofectamin™ 2000 (Invitrogen, Life technologies, Karlsruhe, Germany) according to the manufacturer's instruction, with minor modification adapted to the cell line. The day before transfection 1 to 2 x 10^6 cells were seeded in a 6 cm Petri dish. Next day cells were washed with D-PBS (pH 7.4) to remove the serum, and 2.5 ml of DMEM serum free medium was added. DNA-Lipofectamin complexes were made as per instructions and 1:2 ratio of DNA:Lipofectamin™ 2000 was used.

For a 6 cm Petri dish, respectively 10 µg DNA was diluted into 500 µl DMEM serum free medium and 20 µl of Lipofectamin was diluted into 500µl of DMEM serum free medium. After 5 min incubation time at room temperature, both were mixed and incubated at room temperature for 20 min. The mixture was dropwise added to the cells. Transfection efficiency was estimated 24 h after transfection by checking eGFP expression by FACS.

2.3.3 FACS measurement

This method was used to assess eGFP expression by transfected cells, splenocytes or peripheral blood cells (PBL). The cells to be tested were harvested, washed 1 time with FACS buffer (3% FCS in PBS) and pelleted by spinning down at 1500 rpm for 5 min. Cells were resuspended in 500 μl FACS buffer containing 10 μg/ml propidium iodide to exclude dead cells. Acquisition and analysis were done using BD Cellquest Pro™ Software.

2.3.4 Luciferase assay

The cells were trypsinized, washed 2 times in D-PBS and counted using the hemocytometer. Cells were plated at doses of 1×10^4 in black 96-well cell culture plate in 100 μl D-PBS and 100 μl luciferin (600 μg/ml) were added to start the enzymatic reaction. Immediately after luciferin addition, photon emission at different time points was obtained by taking successive picture with the IVIS® 100 imaging system. Quantification of the signal was done by using the IVIS Living Image Software (Xenogen).

2.3.5 T cell proliferation assay (B3Z assay)

Presentation of SIINFEKL peptide was assessed using the B3Z T-cell hybridoma (Karttunen et al., 1992). B3Z is a lacZ-inducible CD8 + T-cell hybrid specific for OVA peptide 257-264 (SIINFEKL) presented on murine H2-K^b MHC class I molecules. The lacZ assay utilizes a reporter construct consisting on the bacterial ß-galactosidase gene (lacZ) under the transcriptional control of the nuclear factor of activated T cells (NF-AT) element of the human interleukin-2 (IL-2) enhancer. The presentation of the SIINFEKL epitope by murine K^b to B3Z cells result in the IL-2 dependent induction of galactosidase (ß-gal) synthesis and intracellular accumulation of ß-galactosidase by B3Z cells. The amount of ß-gal produced by B3Z T cells can be measured by the hydrolysis of the chromogenic substrate chlorophenolred-ß-d-galactoside (CPRG Calbiochem, Darmstadt, Germany) and is an indication of the amount of SIINFEKL/Kb complexes presented on the surface of cells. For positive control the antigen presenting cells (APC) were pulsed with synthetic SIINFEKL. APC were plate at 1×10^4/well in 96-well plates. To quantify the T cell stimulation, 5×10^4 B3Z cells/well were incubated the APC for 20 hours at 37°C in CO_2 incubator. Cells were pelleted using 2000 rpm for 2min and the supernatant carefully aspirated. The cells were lysed in Z-buffer. Cells release the ß-galactosidase, which reacts with the substrate, to produce red-violet light. The absorption was measured at 595 nm in a 96-well plate ELISA reader (Titertek Multiskan Plus, Germany), with 635 nm as the reference wavelength.

2.3.6 Western blot

2.3.6.1 Precipitation of proteins from bacterial supernatant

A single bacterial colony was inoculated into 50 ml of 100 μg/ml Ampicillin containing LB medium in a 250 ml flask and vigoursly shaken at 37°C overnight. A large number of 5 ml culture (x 10) was inoculated with 500 μl of the overnight culture and cultures were grown to an optical density at 600 nm of approximately 0.7. Cultures were pooled and bacteria were pelleted for 10 min at 4°C and 5000g. Pooled supernatant was filtered through a 0.22 μm-pore-size-filter to remove residual bacterial cells. After 30 min storage at 4°C, trichloroacetic acid was added to the filtrate in order to obtain a final concentration of 10% and stored overnight at 4°C. Protein precipitates, which were collected by 1 h centrifugation at 4°C and 15 000g, were carefully washed with 1 ml ice-cold acetone, and acetone was removed by evaporation at room temperature. To solubilize the precipitate, 50 μl of 2x SDS-PAGE loading dye and 50 μl of a saturated Tris-H$_2$0 solution were added to the samples, followed by incubation at 95°C for 15 min for protein denaturation.

2.3.6.2 Cell lysate

The cells were grown till 70% confluency prior to harvesting. The cells were trypsinized, washed 2 times in D-PBS and counted using the hemocytometer. The cells were lysed in ice-cold lysis buffer (1% NP-40 in TBS) with 1 protease inhibitor tablet added per 50 ml lysis buffer. The cells were lysed at a concentration of 10^7 cells/ml. Lysis was done for 60 min at 4°C followed by centrifugation at 4000 rpm for 10 min to remove the nuclei and cell debris. The cells supernatant was further cleared by another round of centrifugation at 12 000 rpm for 10 min at 4°C. Supernatant was mixed with 6x SDS-PAGE loading dye, denaturated by boiling 10 min and centrifuged 2 min at full speed.

2.3.6.3 SDS-Polyacrylamide (PAA) Gel Electrophoresis

PAA gels from 10-15% were used to separate proteins according to their molecular weights. Before electrophoretic separation, proteins were prepared either from bacterial supernatant (see § 2.3.5.1) or from cell lysates (§ 2.3.5.2). To prepare SDS-PAA gels, the following components for the separating gel listed in the table were mixed together and poured between glass plates (20 x 20 cm). The resolving gel was covered with 2-propanol and let at least 20 min to polymerize. Then, the 2-propanol was removed and the stacking gel was prepared according to the table, mixed and poured over the separation gel. The gel comb was laid avoiding air bubbles. After polymerization, gel was attached to the electrophoresis chamber and covered with electrophoresis buffer. The electrophoresis was carried out for 16 h at 180 mA and 90 V.

Resolving gel	12%	Stacking gel	5%
30% Acrylamid	12 ml	30% Acrylamid	1.7 ml
1.5 M Tris HCl (pH8.8)	7.5 ml	1.0 M Tris HCl (pH8.8)	1.25 ml
20% SDS	0.6 ml	20% SDS	0.05 ml
10% APS	0.3 ml	10% APS	0.1 ml
TEMED	0.012 ml	TEMED	0.01 ml
Water	9.9 ml	Water	6.8 ml

2.3.6.4 Electrotransfer of proteins from SDS-PAGE gel to membrane

After separation by SDS-PAGE, proteins were transferred to a polyvynilidene fluoride (PVDF) membrane. For this, 9 pieces of GB004 Whatman filter paper were cut at the gel size. For the blot, the graphite plates from the transfer equipment were cleaned with dH_2O. 3 pieces of whatman paper were soaked in concentrated anode buffer, 3 pieces were soaked in anode buffer and the pieces were piled on the transfer plate. The membrane was moistened with methanol and laid on the filter pile. The protein gel was taken out from the glass plates, the stacking gel was cut out and the resolving gel was carefully laid on the membrane. Finally 3 pieces of Whatman paper were soaked in the cathode buffer and laid on the gel. Air bubbles were eliminated with a glass pipette. After the cathode plate was put in place, and transfer was done for 1.5 h at 50 V and 180 mA.

2.3.6.5 Immunoblotting

Following transfer, the membrane was placed with the protein side up into a container filled with blocking solution (5% skimmed milk, 0.1% Tween 20 in 1x PBS) and let overnight at 4°C with shaking. Next day, the membrane was transferred in a plastic box and diluted primary antibody in blocking solution was added. After 1 h incubation at RT, the membrane was rinsed twice and then washed 3 times, 10 min each, with washing buffer (0.1% Tween 20 in 1x PBS). The membrane was then incubated with appropriated diluted horseradish peroxidase (HRP) conjugated secondary antibody for 1 h at RT with shaking. Following 3 washes as described above, chemiluminescence detection was performed using Enhanced Chemiluminescence Supersignal Dura West Extended (Pierce PerBio, Bonn, Germany) according to the manufacturer´s instructions. Blots were visualized by using a Lumi-Imager.

C. Results

1. Selection of an optimal luciferase for BLI

Several luciferases such as firefly luciferase (Fluc) and renilla luciferase (Rluc) are commercially available. Of these, firefly luciferase is the most commonly used for BLI, but it is not yet been thoroughly tested which luciferase is optimal for BLI. Because signal attenuation by tissues is lower for red light, red luciferases appear to be advantageous for BLI, but a comparison with other luciferase is missing. Recently, green (CBGr99, CBGr68) and red (CBRed) luciferases from yellow click beetle (*Pyrophorus plagiophthalamus*) have been cloned and modified for optimal expression in mammalian cells. Because of the higher percentage of red light emission, it has been suggested that CBRed and Fluc are the most appropriate luciferases for BLI (Zhao et al., 2005). However, a quantitative comparison of the total photons emitted at the various wavelengths of the spectra, especially in the red wavelengths range, has not been performed. Such measurements are required together with *in vivo* BLI studies for comparitive assessment of the various luciferases for BLI. For such comparisons, it is critical to generate cells expressing equimolar amounts of the different luciferase proteins. Coexpression of a protein with a fluorescent protein allows to refer the amount of protein present in a cell. Therefore, we have combined the respective luciferases expression to the enhanced green fluorescent protein (eGFP) expression with a "self cleaving" 2A peptide. This allowed a quantitative comparison of three different luciferases (Fluc, CBGr99 and CBRed). In the following sections, the photon yield of each luciferase *in vitro* and sensitivity of detection *in vivo* is compared by using stable clones having a similar eGFP expression, thereby the same amount of luciferase protein.

Generation of eGFP-2a-Luciferase constructs

There are generally three ways in which two or more genes can be co-expressed. First, two different genes can be fused together in-frame to produce a chimeric protein, guaranteeing the simultaneous expression of both genes. Although some functional fusion proteins have been successfully expressed (Germann et al., 1989), this strategy may not work for all combinations of proteins as some protein fusions could result in protein misfolding or mistargeting. The second strategy for co-expression involves the design of bicistronic constructs, in which two genes separated by an internal ribosome entry site (IRES) sequence are expressed as a single transcriptional cassette under the control of a common promoter. The intervening IRES sequence functions as a ribosome-binding site for efficient cap-independent internal initiation of translation. Such a design enables coupled transcription of

both genes, followed by cap-independent initiation of translation of the first gene and IRES-directed cap-independent translation of the second gene. This approach is problematic because multiple proteins are often not expressed at the same level (Lee et al., 2001a). The third and only recently established technique is the use of "self-cleaving" 2A peptides, or 2A like sequences from viruses to generate multicistronic vectors. This system consists on the association of two proteins by the 2A peptide consensus motif (2A, Asp-Val/Ile-Gluc-X-Asn-Pro-Gly; 2B, Pro) [Fig. 5A]. This motif is extremely rare and through a ribosomal skip mechanism the 2A peptide impairs normal peptide bond formation between the 2A glycine and the 2B proline without affecting the translation of the 2B [Fig. 5B].
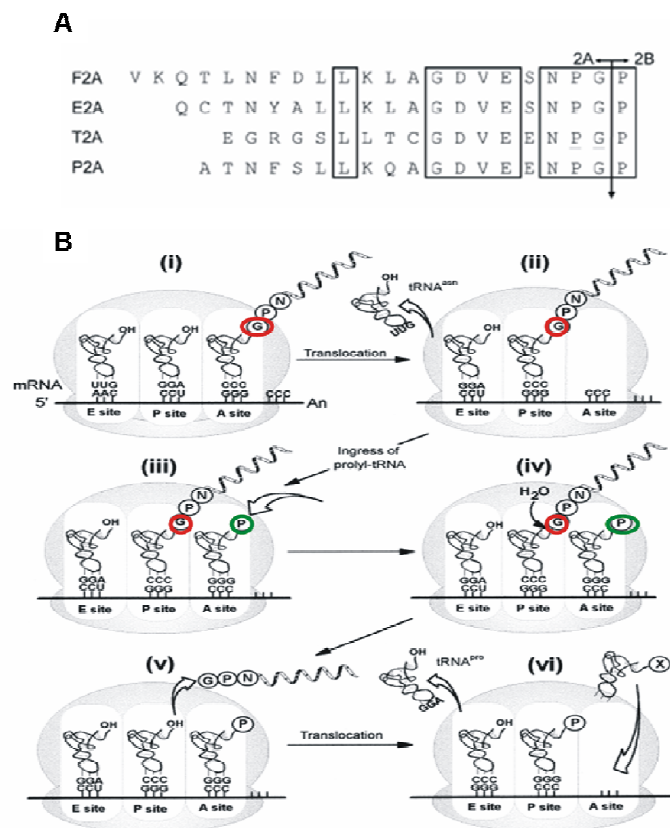
Figure 5 : 2A sequences, scheme of activity

(A) Amino acid sequence of the 2A regions of foot-and-mouth disease virus (F2A), equine rhinitis A virus (E2A), thosea asigna virus (T2A) and porcine teschovirus-1 (P2A; used later to make the construct). Conserved residues are boxed. The cleavage point between the 2A and 2B peptides, and thus the N- and C- terminal cistrons, is indicated by the arrow. (B) The stage following the addition of the ultimate residue of 2A is shown (step i). Peptidyl(2A)-tRNA is translocated from the A to the P site (step ii), allowing the ingress of propyl-tRNA (step iii). Propyl-tRNA is unable to attack the peptidyl(2A)-tRNA^{Gly} ester linkage, and hydrolysis of the glycyl-tRNA ester bond releases the nascent peptide (step iv and v). Deacylated tRNA is now present in the P site (mimicking peptide bond formation) and allows the translocation of propyl-tRNA (rather than the normal peptidyl-tRNA) from the A to P sites (step vi). Synthesis of the peptide C-terminal of 2A proceeds normally, although recommencing with proline.

It has been demonstrated that using 2A peptides leads to the stoichiometric coexpression of proteins (Holst et al., 2006; Szymczak et al., 2004). For the present study we have decided to link the respective luciferases to eGFP using the P2A peptides [Fig. 6] and to use eGFP as a reporter for the amounts of the luciferase protein expressed in a cell.
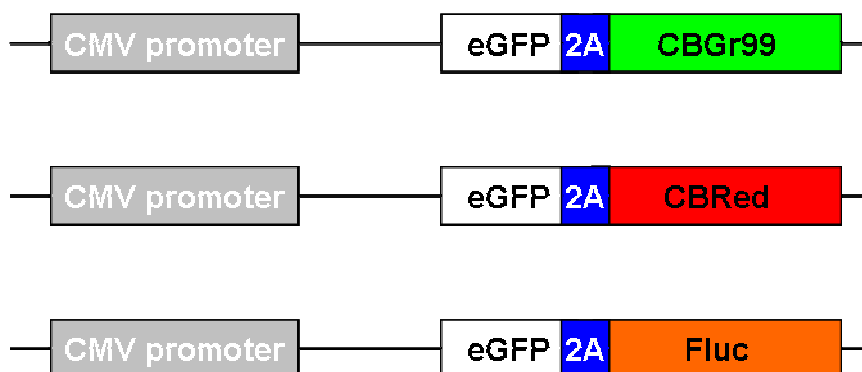
Figure 6 : 2A constructs

Schematic of the 2A-linked eGFP:luciferase constructs used. The CMV promoter is used to express the 2A-linked construct.

Cloning of the 2A constructs

pCMV-eGFP-2A-CBGr99: An "eGFP-2A-CBGr99" cassette was produced by recombinant PCR and inserted under the control of the CMV promoter. Both sequences, eGFP and CBGr99, were PCR amplified in order to add the P2A sequence in 3′ of the eGFP and in 5′ of the CBGr99, respectively. The overlap in sequence, constituted by the 2A sequence, allows the two fragments to recombine after their mixture, denaturation and renaturation. These extended segments, eGFP-2A-CBGr99, served as a template for the secondary reamplification of the combined sequences using the outermost two of the four primers employed to produce the primary fragments. The recombined PCR product was digested with *Hind III* and *Bam HI* to allow its insertion in the pCMV-Cre plasmid digested with *Hind III* and *BCl I.*

pCMV-eGFP-2A-CBRed: As CBGr99 and CBRed have 99% DNA identity, pCMV-eGFP-2A-CBRed was constructed by exchanging a part of the CBGr99 sequence in the pCMV-eGFP-2A-CBGr99 plasmid by the CBRed sequence from the pCBRed-basic plamid using the *Bst XI / Xho I* restriction sites.

pCMV-eGFP-2A-Fluc: The Fluc sequence was PCR amplified from the pGL3 plasmid using chimeric primers. The forward primer contained a part of the P2A cassette in 5′ and 20 nucleotides homologous to the Fluc in 3′. The reverse primer containing 20 nucleotides homologous of the Fluc polyA tail. The digestion of the resulting PCR products with _Bsm BI_ and _Sal I_ followed by its ligation in pCMV-eGFP-2A-CBGr99 digested with the same enzyme allowed the replacement of the CBGr99 sequence.

Linker Constructs: A portion of eGFP linked to the CBGR99 sequence by a (G4S)$_3$ linker from pCMV-DTR-linker-eGFP-linker-CBGr99 plasmid (G.Küblbeck, DKFZ, Heidelberg) was first excised as a _Bsr GI-Sph I_ fragment and inserted in place of eGFP-2A-CBGr99 sequence in the _Bsr GI-Sph I_ sites of the pCMV-eGFP-2A-CBGr99 plasmid to generate the pCMV-eGFP-linker-CBGr99 plasmid.

The pCMV-eGFP-linker-CBRed was made by exchanging a part of the CBGr99 sequence in the pCMV-eGFP-linker-CBGr99 plasmid by the CBRed sequence from the pCBRed-basic plamid using the _Bst XI/Not I_ restriction sites.

The linker plus Fluc were amplified together by PCR from the pGL3 plasmid using chimeric primers. The forward primer contained the sequence encoding for the linker sequence in 5′ and 20 nucleotides homologous of the Fluc polyA tail. The resulting PCR fragment linker-Fluc was then digested with _Cfr 9I/Sal I_ and inserted in place of linker-CBGr99 in the pCMV-eGFP-linker-CBGr99 plasmid, to obtain the plasmid pCMV-eGFP-linker-Fluc.

2A cleavage and generation of stable clones

For verification of correct cleavage, MO4 cells were transfected with the 2A-linked constructs. eGFP-2A production was detected by Western blot analysis using a GFP antibody [Fig. 5A]. For each 2A linked construct, migration of the eGFP-2A protein was consistent with the predicted molecular weight [Fig. 7A, lane 4-6] which is slightly higher than the wild type eGFP [Fig. 7A, lane 7] due to the presence of the "2A tail" in C-terminal. Notably, no uncleaved eGFP-2A-Luciferase could be found, indicating 100% cleavage efficiency. Non cleavable versions of the eGFP-2A-Luciferase constructs were made by exchanging the 2A sequences with a linker sequence ($(G_4S)_3$), and were used to indicate the position of uncleaved material [Fig. 7A, lane 1-3]. Because antibodies against click beetle luciferases are not available and antibodies against Fluc are not useful for Western blot in our hands we could not demonstrate the cleaved luciferases. However, from MO4 cells transfected with pCMV-eGFP-2A-CBGr99, we have generated several stable clones with distinct eGFP expression levels [Fig. 7B]. *In vitro* analysis of eGFP expression and luciferase activity reveals a high degree of correlation between eGFP mean fluorescence intensity (MFI) and light production by CBGr99 ($r^2 \sim 0.9$) [Fig. 7C] Together with the published stoichiometric coexpression in the bicistronic 2A system (Holst et al., 2006), these data demonstrate the usefulness of the eGFP expression for a measure of expression of the associated luciferase protein.
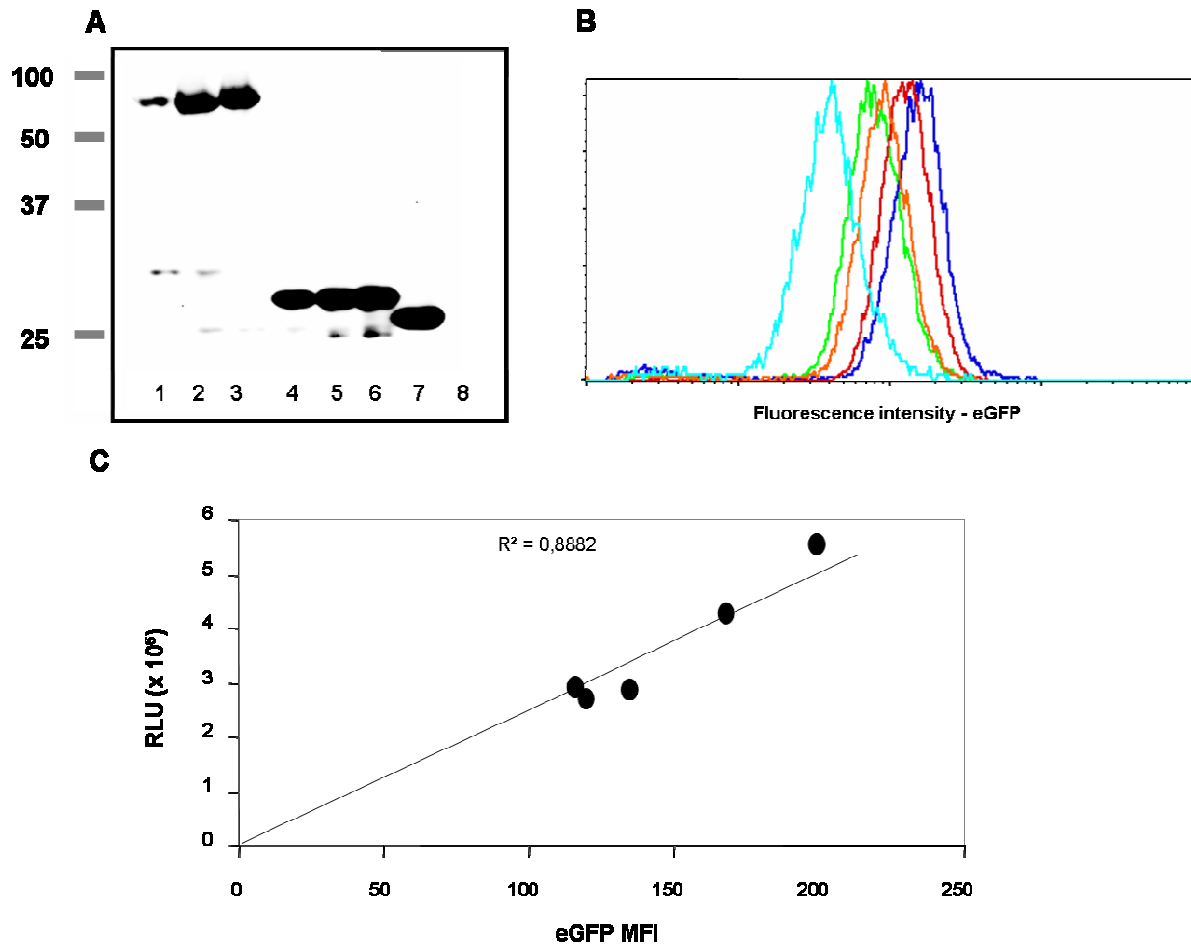
Figure 7 : 2A cleavage and coexpression of eGFP and CBGr99

(A) Western blot with an anti-GFP antibody of transiently transfected cells, lanes 1-3 non-cleavable constructs containing Fluc (lane 1), CBGr99 (lane 2) and CBRed (lane 3). Lanes 4-6 cleaved eGFP band of transient transfectants expressing 2A linked constructs containing Fluc (lane 4), CBGr99 (lane 5) and CBRed (lane 6). Lane 7 native eGFP, lane 8 untransfected cells.   (B) FACS histograms showing eGFP expression of stable transfectants expressing eGFP-2A-CBGr99 (C) Correlation of eGFP and the click beetle luciferases activities in stably transfected MO4 cells. Mean fluorescence intensities (MFI) are plotted against corresponding RLU for CBGr99 in the stable cell lines. Activity of the 2 proteins shows excellent correlation (r^2~ 0.9)

We have selected for each luciferase a clone with similar eGFP expression [Fig. 8A]. In these stable clones, complete cleavage was found with comparable intensity of the eGFP bands [Fig. 8B], which is in agreement with the identical fluorescence intensities shown in figure 7C. These clones were used to perform luciferase comparison *in vitro* and *in vivo*.
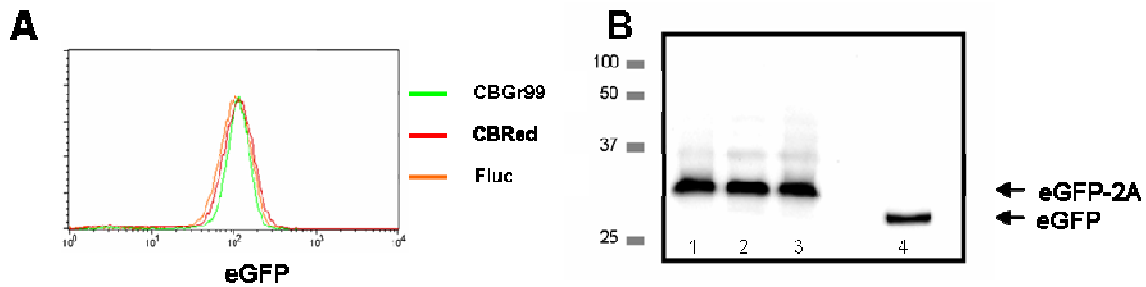
Figure 8 : eGFP expression of the selected stable clones

(A) eGFP expression analysis by flow cytometry of the stable transfectants expressing eGFP-2A-CBGr99, eGFP-2A-CBRed, or eGFP-2A-Fluc. (B) Western blot for cleaved eGFP of the stable transfectants, lane 1: eGFP-2A-Fluc ; lane 2: eGFP-2A-CBGr99; lane 3: eGFP-2A-CBRed; lane 4: transient transfection with pEGFP-N3 plasmid.

Luciferase comparison *in vitro*

For comparison of light emission, the MO4 cell lines expressing equimolar amounts of the different luciferases were imaged. Although the luciferases utilize the same substrate, D-luciferin, the kinetics of the enzymatic activities may differ. Therefore, imaging of the cells was performed every minute after luciferin addition. We could show that the kinetics and maximum photon yield are indeed different [Fig. 9A]. CBGr99 clearly displayed the highest photon yield and is characterized by an enzymatic activity that peaks at about 11 min after addition of D-luciferin. For CBRed and Fluc, the maximum is reached at about 27 min and 35 min, respectively [Fig. 7A]. The photons emitted in the red part of the spectrum (above 600 nm) are critical for *in vivo* BLI as they are less absorbed by mammalian tissues.

To estimate the light that is emitted in the red-orange part of the spectrum, collection of orange-red light was performed using a DsRed2-1 filter (pass band 575-600 nm). CBGr99 activity peaks at about 10 min after addition of D-luciferin whereas for CBRed a maximum was after about 21 min and for Fluc after about 32 min [Fig. 9B]. CBGr99 emits more orange-red photons than CBRed in the early phase of the enzymatic activity but after 16 min, CBRed displayed a strongest photon yield. Fluc clearly emits fewer orange-red photons [Fig. 9B]. These observations do not allow to conclude that CBGr99 emits more photons above 600 nm. However, they strongly suggest that despite an emission spectrum, which is mainly in the green wavelengths, CBGr99 is a good candidate for *in vivo* BLI.
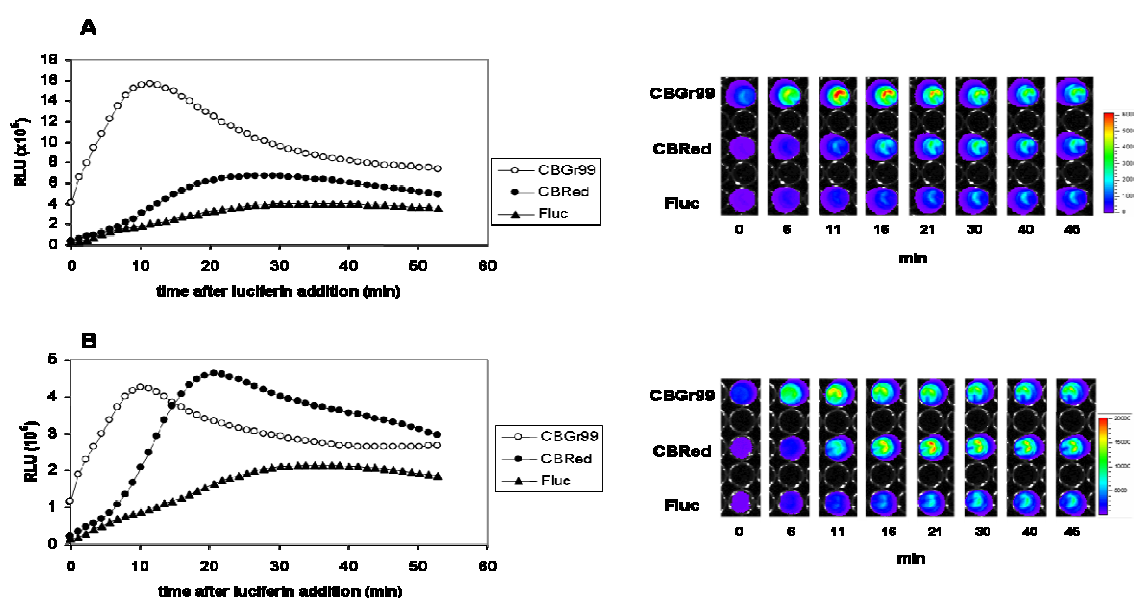
Figure 9 : **Luciferase comparison *in vitro*.**

Stably transfected MO4 cells were plated in a black 96 well plate and imaged for 1 min (45 times) (A) without emission filter, (B) with a DsRed2.1 emission filter. The graph of RLU versus the time allows direct comparison of the different luciferases.

Luciferase comparison *in vivo*.

Our *in vitro* studies have shown that CBGr99 is potentially a good candidate for BLI. However, tissues have a strong influence on the detection of bioluminescence reporters *in vivo*. Therefore, I evaluated the capacity to detect light emission of the stable clones *in vivo* placed in different locations, either (1) underneath the skin (subcutaneous), (2) in the peritoneal cavity (intraperitoneally), or (3) in a highly vascularized organ such as the lung. In the subcutaneous model, 30 000 cells of each clones were injected into the same mouse. With this approach the luciferases are directly comparable in presence of the same amount of injected luciferin. In the subcutaneous model the cells are superficially located in the mouse; thereby light absorption due to hemoglobin is low. As observed *in vitro*, the signal intensity from the CBGr99 luciferase is much higher compared to the two other luciferases [Fig. 10].
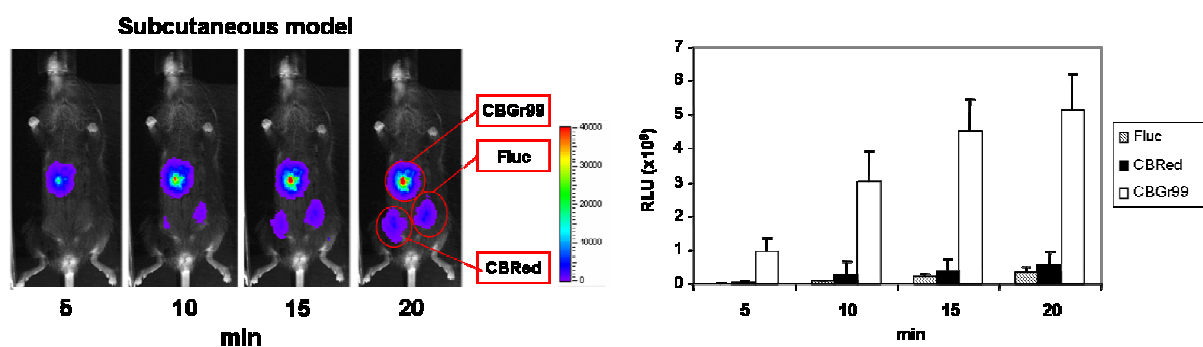
Figure 10 : **Luciferase comparison in the subcutaneous model**
Mice were injected subcutaneously injected with 30 000 cells of each stable clone and imaged at different times after D-luciferin injection. A representative animal is shown. The signal intensity from 5 mice were averaged and plotted relative to the time after luciferin injection.

In the intraperitoneal model, where the cells are located deep in the mouse, the presence of organs like the gut and kidneys will lead to higher tissue absorption than in the previous model. Probably because of a higher absorption of the CBGr99 signal, BLI of cells injected intraperitoneally (1×10^6 cells) showed that the differences between the various luciferases are less pronounced. However, the sensitivity of detection of CBGr99 remains superior in the first 5 min [Fig. 11A] and then becomes similar to CBRed in the next 15 min [Fig. 11A]. The highest sensitivity of CBGr99 at the early time points can be explained by a higher emission of photons in the red part of the spectrum [Fig. 11A].

For comparison of BLI of a strongly vascularized organ, we have used the lung model that presents two main disadvantages for BLI (1) Photons must traverse through a deep, highly vascularized and hemoglobin rich tissue (2) Scattering of the light is also caused by the presence of air/alveolar boundaries and lung/muscle junctions. Because intravenously injected cells will be sequestrated in the capillaries of the lung tissues, mice were imaged directly after intravenous injection of the respective clones (0.5 x 10^6 cells). As suggested by the previous observation, Fluc is less sensitive than the click beetle luciferases (CBluc) [Fig. 11B]. As already observed in intraperitoneal model, the bioluminescence signal emitted by the CBGr99 luciferase is greater in the first 10 minutes and becomes similar to the CBRed in the last time points [Fig. 11B].
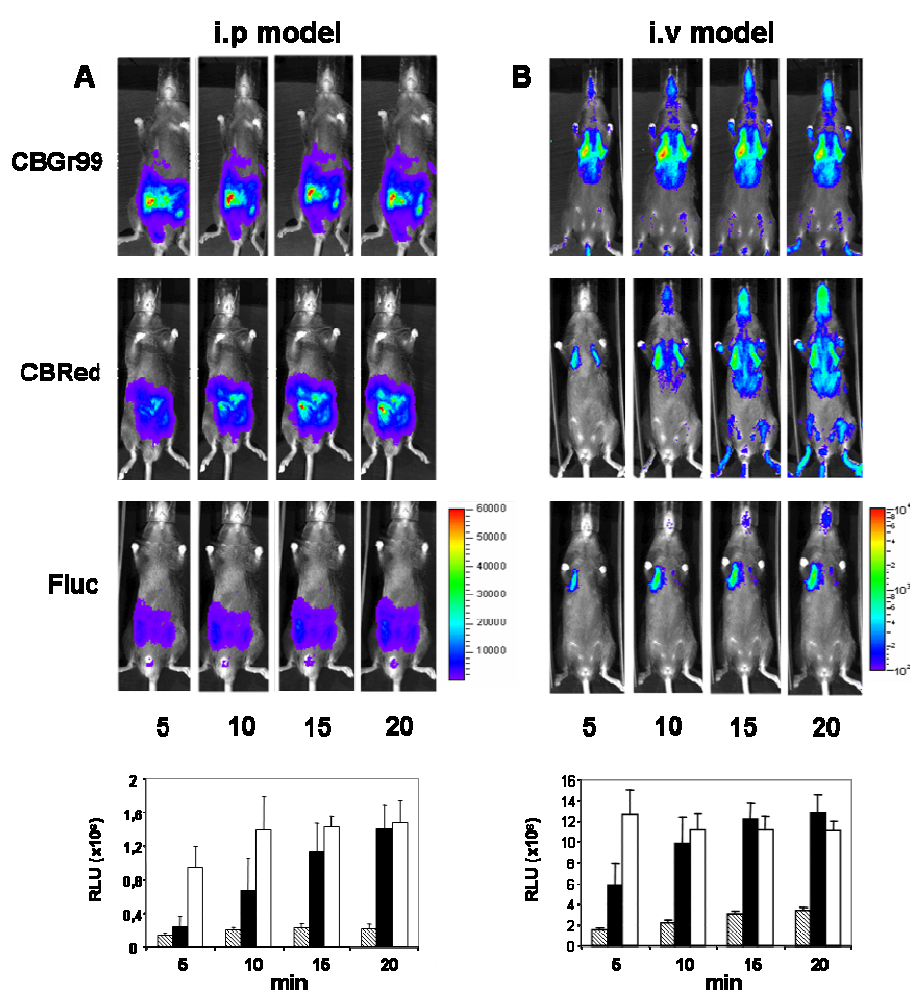
<u>Figure 11 :</u> Luciferase comparison in the i.p. and i.v. model

Mice were injected with stable transfectants expressing eGFP-2A-CBGr99, eGFP-2A-CBRed or eGFP-2A-Fluc, respectively, and imaged at different times after D-luciferin injection. Representative animals are shown. The signal intensities from three mice per group were averaged and plotted relative to the time after luciferin injection. (A) Intraperitoneal model. BLI signal of 1 x 10^6 cells injected i.p. (B) Lung model. BLI signal of 0.5 x 10^6 cells injected i.v.

Altogether these results clearly illustrate the superiority of the CBlucs over the Fluc which is the most commonly used in reported BLI studies. The comparison of the CBLuc has shown that depending on the time point, CBGr99 has either a superior or a similar sensitivity *in vivo* than CBRed. Despite a high attenuation of its signal *in vivo*, the CBGr99 luciferase still produces a higher or a similar amount of red photons (depending on the time point). These properties make CBGr99 highly suitable for BLI.

2. BLI to follow tumor growth in mice

Monitoring of tumorigenesis and metastasis *in vivo*

The Fluc has been used as reporter gene in both *in vitro* and *in vivo* assays. This luciferase has been used to tag tumor cells for the purpose of monitoring growth *in vivo* (Edinger et al., 1999). Temporal measurement of tumor cell growth was quantitative and permitted spatio temporal evaluation of tumor growth. Moreover, Fluc and its substrate, luciferin, have been shown to be non-toxic to mammalian cells (Sweeney et al., 1999). We have shown that CBGr99 luciferase is more suitable for BLI than Fluc (see chapter C 1.4). To verify whether CBGr99 is also appropriate to follow tumor growth *in vivo*, we have further characterized, a stable MO4 transfectant expressing CBGr99. First, a stable clone displaying a good antigen presentation was selected. For this clone, the sensitivity of detection was determined *in vitro* and *in vivo*. Second, proliferation of this clone was assessed *in vivo* to ensure that CBGr99 is appropriate for monitoring tumor growth *in vivo*.

Antigen presentation

MO4 is a melanoma cell line that stably expresses the chicken ovalbumin protein (OVA). OVA is a well-characterized antigen with two defined CTL epitopes: ova257-264 (Rotzschke et al., 1991) and ova176-183 (Lipford et al., 1993). The OVA peptide 257-264 (SIINFEKL) is the immunodominant peptide. In therapeutic studies in mice, SIINFEKL is often used as a model antigen because of abundance of tools allowing the observation of the immune response. MO4 cells are usually grown under antibiotic selection (G418) to make sure they maintain OVA expression. Using the 2A technology, we have produced several stable transfectants that coexpress eGFP and CBGr99 (see chapter C 1.2). To obtain a clonal population we have selected stable transfectants based on their eGFP expression [Fig. 7B] starting from a single cell. Therefore, the selection process was done in the absence of antibiotics to avoid an excessive stress for the cell. To have a cell line displaying a good SIINFEKL presentation, we have checked the ability of these clones to efficiently present the SIINFEKL peptide by the B3Z assay. B3Z is a lacZ-transfected SIINFEKL-specific CTL clone. Recognition of MHC I complexed OVA peptides leads to transcriptional activation of lacZ gene resulting in production of ß-galactosidase. Enzyme activity correlates with amount of galactosidase synthesized by transcription of the lacZ gene and hence with peptide presentation. As shown in figure 12, most of the clones still present the SIINFEKL peptide despite the absence of selection in cell culture. The clone 10 has shown a presentation of

SIINFEKL on MHC I which is almost as high as to the parental B16F10 cell line loaded with SIINFEKL and greater than the other transfectants. Therefore, we have used clone 10, denoted MO4/GL2A-10, for subsequent studies.
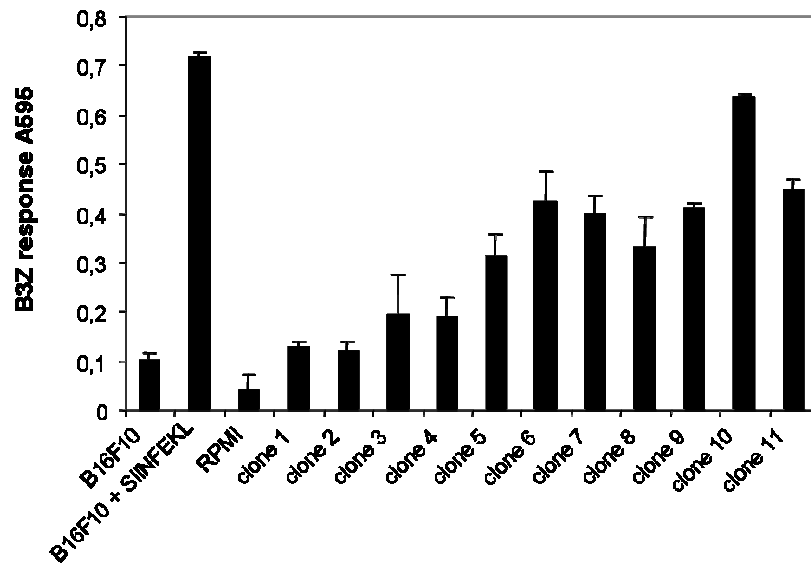
Figure 12 : **SIINFEKL presentation by stable clones**

1 x 10^4 cells/well were co-cultured with B3Z cells for 20 h and the lacZ was performed according to the protocol described in Material & Methods (§ 2.3.5)

Sensitivity of detection.

To assess the relationship between bioluminescent signal intensity and cell numbers, we prepared a dilution series of MO4/GL2A-10 cells (range 100- 10 000 cells per well) and measured the luminescence for a given volume (100 µl) of cell suspension after D-luciferin addition [Fig. 13A]. Quantification of the luminescence signal demonstrates a linear relationship between cell numbers and light emission after addition of D-luciferin [Fig. 13B]. Hence it is important to notice that the MO4/GL2A-10 cells have a relatively good sensitivity of detection *in vitro*. As shown in Figure 10A, as few as 100 cells can be detected *in vitro*. We also estimated the sensitivity of detection *in vivo* by injecting a serial dilution of MO4/GL2A-10 cells (range 5000-1250 cells) subcutaneously in mice. BLI of these mice has indicated that approximatively 2500 MO4/GL2A-10 cells [fig 13C] can be detected when superficially located in mice, namely subcutaneously.
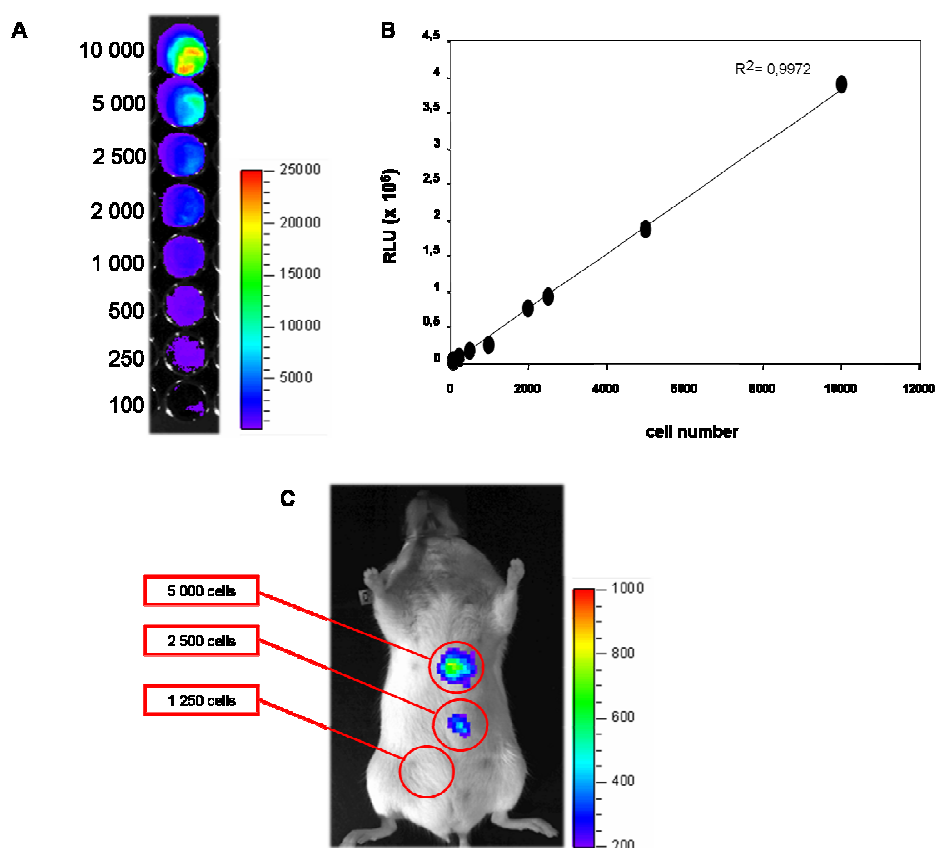
Figure 13 : *In vivo* **BLI of MO4/GL2A-10 cell line.**

(A) MO4/GL2A-10 were diluted from 10 000 to 100 cells, plated in black 96-well plate, and imaged for 1 minute after addition of D-luciferin. (B) Correlation between cell number per well and bioluminescence (RLU). (r² = 0.99). (C) Serial dilution of MO4/GL2A-10 cells (range 5000-1250) were subcutaneously injected in a C57Bl/6 Tyr -/- mouse and imaged for 5 min after i.p. administration of D-luciferin.

To estimate the attenuation of the signal due the black fur which is a strong absorber of light, black and white mice were subcutaneously injected with 50 000 MO4/GL2A-10 cells and imaged. The white mice that we have used C57Bl/6 mice are albino due to a spontaneous mutation of the tyrosinase gene (C57Bl/6 Tyr-/-). As shown in figure 14, the sensitivity of detection in black mice is significantly reduced compared to white mice (~10 times lower). When black mice are shaved, the light emission signal is very similar to the signal observed in white mice. Therefore, subsequent experiments were performed with shaved C57Bl/6 black mice which are better characterized than the white C57Bl/6 Tyr-/- mice.
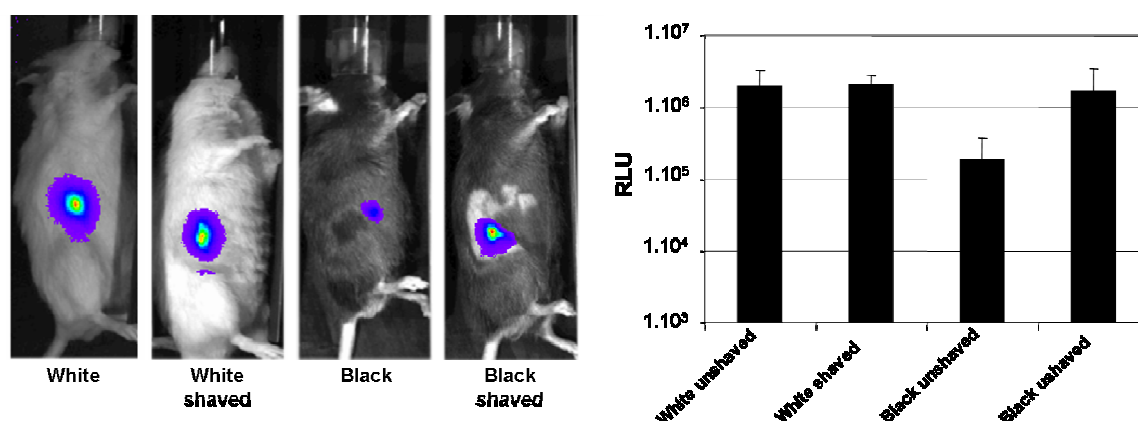
Figure 14 : Black vs White mouse for BLI

50 000 MO4/GL2A-10 cells were subcutaneously injected in the indicated mice and imaged after i.p. administration of D-luciferin. A representative animal is shown. The signal intensity from 3 mice were averaged and plotted.

Monitoring of tumor growth by BLI

Subcutaneous tumor growth

C57Bl/6 mice inoculated with M04 cells subcutaneously develop fast growing tumors that lead to death 20 to 25 days after tumor inoculation. Tumor volume is estimated after measurement of the tumor diameter with a caliper. To check whether MO4/GL2A-10 melanoma cells can be used to monitor subcutaneous tumor growth in mice, we injected 0.5 x 10^6 cells subcutaneously. Tumor growth was then monitored by BLI [Fig. 15A] and by external caliper measurement [Fig. 15C]. Tumor growth was measured beginning on day 1 and weekly thereafter. By day 1, when tumor is still not detectable by optical inspection a luminescence signal was detectable at the site of injection [Fig. 15A]. Evidence of tumor growth was already visible at day 9 by a signal increase whereas the tumor is again hardly visible by eye. The signal significantly increases over the next 21 days with a similar to that observed with the caliper method [Fig. 15B]. Linear regression analysis showed that luminescence correlates to the tumor volume [Fig. 15C; $r^2 > 0.9$]. No apparent signal was detected from sites other than the site of injection indicating that the MO4/GL2A-10 cells seem not to metastasize.
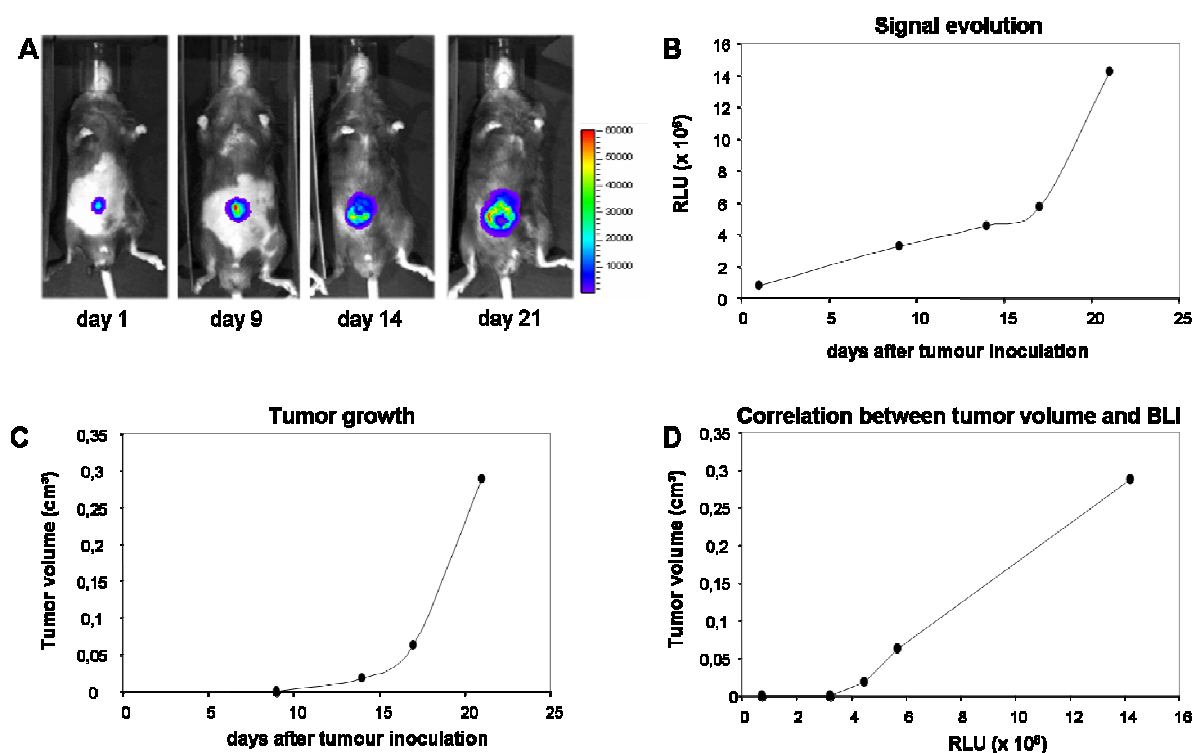
Figure 15 : Monitoring subcutaneous tumor growth *in vivo*.

MO4/GL2A-10 (0.5 x 10^6) were injected subcutaneously into C57Bl/6 mice and tumor growth followed over time. (A) In vivo BLI of a representative mouse is shown. (B) Bioluminescence signal (RLU) from tumors was quantified and is displayed over time. (C) Tumor volume estimate after caliper measurement is displayed over time. (D) Correlation between tumor volume and bioluminescence signal.

In vivo analysis of metastasis colonization

One of the current models for metastasis of melanoma and other tumors is lung tumor formation after intravenous injection of tumor cells. In this model, MO4 tumor nodules are usually quantified by counting the black nodules on the outside of an excised lung. This methodology requires euthanasia and allows analysis at only one single time point. To overcome this deficiency, we have intravenously injected 0.5×10^6 MO4/GL2A-10 cells in mice and imaged them over a period of 36 days. Immediately after injection the cells were detectable in the lung. At day 6, the signal is strongly decreased or absent. The absence of signal probably indicates an initial clearance of most of the tumor cells. At day 11, the cells were detectable at the anatomical site of the lung. Subsequent time points showed an increase of the luminescence signal indicating metastasis colonization until death approximatively 40 days after cells inoculation [Fig. 16].
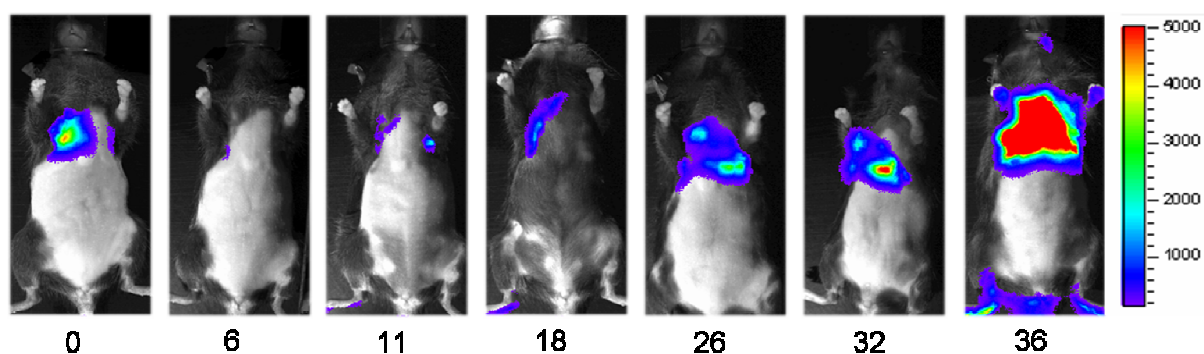
Figure 16 : *In vivo* **analysis of tumor cell lung colonization.**

MO4/GL2A-10 (0.5 x 10^6) were injected intravenously into C57Bl/6 mice. In vivo BLI of a representative mouse is shown.

Generation of autochthonous hepatocarcinoma model for BLI

We have previously shown that CBGr99 is suitable for monitoring transplantable tumor growth via BLI. Although transplantable models are frequently used for experimental tumor studies they do not reflect the clinical situation of cancer formation. Conditional autochthonous tumor model are more useful for mimicking tumor development as it occurs in humans. For example a conditional transgenic hepatocarcinoma model (AST: Albumin-Stop-Tag) has been established in our laboratory (Stahl, 2004). In this model, the SV40 Tag oncogene (Tag) is under the control of liver-specific promoter of mouse albumin (Alb) (Sandgren et al., 1989; Shiota et al., 1992) and can be induced at a desired time point by Cre recombinase. The activation of the transgene is achieved by intravenous injection of an adenovirus encoding the *cre* gene. Hepatocarcinoma development in these mice is dependent on the adenovirus dose and is characterized by the formation of several nodular adenomas in the liver. Because an increase in alanine aminotransferase (ALT) level reflects the presence of lesions in the liver, the measurement of its level in the serum is, so far, the only way to detect the presence of tumors without sacrifying the mice. This method may indicate the presence of tumor, but ALT levels do not correlate with tumor size.

To be able to monitor tumor growth, I have generated a conditional reporter mouse designed ASC (Albumin-Stop-CBGr99), that expresses exclusively in the liver the CBGr99 luciferase preceded by a floxed STOP cassette. By breeding the ASC with the AST mice, a binary transgenic model (ASCT mice) was established in which the conditional expression of two transgenes, Tag and CBGr99, can be induced simultaneously in the same liver cells by injection of adenovirus encoding *cre*. We evaluated in this mouse model the possibility to monitor hepatocarcinoma formation over the course of several weeks by BLI.

Generation and characterization of ASC mice

To generate transgenic mice expressing the CBGr99 luciferase in an inducible manner specifically in the liver, a Stop-CBGr99 cassette was inserted into the ATG-including exon of the albumin gene through homologous recombination of a bacterial artificial chromosome (BAC) clone containing the albumin gene. There are several advantages of using BACs as compared to a single promoter sequence. (1) BACs have a high stability in terms of their propagation in recombinant deficient *E.coli* host cells, (2) BACs can be modified in *E.coli* to insert transgenes at a desired position and (3) the large size of the insert in BACs of approximately 150-200 kb provides less integration dependency of transgene expression.

Construction of the Stop-CBGr99-FlpAmp cassette

To generate the pFstop-CBGr99-FlpAmp construct, the pCBGr99-Basic vector (Promega) was used as starting vector. This plasmid was digested by *Hind III* followed by blunting with Klenow polymerase. In parallel the Fstop cassette was isolated from pAST plasmid (G.Küblbeck, DKFZ, Heidelberg) with *EcoR I* and blunted with Klenow polymerase to allow its insertion upstream of the CBGr99 gene. The intermediate plasmid, pFstop-CBGr99, was opened with *Sal I* and subsequently blunted using Klenow polymerase. The Flp-Amp cassette was released from the pCMV-Cre plasmid (G.Küblbeck, DKFZ, Heidelberg) with *Xho I/Nhe I* and blunted before its ligation downstream to the CBGr99 gene. The Fstop-CBGr99-FlpAmp cassette was then PCR-amplified from the template plasmid using chimeric 60 nucleotides primers. The 3′ 20 nucleotides of each primer were homologous to the targeting cassette used for amplification, while the 5′ 40 nucleotides were homologous to the first exon of albumin where the cassette has to be targeted by recombination. The primers were designed to target precisely the cassette in frame with the albumin start codon.

Zeocin and Ampicillin gene were amplified in same way by PCR to allow the replacement of the *LoxP* site present in the BAC plasmid by homologous recombination.

Modification of the albumin gene containing BAC

To obtain a BAC containing the mouse albumin gene, the CHORI database was screened. The RCPI23-14C7 clone was assumed to be the best candidate because of the presence of the complete 5′and 3′ regulatory regions, owing to the central position of the albumin gene in the BAC. After transfer of the selected BAC into EL 250 bacteria, it was modified by homologous recombination to express the Stop-CBGr99 cassette under the control of the albumin promoter. BAC DNA was introduced in EL 250 bacteria that contain a defective prophage [Fig. 17A] that protect and recombine electroporated linearized DNA (Yu et al., 2000). The PL operon encoding *gam* and the red recombination genes, *exo* and *bet*, are under the tight control of the temperature-sensitive λ repressor. Recombination functions can thus be transiently supplied by shifting the culture to 42°C for 15 min [Fig. 17B]. Gam inhibits the *E.coli* RecBCD nuclease from attacking the electroporated linear DNA, while Exo and Beta generate recombination activity. To insert the cassette, containing the Stop-CBGr99 sequence and a selection marker gene (Ampicillin) into the exon 1 harboring the translational start of the albumin protein, two amplified recombigenic arms of 40 base pairs were added on both sides of the cassette by PCR. The selectable marker can, however, interfere with the subsequent function of the targeted locus. Therefore the selectable marker was flanked with

FRT sites, so that, it can be removed from the targeted locus by Flp Recombinase. In the EL 250 bacteria, the defective prophage contains an arabinose inducible *flpe*. *flpe* is a genetically engineered *flp* that has a higher recombination efficiency than the original *flp* gene. The selective marker can thus be removed by incubating the bacteria with L-arabinose [Fig. 17C]. Because of the presence of two *loxP* sites in the BAC plasmid, it is possible that Cre expression leads to the deletion of the BAC from the mouse genome. Therefore two homologous recombinations were performed using a cassette encoding resistance to Ampicillin and Zeocin to replace these two *loxP* sites. The modified BAC was linearized prior microinjection in oocystes. (For more detailed information concerning the BAC modification see material and methods § 2.1.15.2)
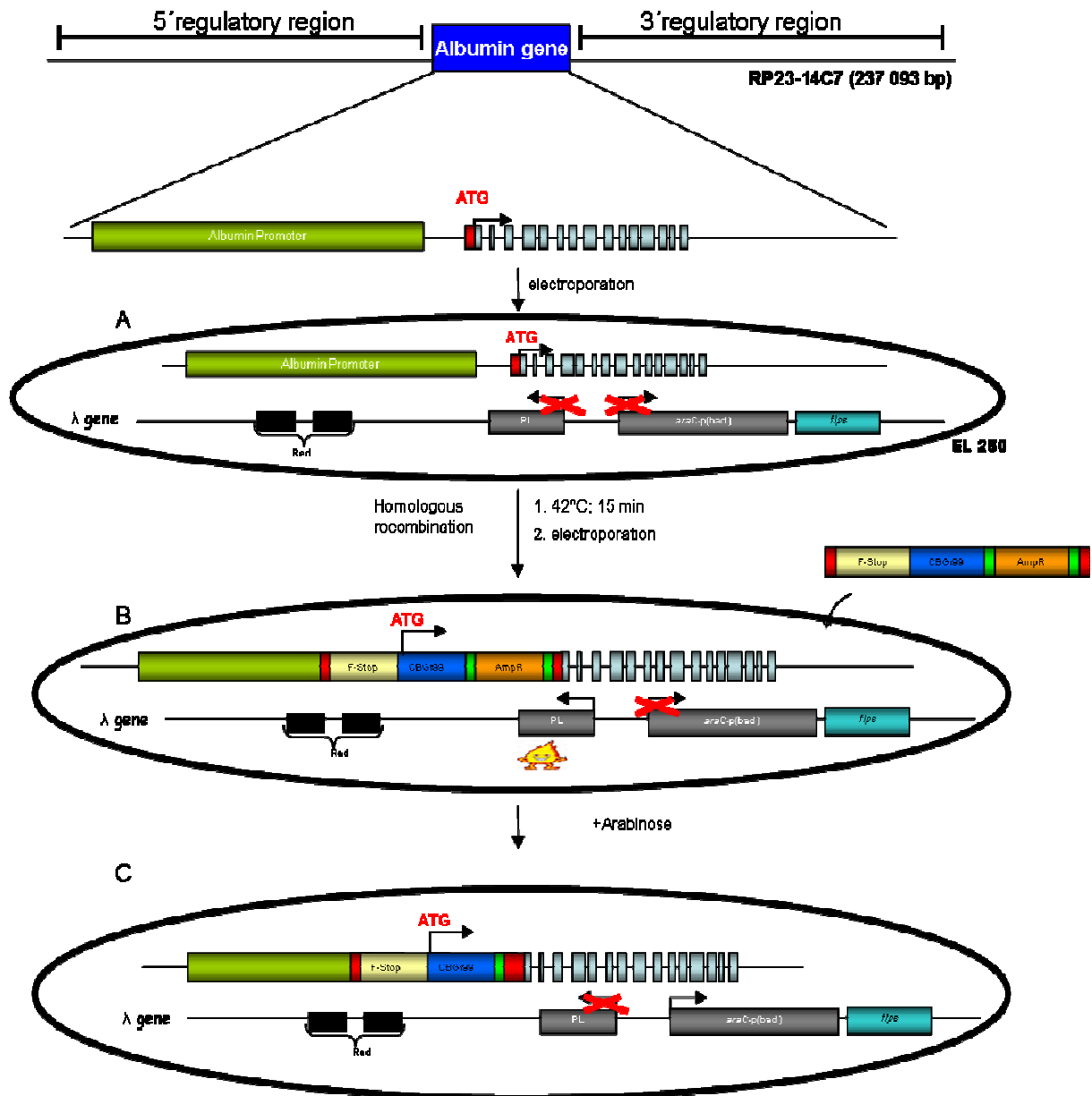
Figure 17 : **General strategy for BAC preparation**

(A) The first step consists in the introduction of BAC DNA into the EL250 bacteria strain which contains the λ gene. This is performed by electroporation using the Gene Pulser® from Biorad. (B) A temperature-sensitive promoter, PL, drives expression of the red gene which is able to recombine electroporate linearDNA produce by PCR with short homology regions at their ends (40 bp homology region, red square). Recombination function is supplied by shifting the culture to 42°C during 15 min. The linear DNA contains an Ampicillin cassette, flanked by FRT sites (Green square), which allows selection of the positive clones after recombination. (C) The promoter of the araBAD operon, which can be induced by L-arabinose, controls the expression of the flpe gene. Expression of the flpe gene allows the removal of the selective marker in order to avoid interference with the subsequent function of the targeted locus.

Screening of founder mice

Following microinjection into B6D2F1 oocystes, 8 live offspring mice were tested for the presence of the transgene at 5 weeks of age. For this, the presence of the CBGr99 transgene within the mouse genome tail biopsies was analyzed by Southern blotting. For identification of the CBGr99 transgene a 664 bp Dig labeled probe generated by digestion of pCBRed-basic plasmid with *Pvu II* was applied [Fig. 18]. From the 8 founders obtained, 1 male harbored the CBGr99 transgene.
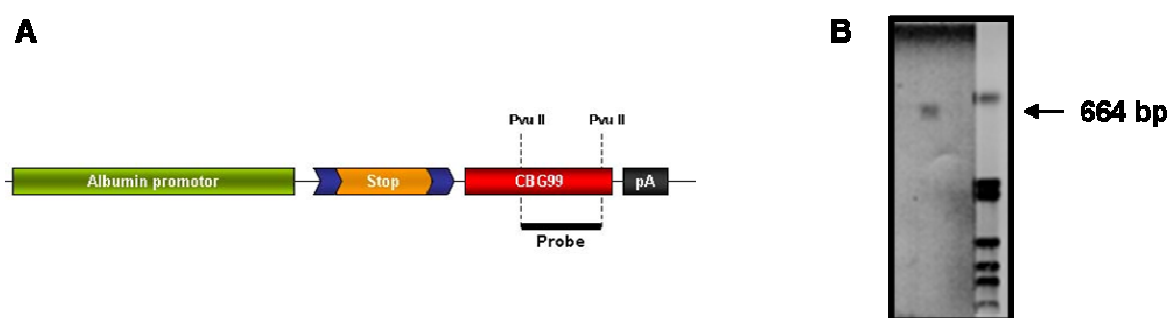
Figure 18 : ASC transgenic mice carry the transgene as shown b southern blot

(A) Location of the 664 bp Dig labelled probe within the Alb-Stop-CBGr99 construct is shown. (B) Representative Southern blotting of a positive mouse.

The positive founder mouse was designed ASC and mated with AST mice and presence of transgenes in the F1 generation was assessed by Southern blotting for CBGr99 (as shown previously) and by PCR for SV40 Tag [Fig. 19]. Single transgenic for CBGr99 as well as the double transgenic were kept for further studies.
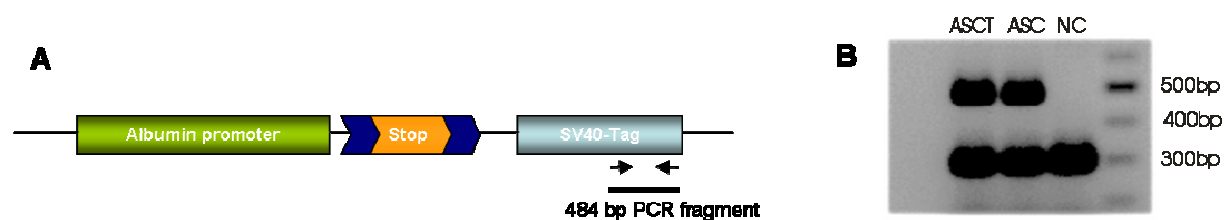
Figure 19 : ASC and ASCT transgenic mice carry the transgene as shown by PCR

(A) Location of Tag specific primer within the transgene used to generate the 484bp PCR product. (B) Recovered genomic DNA from proteinase K digested AST and ASCT mouse tail biopsies were subjected to Tag PCR. Depicted are a positive PCR for each transgenic line as well as a negative control (NC).

Characterization of ASC and ASCT mice

Unrecombined mice

Because a STOP cassette can be leaky (Willimsky and Blankenstein, 2005), ASC and ASCT mice were imaged before injection of Cre-recombinase encoding adenovirus. A luciferase signal showed that the STOP cassette is leaky in ASC mouse [Fig. 20]. Considering that a luminescence signal is very low when it is below 600 counts per pixel, we can conclude here that the signal is very low [see scale, Fig 20]. To verify that this leakiness of the STOP cassette is not leading to spontaneous hepatocarcinoma development or spontaneous signal increase, 15 ASCT mice were imaged. At the age of 12 to 14 months all mice displayed comparable signals as the young unrecombined mice. Their liver did not show any signs of hepatocarcinoma development after sacrifice (data not shown).

unrecombined
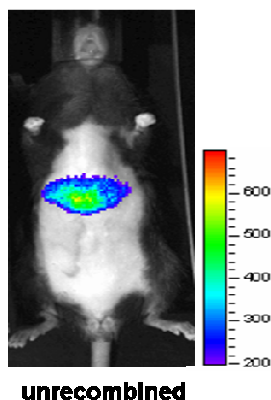
<u>**Figure 20 :**</u> **Leakage in ASC model.**

ASC mice were imaged immediately after intra-peritoneal injection of luciferin (180μg/g of body weight). 5 min exposure time, A position and medium resolution picture setting were applied. A low signal from the liver is observed in unrecombined mice.

Recombined mouse

In order to induce recombination, different doses of adenovirus encoding Cre were injected intravenously to ASC and ASCT mice. 1 day after injection, a strong signal increase was observed showing efficient recombination and specific luciferase expression in the liver [Fig. 21A]. The signal increase observed after Adeno-Cre injection is 30, 170 and 350 fold higher than in the unrecombined mice after injection of 1.25×10^8, 2.5×10^8 and 5×10^8 i.f.u., respectively. The relationship between signal increase and viral dose is non linear with dramatic luminescence signal increase resulting from small increase in viral doses [Fig. 21B]; e.g from 30 to 170 fold signal increase when viral dose is doubled (from 1.25×10^8 to 2.5×10^8 i.f.u.). This observation correlates with a previous study showing that Kupffer cells in the liver take up the adenovirus and thereby reduce transgene delivery to the hepatocytes (Tao et al., 2001). Once Kupffer cells are saturated, efficient gene delivery to hepatocytes can be achieved more efficiently explaining the highest induction of luciferase expression per virus particles with high viral dose.
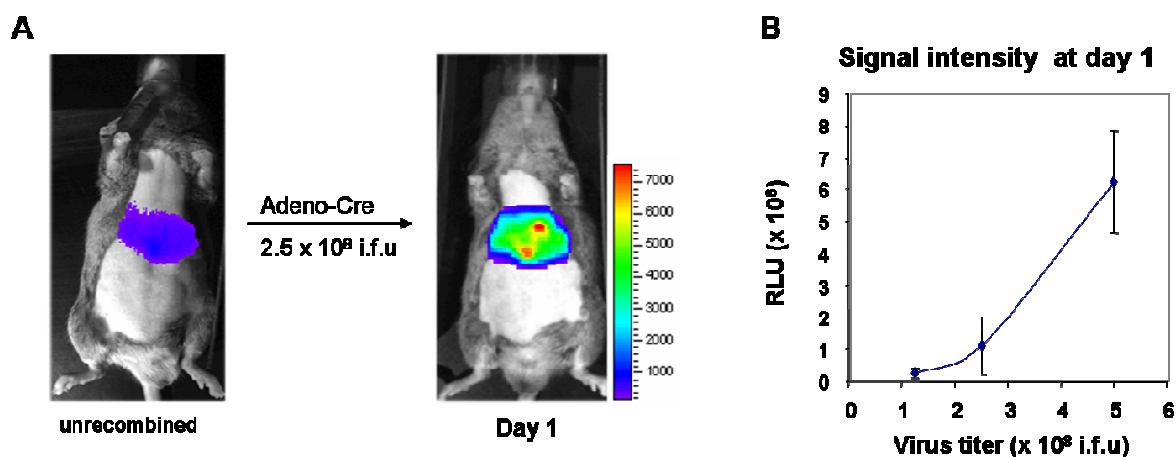
Figure 21 : **Induction of luciferase expression**

1 day after adenovirus injection, mice showed a strong increase in luciferase signal due to the deletion of the stop cassette. (A) Imaging illustrates the signal increase after injection of 2.5×10^8 i.f.u. (B) The graph shows that signal intensity is dependent on the virus titer.

After induction, the mice were weekly imaged in order to see whether hepatocarcinoma growth induced by SV40-Tag expression in ASCT mice could be followed by BLI [Fig. 22A]. In parallel the presence of tumors was estimated by measurements of the ALT levels in the serum. For negative controls, the same measurements were performed in ASC mice. In ASC mice, both ALT and luciferase activity were stable over the time [Fig. 22 (B and C)] whereas ASCT mice showed increased level of ALT as well as increased luciferase signals [Fig. 23 (B and C)], thus indicating tumor development.
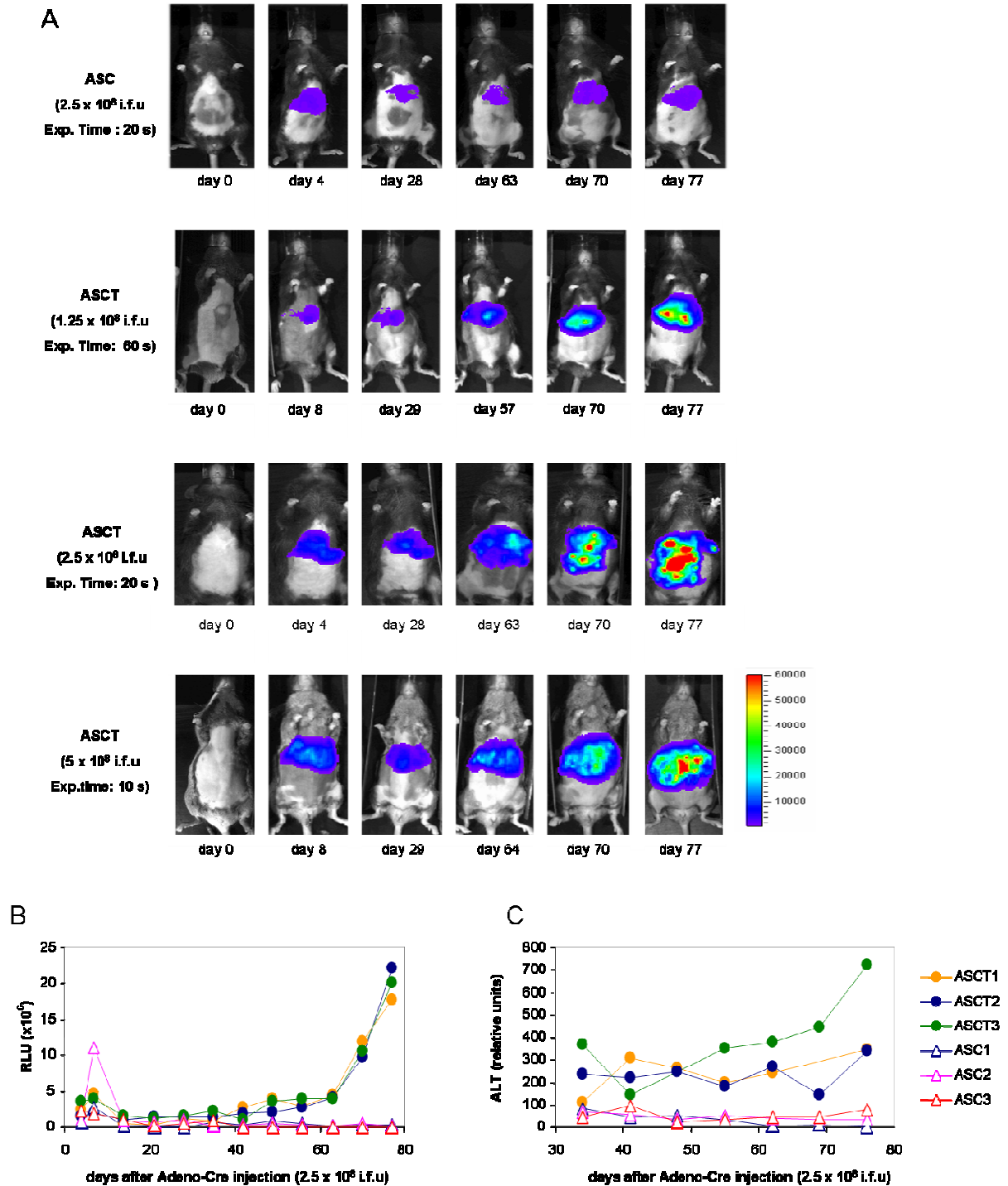
Figure 22 : BLI of hepatocarcinoma growth

 (A) Longitudinal measurement of ASCT induce hepatoma tumor growth from individual mice 6 images of representative ASC and ASCT mice were after adeno-Cre injection of indicated doses of virus.(images taken 10 min after i.p D-luciferin administration; acquisition time indicated in the figure, high resolution) the numbers of days annotating each individual images refers the time post-adeno-Cre injection. (B) Graph depicting the longitudinal measurement of light emission from individual mice (3 mice/groups). Light emission is expressed as relative light units. (C) Graph depicting the longitudinal serum level of ALT.

For 1.25×10^8, 2.5×10^8 and 5×10^8 i.f.u of injected virus, most of the mice (16/17 mice) showed a significant signal increase that was observed 40 to 60 days after virus injection [Fig. 23]. In all cases, signal emission was confined to the liver, demonstrating that in this model tumor development is indeed restricted to the liver.
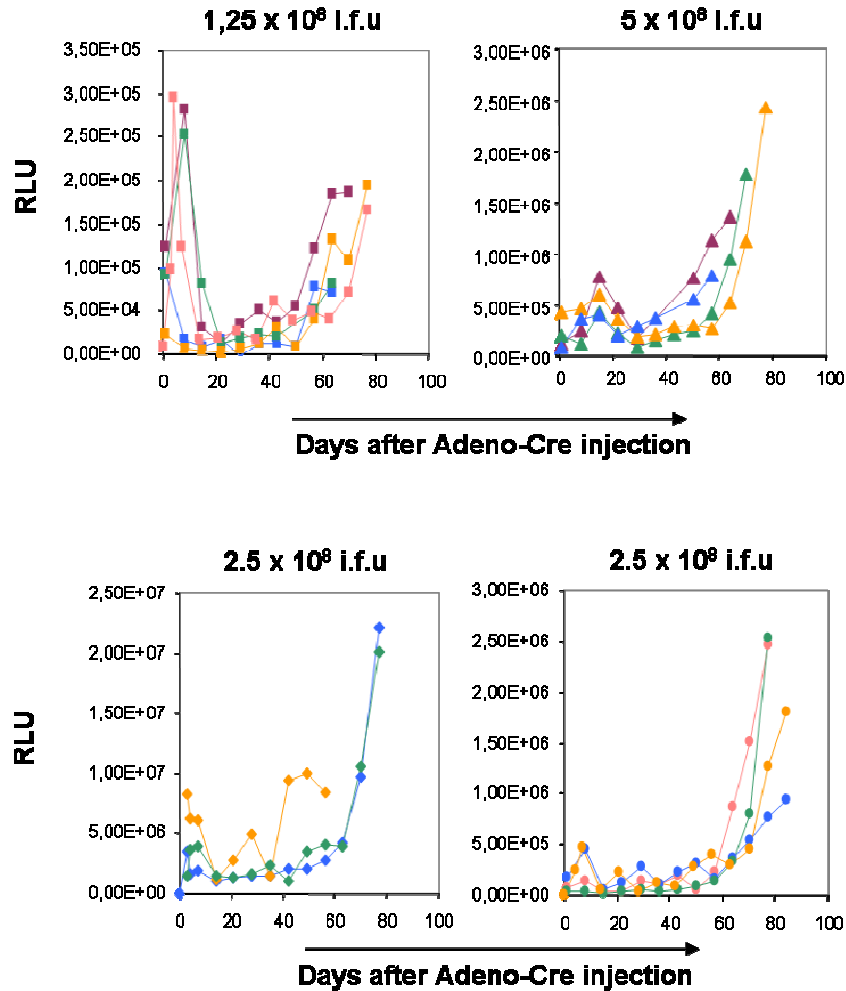
Figure 23 : Luminescence signal evolution in ASCT mice and observation ex vivo

(A) Longitudinal measurement of ASCT induced hepatoma tumor growth from individual mice. Graph depicting the longitudinal measurement of light emission from individual mice after injection of the indicated dose of Adeno-cre. Light emission is expressed as relative light units.

At the final time point, mice were sacrificed and inspected for the presence of tumors. All mice that have shown signal increase displayed large tumor nodules that are luciferase positive in the liver [Fig. 24A]. Large nodules were also observed in the mouse that did not display luminescence signal increase within 60 days after virus injection. Only 2 nodules were luciferase positive [Fig. 24B] and the luminescence signal increase was visible around 80 days after Adeno-Cre injection [Fig. 24C]. We can hypothesize that a majority of cells that were infected with the virus have switch on Tag expression leading to the formation of nodules whereas CBGr99 was kept silent. However, in some cells both transgenes were induced which led to the 2 luciferase positive nodules. In the case of this mouse, the luminescence signal does not efficiently correlate with tumor formation. We have seen here that the probability of having a signal reflecting hepatocarcinoma growth is high (16/17) therefore we can conclude that the ASCT mice serve as a suitable model for hepatocarcinoma monitoring by BLI.
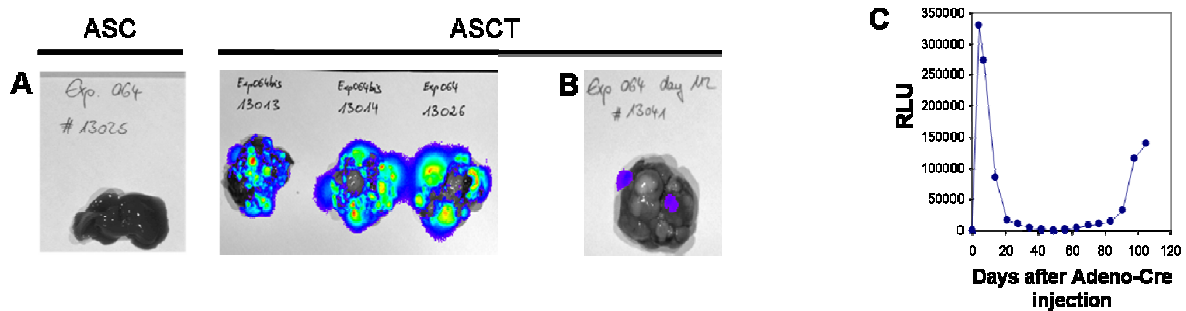
Figure 24 : *Ex vivo* **observation of liver from ASCT mice**

Ex vivo visualization of CBGr99 expressing liver nodules by BLI (A) in the general situation (B) in the mouse 13041. (C) Graph depicting the longitudinal measurement of luminescence signal in the mouse 13041

3. Bioluminescence imaging of tumors in live animals with bacteria encoding luciferase and their usage in tumor therapy

Recent observations in murine models with facultative anaerobic bacteria (Pawelek et al., 1997), as well as data generated more than 30 years ago with obligate anaerobic bacteria (Moese and Moese, 1964), indicate that some bacteria species can preferentially replicate and accumulate within tumors. Making use of BLI, tumor colonization in nude mice has been visualized using *E.coli* and three attenuated pathogens (*Vibrio cholerae, Salmonella typhimurium, and Listeria monocytogenes*) transformed with plasmid encoding the Lux operon (Tani et al., 2004). Starting from these observations, we have investigated whether or not *Vibrio cholerae* (*V.cholerae.lux)* and *E.coli* (*Top10.lux*) expressing the lux operon would also target tumors in immunocompetent mice which are able to mount an immune response against the bacteria. In addition to imaging, we have used *E.coli* expressing luciferase in an inducible fashion as delivery vectors for interleukins (GMCSF; IL-2) in order to enhance elimination of tumors by the immune system.

Visualization of tumors

Subcutaneous model

V.cholerae colonization

To follow tumor targeting by *V.cholerae.lux* in immunocompetent mice, we injected C3H mice (n=5) carrying subcutaneous AG104A fibrosarcoma tumors (~ 500 mm³) with 1×10^8 cells of light emitting *V.cholerae.lux*. 20 minutes after injection of bacteria the luminescence signal was only visible at the anatomical site of the liver. 24 hours later the bacteria were still located in the liver but now a strong luminescence signal was visible at the tumor site suggesting tumor colonization by the bacteria. At day 7, the bacteria had disappeared from the liver, probably due to the immune response whereas the signal intensity from the tumor was increased indicating efficient replication of the bacteria in the tumor. From day 7 on, the signal started to decrease until no luminescence was visible around day 30 [Fig. 25]. In these studies 100% (5/5 mice) of the tumors have been targeted by the bacteria.
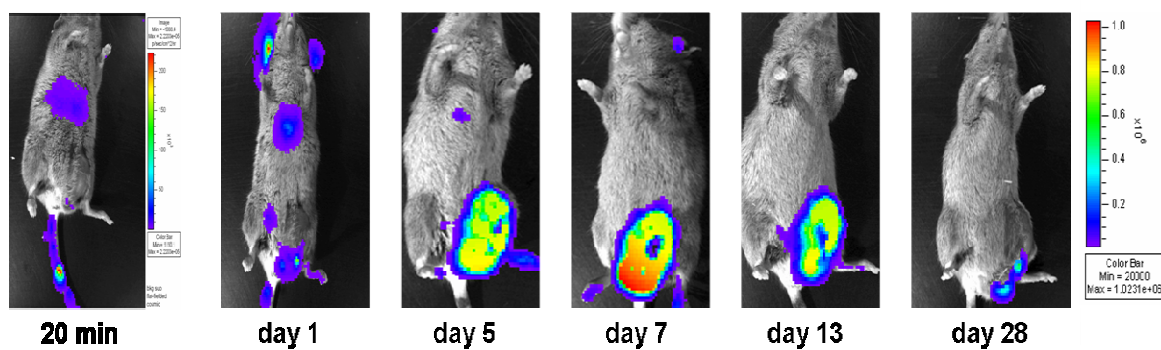
Figure 25 : **Tumor colonization by** *V.cholerae.lux*

AG104A tumor bearing mice (n=5) were infected by intravenous injection of V.cholerae.lux. Mice were imaged at the indicated time point after bacteria infection. Representative animals are shown.

The monitoring of tumor growth showed that V.cholerae.lux does not affect tumor progression [Fig. 26].
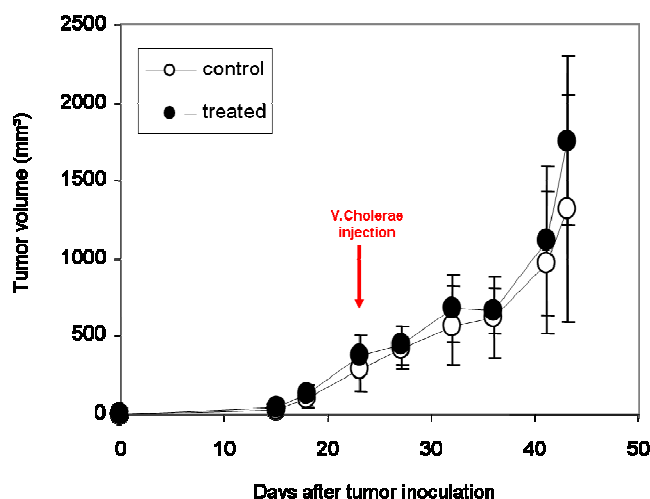
Figure 26 : **Tumor growth of AG104 A tumors after** *V.cholerae* **injection.**

(A) AG104A were s.c. injected into the shaved abdomen of mice. After developing tumors (≈500 mm³), mice were treated as indicated and volumes of the tumors were determined. Points: mean tumor volumes of groups of five mice in a typical experiment. Control: PBS control. Treated: injected with 10^8 V.cholerae cells at indicated time (red arrow).

The plasmid encoding for the *lux* operon is not integrated in the *V.cholerae.lux* genome. Therefore, loss of signal after 28 days may be due to the loss of the plasmid encoding the *lux* operon in absence of antibiotic selection *in vivo*. Alternatively, the immune system may have cleared the bacteria. In order to see if loss of the plasmid would be responsible, we used *E.coli* (*Top10-lux*; provided by Dr. Loessner) that has the *lux* operon stably integrated into their genome. In these bacteria, the lux operon is under the control of the P_{BAD} promoter of the arabinose operon [Fig. 27 A and B] (Lee et al., 1980).

L-arabinose-inducible expression

The ability to express cloned gene under a control condition is often very useful. These systems have been usually generated to have low basal level of expression to minimize the effects of exposing bacteria to toxic gene products during growth. The P_{BAD} promoter is an inducible promoter which turns on the transcription machinery in presence of L-arabinose; in its absence, transcription occurs at very low levels (Lobell and Schleif, 1990). The P_{BAD} promoter is widely used to positively control expression in bacterial culture (Guzman et al., 1995). Together with our collaborators (Dr. Loessner, HZF, Braunschweig), we showed that gene expression could also be induced *in vivo* when L-arabinose is administrated systemically (Loessner et al., 2007a). *Salmonella typhimurium* SL7207 carrying the Fluc or the lux operon under the control of the P_{BAD} promoter were engineered [Fig. 26 A and B] and injected intravenously into mice bearing CT 26 tumor of around 0.5 cm diameter. 3 days after injection of bacteria, we have determined by *in viv*o BLI very low luciferase activity. Intraperitoneal injection of L-arabinose led to a strong induction of luciferase expression that peaks 5 hours after injection [Fig 27 C and D]. These experiments show that the P_{BAD} promoter can be efficiently induced *in vivo* when L-arabinose is administrated systemically.

The lux operon is integrated in the bacterial chromosome whereas the Fluc is transiently express. The lower luminescence intensity observed with the lux operon may be explained by the single copy of lux operon present in the carrier bacteria but also by the different photon yields of the two enzymatic reactions.
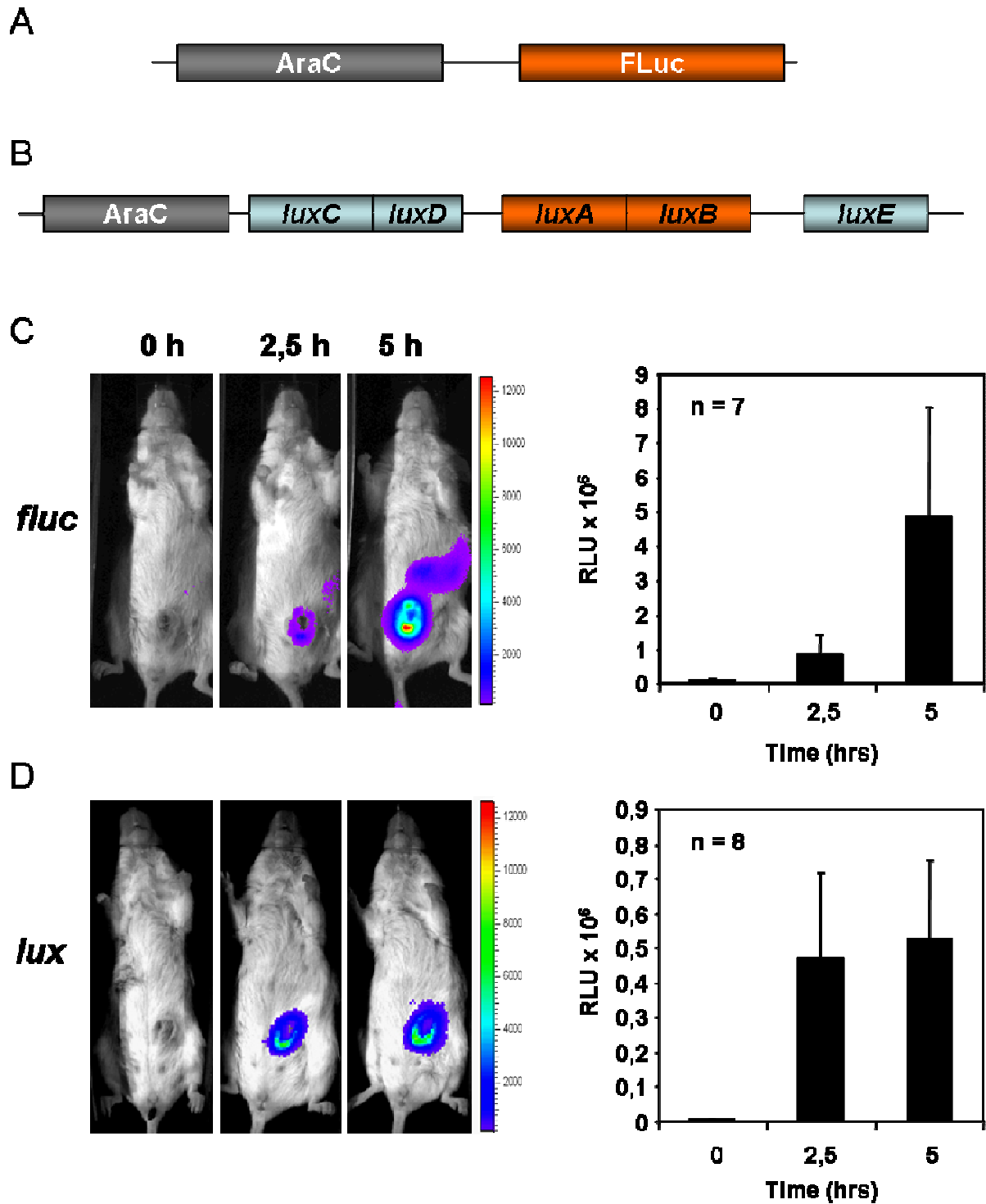
Figure 27 : *In vivo* **BLI of L-arabinose-induced bacterial luciferase**

Representation of the plasmids encoding for the inducble expression of (A) Fluc and (B) lux operon. Tumor bearing mice were infected with S.typhumurium harbouring the inducible (C) Fluc plasmid or (D) the lux operon. 3 days post infection, mice were intraperitoneally injected with 120 mg L-arabinose. Images of mice were acquired before (0 h) or after L-arabinose administration at the indicated time points. Representative mouse is presented.

Top10.*lux* tumor colonization

E.coli bacteria (*Top10.lux*) that have the lux operon under the control of the P_{BAD} promoter integrated in the bacterial chromosome. The use of these bacteria allowed us to investigate whether tumor colonization is transient. C3H mice bearing AG104A tumors (~ 500 mm³) were i.v injected with *Top10.lux* and tumor colonization was followed by *in vivo* BLI of the mice 5 hour after L-arabinose injection. Monitoring of the mice (n=10) showed again an initial increase of the luminescence which started to decrease in the tumors after about 6 days [Fig. 28A]. The luminescence signal peaked around day 6 and became non-visible around day 14. The complete clearance of the *Top10.lux* luminescence signal suggests that the bacteria were eliminated by the host's immune system. The single *lux* operon copy due to the chromosomal integration may explain the lower light intensity observed with *Top10.lux* in comparison to *V.cholerae.lux* where the plasmid encoding for the lux operon is transiently expressed [Fig. 28B]. Thereby, the earlier clearance of the luminescence signal observed with Top10.lux may be explained by a low luminescence signal which could not be detected or by a difference of colonization capacity between the 2 strains. Again, tumor colonization by bacteria was observed in all mice. No effect on tumor growth was observed [Fig. 27C].
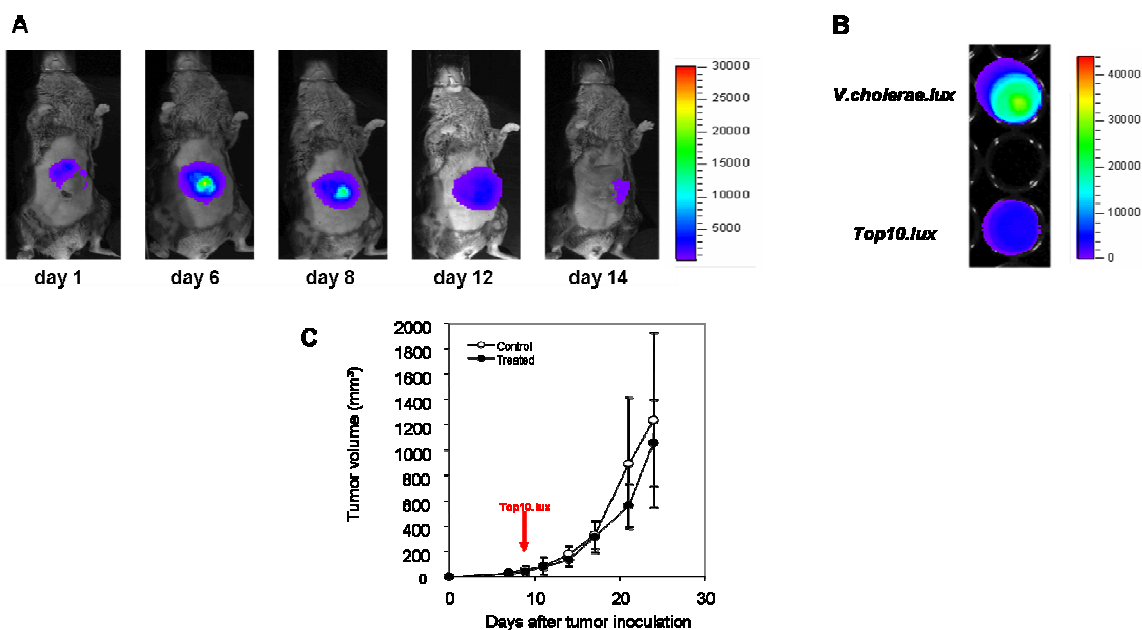
Figure 28 : *In vivo* **BLI of AG104A colonization by** *Top10.lux*

(A) AG104A tumor bearing mice were infected by i.v injection of Top10.lux and imaged at the indicated time point. Representative animals are shown. Imaging was performed 5 hours after i.p administration of 120 mg of L-arabinose. (B) 10⁸ bacteria of the indicated strain were imaged to compare their light emission (C) AG104A tumor cells were injected s.c in mice. After development of tumors (~500 mm³), mice were treated as indicated and volumes of the tumors were determined. Points: mean tumor volumes of groups of five mice in typical experiments. Control: PBS control. Treated: injected with 10⁸ Top10.lux cells at indicated time (red arrow).

To ensure that the tumor targeting by bacteria is not only restricted to the AG104A fibrosarcoma we have performed similar experiments in additional tumor models namely the RMA and B16 tumors [Fig. 29]. These experiments have shown here that bacteria are able to target and to transiently colonize all transplantable tumors investigated so far. In all cases tumor colonization by bacteria had no effect on tumor growth (data not shown).
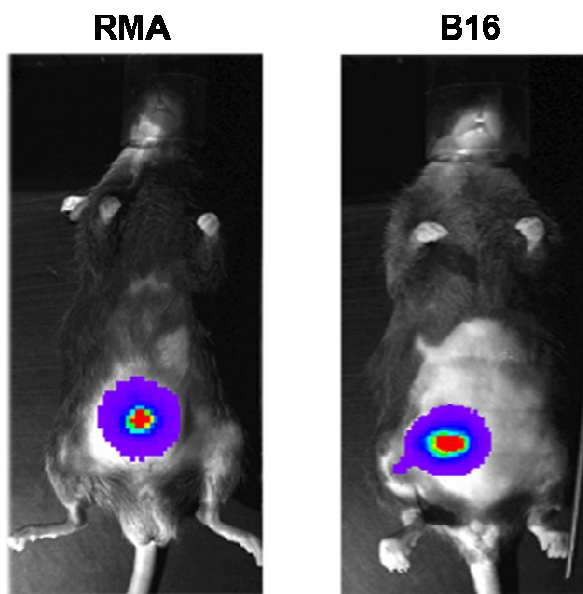
Figure 29 : *In vivo* **BLI of tumor colonization by** *Top10.lux*

(A) Tumor bearing mice were infected by intravenous injection of Top10.lux. Mice were imaged at the indicated time point after bacteria infection. Representative animals are shown. Imaging was always performed 5 hours after intraperitoneal administration of 120 mg of L-arabinose.

Following these observations we focused on the use of bacteria as a carrier to target immunostimulatory proteins, such as interleukins, to tumors. However, most bacterial systems for the presentation of recombinant proteins rely on the expression of proteins in the cytoplasm of bacterial carriers; the proteins are thus only accessible to the host immune system upon disintegration of the bacteria. As an alternative to cytoplasmic protein expression, several systems for exporting proteins from the cytoplasm of live-attenuated bacterial vaccines have been developed. Therefore, we have produced bacteria that efficiently secrete interleukins to allow their contact with the targeted cells.

Bacteria secreting interleukin

Usually recombinant proteins are expressed intracellularly in bacteria. To allow secretion of these proteins into the tumor environment, a secretory system needs to be used which allows protein secretion through the bacterial membrane. Secretion of recombinant proteins in Gram-negative bacteria requires specific translocation of the exoprotein across the inner and outer membrane and depends on naturally occurring secretion systems. Gram-negative bacteria have evolved five basic protein secretion mechanisms, which are classified as type I to type IV secretion systems and autotransporters, also referred to as type V secretion systems (Henderson et al., 2000; Lory, 1998). The type I secretion systems combine a number of features that make them superior to other secretion systems for recombinant protein delivery (Binet et al., 1997). Among the type I secretion systems the *Escherichia coli* HlyA system is currently the only protein exporter which has been developed to a versatile and universally applicable secretory expression system (Gentschev et al., 1996).

The Hly secretion system.

The plasmid-encoded HlyA secretion system initially characterized by Goebel and coworkers (Hess et al., 1990; Vogel et al., 1988) comprises four structural genes, organized in a single transcriptional unit. Besides the genes for HlyA (*hlyA*), the ABC translocase (*HlyB*), and the membrane fusion proteins component (*HlyD*), the operon encodes an acetylase (*hlyC*) required for posttranscriptional activation of HlyA [Fig. 30A]. The operon is transcribed from a promoter complex (P_{hly}) upstream of the Hly C. The secretion signal (HlyAs) necessary for recognition of the target protein by the HlyA secretion machinery is located at the C-terminal end of the HlyA, comprising the last 61 amino acids [Fig. 30A]. Since the secretional signal does not become released during the secretion process, proteins adapted to hemolysin-mediated transport are generally secreted as fusion proteins, carrying a C-terminal extension of 61 amino acids. In our study we have fused different interleukins with the HlyAs secretion signal for extracellular delivery [Fig. 30B].

A

B
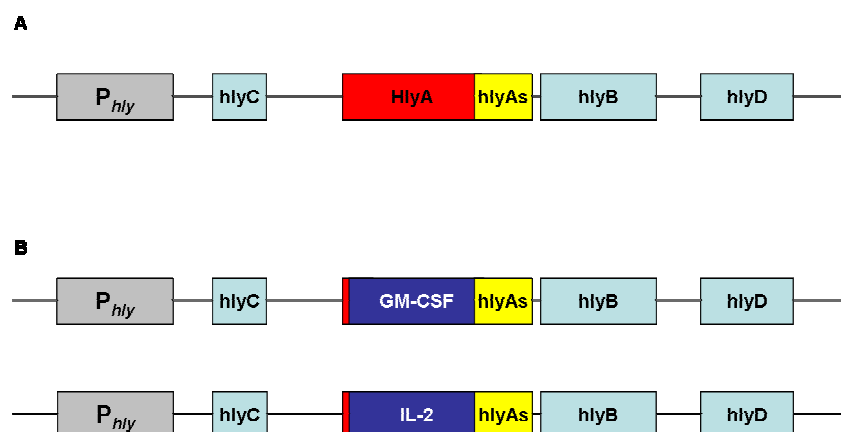
Figure 30 : **Construction of GM-CSF and IL-2 fused to hlyAs.**

(A) Representation of the plasmid encoding for secretion of hemolysin A. (B) Representation of plasmids encoding for the secretion of GM-CSF-HlyAs and IL-2-HlyAs fusion proteins.

Interleukins

Since its initial discovery (Morgan et al., 1976), cytokine based immunotherapy has been vigorously and extensively investigated for cancer treatment. However, so far most cytokine-based therapy trials have not fulfilled the expectations. One of main obstacles is the difficulty of achieving therapeutically relevant dosages in patients without generating excessive tissue toxicity. Deliverance of cytokines locally with a bacterial carrier has the potential of generating sustained high local concentration of immunostimulatory cytokine without raising the systemic levels of cytokines, which is responsible for most of the observable toxicity. Interleukin-2 (IL-2) and Garanulocyte-Macrophage Colony Stimulating Factor (GM-CSF) are two potential candidates for immunotherapeutic studies. IL-2 stimulates natural killer cells, preactivates cytotoxic T cells, B cells and macrophages (Smith, 1988). When administrated at very high doses as a single agent, IL-2 was capable of inducing tumor regressions in certain model systems *in vivo* (Donohue et al., 1984; Rosenberg et al., 1985). Whereas GM-CSF has an effect on a number of cell types including monocytes, dendritic cells, eosinophils, and neutrophils (Burgess et al., 1977; Sieff et al., 1985). In preclinical and clinical studies, GM-CSF secreted from tumor cells has been shown to be a potent stimulator of antitumor responses (Dranoff et al., 1993; Sampson et al., 1996; Soiffer et al., 1998; Yu et al., 1997). The consensus from these studies suggests that GM-CSF stimulates antigen presenting cells such as dendritic cells to generate potent immune responses. Hence both interleukins are known to be biologically active without glycosylation (DeLamarter et al., 1985; Sato et al., 1993) which is of importance for bacterial expression as they are not able to carry out mammalian glycosylation and other protein modifications.

GM-CSF construct

GM-CSF cDNA was inserted in a pILH-1 plasmid encoding for the secretion apparatus of *E.coli* hemolysin. The sequence encoding mouse GM-CSF was amplified by PCR using pGMCSF2a plasmid (Dr.S.Weiss; Braunschweig) as template and oligonucleotide F-bfrBI-GM-CSF as forward primer and the oligonucleotide 2.R-PacI-GM-CSF, containing a part of the sequence encoding for the C-terminal of HlyA, as a reverse primer. Digestion of the resulting PCR product with *NsiI* and *PacI* followed by its ligation in pILH-1 plasmid digested with the same enzyme resulted on the pIHL-GM-CSF plasmid.

IL-2 construct

IL-2 cDNA was amplified by PCR using pBlue-IL-2 plasmid as template and oligonucleotide F-RI-HlyA-IL2 as forward primer and the oligonucleotide R-RI-PacI as a reverse primer. Digestion of the resulting PCR product with *NsiI* and *PacI* followed by its ligation in pILH-GM-CSF plasmid digested with the same enzyme resulted on the pIHL-IL-2 plasmid.

Secretion of interleukin in Top10 bacteria.

To verify secretion of GM-CSF-HlyAs and IL2-HlyAs, culture supernatants of recombinant *Top10.lux* carrying the respective plasmid were concentrated and analyzed by Western blotting. In both cases, a specific monoclonal antibody detected a protein band having the expected molecular mass, whereas no specific signal could be found in the supernatants of the untransformed *Top10.lux* strain. All bands displayed the expected molecular weight [Fig. 31]. Therefore, we have successfully produced two recombinant bacteria strains that conditionally express the *lux* operon and efficiently secrete GM-CSF (*Top10.lux*.GM-CSF) and IL-2 (*Top10.lux*.IL-2).
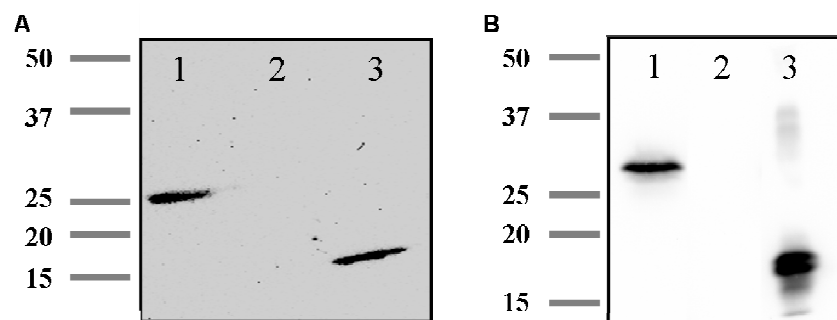
Figure 31 : **Interleukin secretion by *Top10.lux* bacteria.**
(A) Western blot analysis of bacterial supernatant from Top10.lux.GM-CSF. Lane: 1, GM-CSF-HlyAs (25,7 kDa); 2, Top10.lux supernatant; 3, recombinant GM-CSF (14,8 kDa). (B) Western blot analysis of bacterial supernatant from Top10.lux.IL-2. Lane: 1, Il-2-HlyAs (29,1 kDa); 2, Top10.lux supernatant; 3, recombinant Il-2 (15,4 kDa).

Tumor studies with GM-CSF secreting E.coli

The antitumor activity of *Top10.lux*.GM-CSF was determined in C3H mice bearing 500 mm³ (~ day 9) AG104A tumors. 10^8 bacteria were administrated intravenously 3 times at intervals of 72 h and mice were evaluated by BLI for tumor colonization 24 h after each injection of bacteria. Although in all mice colonization with bacteria was observed, the tumor growth was similar to the untreated group and to the group treated with *Top10.lux* [Fig. 32A]. As GM-CSF is believed to enhance the recruitment of dendritic cells to the tumor site and to subsequently increase antigen presentation, we have thought to use the AG104A-Tag cell line that expresses a strong tumor antigen namely Tag. C3H mice bearing 500 mm³ AG104-Tag tumors were treated with 3 intravenous administrations of bacteria as described above. Again tumor colonization was observed in all mice. In the *Top.lux*.GM-CSF group tumor growth was retarded at the day 4 of treatment in comparison to the *Top.lux* and untreated mice. Out of

5 mice, 2 have completely rejected the tumor, whereas the others had a slower growth [Fig. 32B]. These results suggested that treatment with bacteria secreting GM-CSF was efficient to reject tumor in a therapeutic vaccination setting. However, the results obtained with the AG104A-Tag tumor were not reproducible. As shown, in Figure 32C, in subsequent experiments a decreased tumor growth was also observed in tumor bearing mice treated with *Top.lux*. (e.g. in the absence of interleukin). Therefore, the effect of GM-CSF on tumor growth is questionable in this model. The experiment shown in figure 32C suggested that the bacteria themselves might be responsible for the delay in tumor growth.
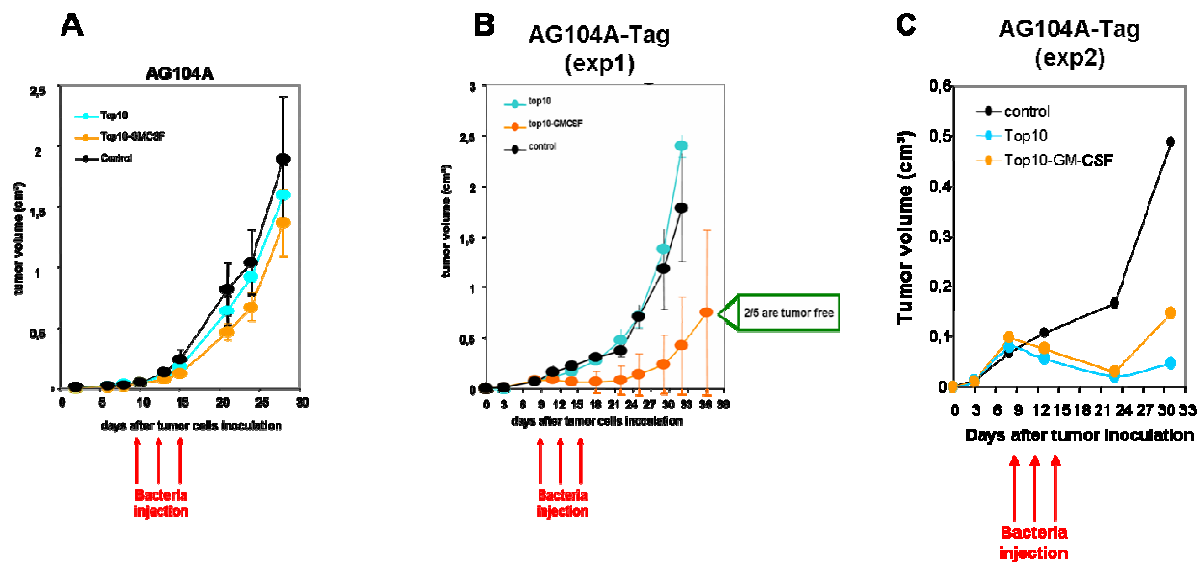
Figure 32 : **Treatment of developing fibrosarcoma by injection of bacteria**

 (A) AG104A and (B) and (C) AG104A-Tag cells were s.c. injected into the shaved abdomen of mice. After developing tumors (≈500 mm^3), mice were treated as indicated and volumes of the tumors were determined. Points: mean tumor volumes of groups of five mice in a typical experiment.

85

Spontaneous tumor model

Alb-Tag model

In section § 3.1, we have shown that bacteria expressing the lux operon can efficiently colonize all transplantation tumors investigated so far. Next, we wished to investigate whether or not autochthonous tumors could also be visualized by luminescent bacteria. A murine model (Alb-Tag) for hepatocellular carcinoma was previously developed in our laboratory (Ryschich et al., 2006). Transgenic mice expressing the Tag oncogene under the control of the albumin promoter/enhancer develop highly vascularized liver cancers. A major advantage of this model over transplanted tumors is that Tag-induced tumors develop spontaneously within the liver. Tumor development is characterized by formation of several adenoma nodules in the liver. A disadvantage of this model is that tumor growth is not visible from the outside.

We have thought to inject light-emitting bacteria in Alb-Tag mice to see whether they will target tumor nodules and thereby allow their visualization. 12 weeks old Alb-Tag mice were intravenously injected with 1×10^8 *V.cholerae.lux* and monitored over the time. As previously shown in the transplantable model, all mice have a luminescence signal originating from the liver as early as 20 min after injection of bacteria [Fig. 33A]. At day 5, 55 % of the mice (5/9) displayed a signal from liver nodules. The signal increased until a maximum which was reached between day 6 and 9, and then gradually decreased and disappeared between day 14 and 21. It has already been shown in this tumor model that mice develop several nodules in the liver. Importantly, only few regions of the liver lighted up (3 mice with 1 signal [Fig. 32A] and 2 mice with 2 distinct signals [Fig. 33B]). The mice that remained negative were rechallenged with bacteria at a late tumor stage. Although, they carried large tumors, none of them has shown tumor targeting [Fig. 33C]. These results show that despite the presence of large tumors in Albumin-Tag mice, tumor targeting by bacteria as determined by BLI is not as efficient as in subcutaneous transplantation tumor models.
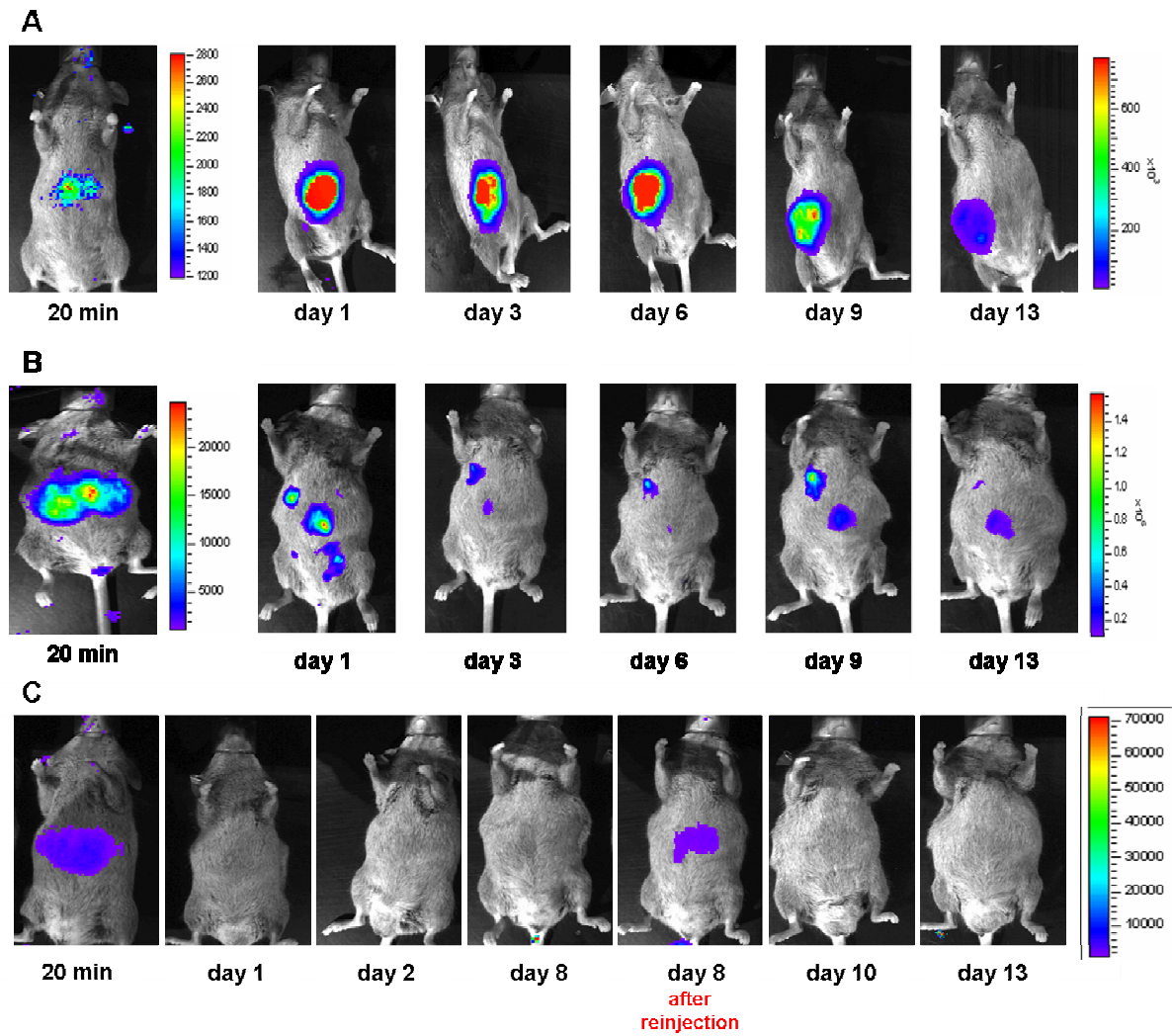
Figure 33 : *In vivo* **BLI of tumor colonization by** *V.cholerae.lux* **in the Alb-Tag model**

Tumor bearing mice were infected by intravenous injection of V.cholerae.lux. Mice were imaged at the indicated time point after bacteria infection. 3 representative animals are shown.

RIP-Tag-5 model

We have also investigated whether or not *V.cholerae.lux* could target tumors in a spontaneous insulinoma model, namely in RIP.Tag-5 mice, expressing the oncogene Tag under control of the rat insulin promotor in the beta-islets of the pancreas. Tag expression starts at the age of 10 weeks and leads in a multistep fashion to formation of hyperplastic islets and to the development of solid insulinoma at about 25 weeks of age (Hanahan, 1985). 7 months old RIP-Tag-5 mice were intravenously injected with 1.10^8 *V.cholerae.lux*. The usual luminescence signal originating from the liver after i.v injection of bacteria is visible 35 min after injection of bacteria. The mice (n=3) were monitored over a period of 3 days and none of the 3 injected RIP-Tag-5 mice were displaying a luminescence signal [Fig. 34]. Here, we have observed that *V.cholerae.lux* does not target tumor in the RIP-Tag-5 model.

Figure 34 : *In vivo* **BLI of tumor colonization by** *V.cholerae.lux* **in the RIP-Tag-5 model**
Tumor bearing mice were infected by intravenous injection of V.cholerae.lux. Mice were imaged at the indicated time point after bacteria infection. A representative animal is shown.

Her2-Neu model

Finally, we studied whether spontaneous developing mammary carcinomas are targeted by *Top10.lux*. The Her-2/neu transgenic (neu-N) mice that express the HER-2/neu oncogene under tissue-specific transcriptional control of the mouse mammary tumor virus (MMTV-LTR) represent a suitable model of mammary carcinogenesis. These mice develop neu-overexpressing spontaneous mammary carcinomas in a stochastic manner beginning at around 4 months. To see whether bacteria would target the breast tumors in this model, 10^8 *Top10.lux* bacteria were intravenously injected in neu-N mice with advanced tumors (5 months old). One day after injection of bacteria, mice were imaged 5 hours after induction of luciferase expression by L-arabinose. All mice tested (7/7) have shown the typical luminescence signal observed from the liver immediately after bacteria injection. However, only one out of the seven mice displayed a luminescence signal from tumors [Fig. 35]. Importantly, among the 8 mammary tumors that are optically visible only 3 showed colonization by bacteria. Monitoring of bacteria colonization in this mouse showed that the luminescence signal stays quite stable over time in the 3 targeted tumors. The mouse had to be sacrified for ethical reasons which prevented us from following the survival of the bacteria in this model. The luminescent signal intensities are different and implicate that each tumor has a different ability to be colonized by bacteria. Several of the biggest tumors remained luciferase negative which indicates that the colonization capacity of the bacteria is not dependent on the tumor size. The 6 other tumor bearing mice remained negative over time, even after re-injection of bacteria [Fig. 35B]. Thus, colonization of mammary carcinoma in Her-2/neu mice by Top10.lux bacteria appears to be very inefficient.
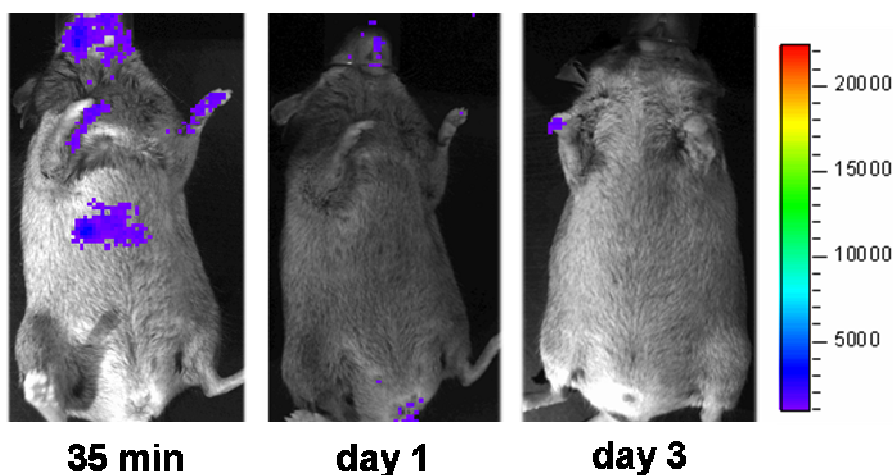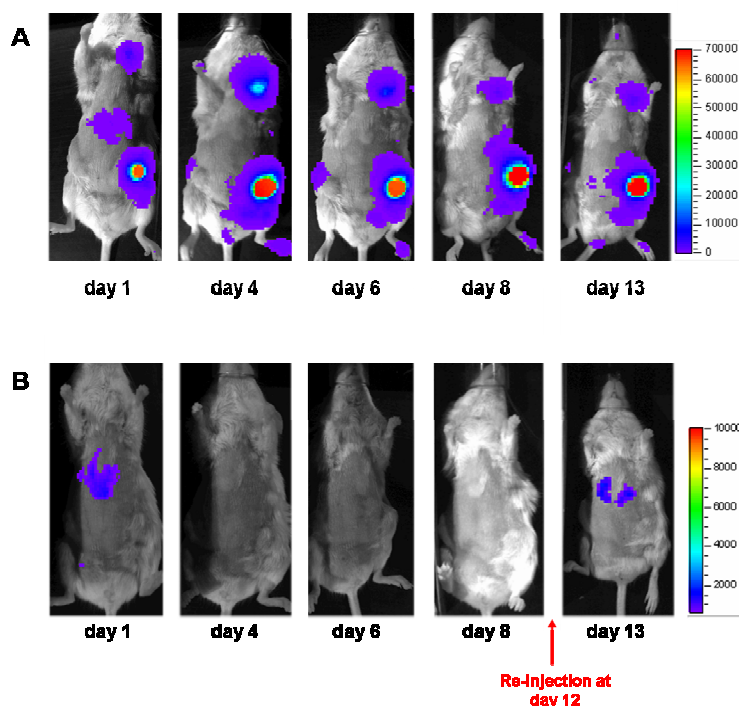
Figure 35 : *In vivo* **BLI of tumor colonization by Top10.lux in the Her-2/neu model**

Tumor bearing mice were infected by intravenous injection of Top10.lux. 5 hours after i.p. administration of L-arabinose mice were imaged at the indicated time point after bacteria infection. (A) The single positive mouse is shown. (B) A representative negative mouse is shown.

In conclusion, using BLI we were able to visualize tumor targeting by *V.cholerae.lux* and *Top10.lux* in immunocompetent mice. However, in subcutaneous transplantation tumors colonization with bacteria was clearly more efficient than in spontaneously developing tumors. These data are summarized in table 3. According to these results bacterial targeting of tumors in patients may not be a promising approach.

Tumor	Origin	Bacteria	Number of mice	Positive (luminescence)
Transplantation tumor models				
AG104A	Fibrosarcoma	*V.cholerae.lux*	10	10
AG104A	Fibrosarcoma	*Top10.lux*	32	32
AG104A.Tag	Fibrosarcoma	*Top10.lux*	43	43
RMA	Lymphoma	*Top10.lux*	17	17
B16	Melanoma	*Top10.lux*	10	10
Autochtonous tumor models				
Albumin-Tag	Hepatoma	*V.cholerae.lux*	9	5*
RIP-Tag	Insulinoma	*V.cholerae.lux*	3	0
Her2/neu	Mammary carcinoma	*Top10.lux*	7	1*

Table 3 : Summary of bacterial targeting and tumor visualization by BLI

* In positive autochthonous tumor mice not all tumor nodules were positive.

4. Generation of a conditional luciferase reporter mouse

Since BLI represents a useful approach for tracking of a cell population *in vivo*, cells expressing luciferase have been generated by transfer of the luciferase gene using retroviral vector (Costa et al., 2001; Kim et al., 2004). However, the use of retroviruses is hampered by the large variation in its transduction efficiency, especially when the genes are to be introduced into primary cells. Infection with retrovirus often requires cell culture and activation which may alter the biological properties of the cells. An alternative approach to *ex vivo* cell labeling by retrovirus is the generation of transgenic mice that ubiquitously express luciferase. Luciferase positive cells can then be transferred with a minimum of *ex vivo* manipulation. To facilitate isolation of cells from the donor animal after monitoring by BLI, a fluorescent protein can be associated to the luciferase. Moreover, it allows multimodality analysis. Luciferase expression can be followed by BLI whereas flow cytometry and immunohistology permit eGFP expression analysis.

Therefore, I wanted to generate a transgenic mouse line that conditionally expresses luciferase and eGFP in all tissues. To this we used an ubiquitous promoter, the chicken-ßActin promoter, to control the expression of an eGFP-2A-CBGr99 cassette. By insertion of a flox STOP cassette between the promoter and the reporter genes, the expression should inducible by Cre recombinase. The mating with Cre deleter mice (Schwenk et al., 1995) would lead to a mouse line, ßactin-eGFP-2A-CBGr99, that ubiquitously expresses GFP and luciferase, whereas, the unrecombined mouse line can be used as reporter mouse for Cre expression.

Generation and Characterization of ßactin-Fstop-eGFP-2a-CBGr99 mouse line

Construct

A targeting construct was engineered for homologous recombination so that upon Cre expression a promoter less eGFP-2A-CBGr99 cassette is activated by an ubiquitously expressed promoter to indicate recombination at a single cell level. A Fstop DNA from pAST plasmid (G.Küblbeck, DKFZ, Heidelberg) was first excised as an *EcoRV–StuI* fragment and ligated into pCMV-eGFP-2A-CBGr99 (see § 1.2.1) cut with *SmaI* to make pCMV-FStop-eGFP-2A-CBGr99. To make pßActin-Fstop-eGFP-2A-CBGr99, pCMV-FStop-eGFP-2A-CBGr99 was cut with *XbaI-HindIII*. The liberated FStop-eGFP-2A-CBGr99 cassette was then ligated into pßactin-16-pl (Dr. C. Probst, ETH Zurich) that has been cut with the same restriction enzymes. Finally, pßActin-Fstop-eGFP-2A-CBGr99 was linearized with *PagI/XbaI* and resuspended into injection buffer prior to injection in oocystes.

Screening of founder mice

The 9 live offspring mice obtained after microinjection C57Bl/6 oocystes were tested for the presence of CBGr99 at 5 weeks of age by Southern blotting (see § 2.2.2.). The 2 positive founders were mated with C57B6/j mice and presence of the transgene in the F1 generation was also checked by Southern blot. For both transgenic lines, the transfer of the transgene to the next generation was observed.

Characterization of ßactin-eGFP-2A-CBGr99 mice

The two transgenic founders were crossed each with a Cre deleter mouse that ubiquitously expresses Cre (Schwenk et al., 1995). BLI was performed from the resultant F1 generation. The results showed that both transgenic lines, denoted ßAc-G2A99/0 and ßAc-G2A99/4 mice, were capable of Cre-dependent luciferase expression [Fig. 36A]. We next measured the difference in bioluminescence from individual tissues by dissecting both transgenic lines after administration of D-luciferin. In the ßAc-G2A99/0 line, we observed that bioluminescence could be switched on in a Cre-dependent manner in all tissues but with variable signal intensities [Fig. 36B]. Brain, thymus, heart, lung, spleen, skin and gut show a strong signal whereas pancreas and lymph nodes have a lower signal and liver and kidney bioluminescence is very weak. Similar observations were made with the second transgenic line, ßAc-G2A99/4, but with much lower signals (results not shown). Therefore we have used the ßAc-G2A99/0 line for subsequent studies.
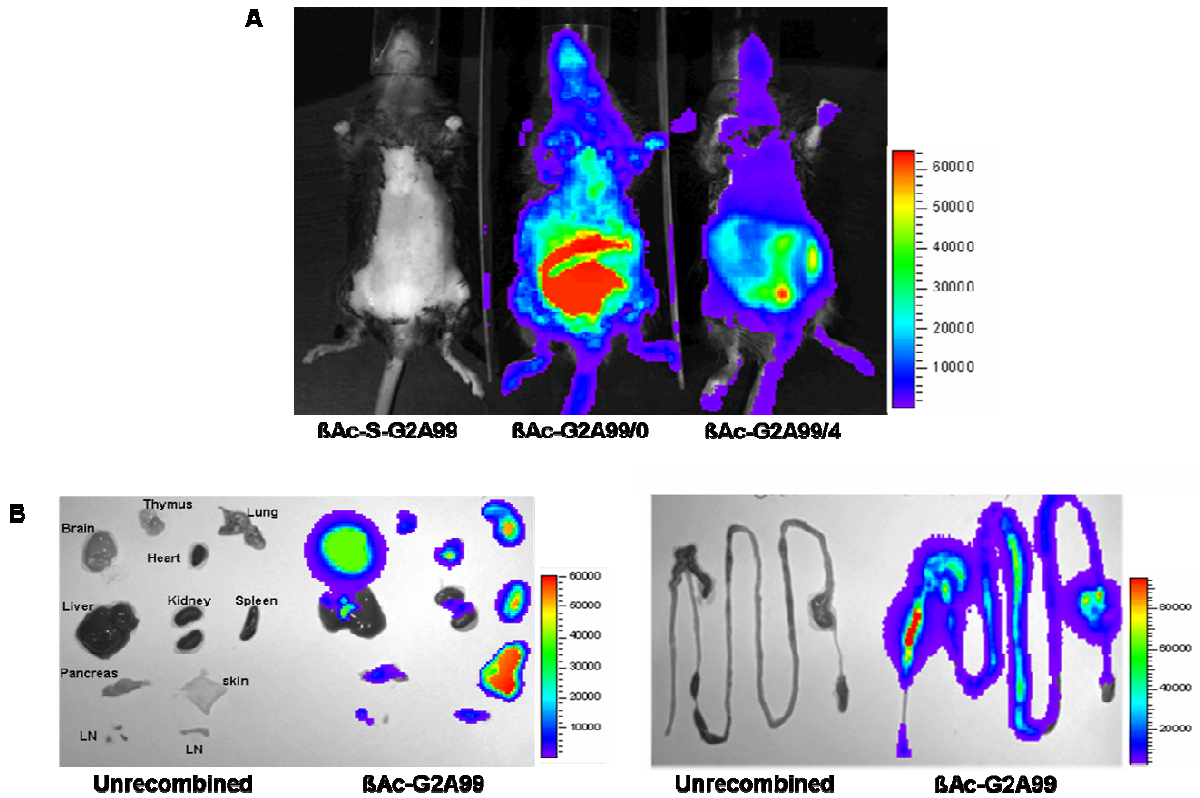
Figure 36 : **Characterization of the ßAc-S-G2A99.**

(A) BLI images of two transgenic lines, ßAc-G2A99, resulting from ßAc-S-G2A99/Cre deleter cross. The mouse in the left is ßAc-S-G2A99, thereby Cre negative, and does not luminesce, whereas the 2 mice in the right are Cre positive and appears to luminesce from all areas of the body (B) Images of organs from recombined and non recombined mice. All organs from the recombined mice luminesce.

93

In order to estimate the sensitivity of detection, splenocytes were imaged *in vitro*. A minimum of 1.25×10^5 splenocytes was required for detection [Fig. 37A]. Since the luciferase signal in lymphocyte appears to be very weak, we asked if transferred cells could be detected in a mouse where tissues absorb most of the emitted photons. Indeed, after transfer of 10×10^6 splenocytes to syngeneic recipients we were not able to see any signal. As the expression of luciferase protein correlates with eGFP expression, splenocytes and peripheral blood cells (PBL) were checked for their eGFP expression. Although the ßactin promoter is supposed to be ubiquitously expressed, Figure 36B shows only a small percentage of the cells express eGFP. Probably this explains the low sensitivity of detection *in vitro* and *in vivo*. From this data we estimate that approximately 2000 eGFP positive splenocytes are detectable *in vitro*. FACS sorting of the small percentage of eGFP positive cells would be too tedious and require too many donor mice. Therefore, and unfortunately, we have to conclude that the ßAc-G2A99/0 is not suitable as universal cell donor.
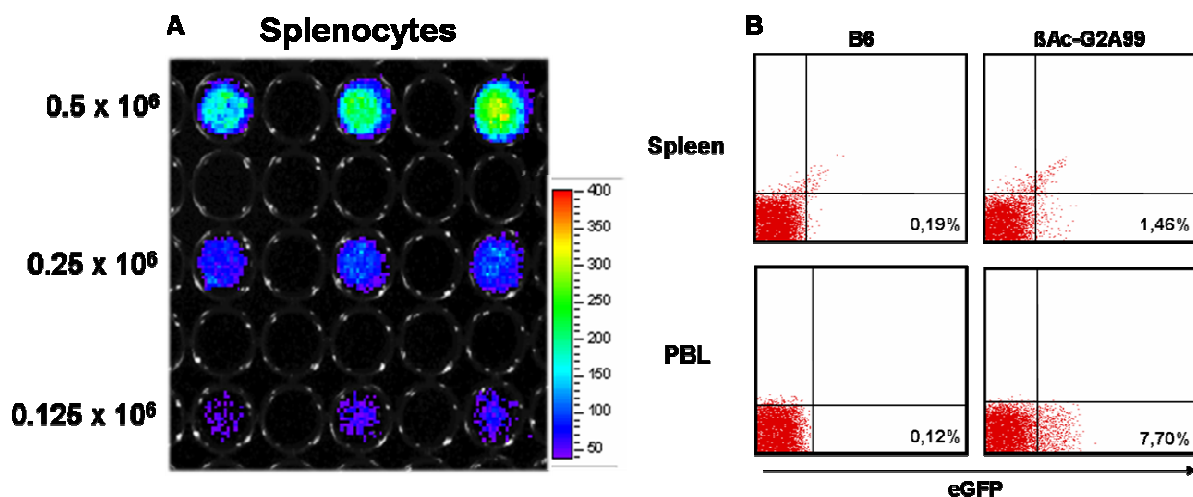
Figure 37 : **Sensitivity of dectection on BLI study *in vitro*.**
(A) Luciferase assay in vitro of splenocytes from 3 individual ßAc-S-G2A99/0 mice. (B) Flow cytometry analysis for eGFP to measure the percentage recombination in splenocytes and in PBL of ßAc-G2A99/0 mice.

Generation and characterization of CAG-CBGr99-2A-mCherry mouse line

As we failed to generate a conditional mouse line that can be used as a source of cells for transfer we envisaged a new transgenic line that constitutively and ubiquitously expresses a CBGr99-2A-mCherry cassette. This cassette contains the CBGr99 luciferase associated to a monomeric red fluorescent protein (mCherry) with the 2A system. The cassette is under the control of a composite promoter that combines the human cytomegalovirus immediate-early enhancer and a modified chicken ß-actin promoter (CAG). The CAG promoter is a very strong and ubiquitous promoter. It has been shown to produce high levels of expression both *in vitro* and *in vivo* (Okabe et al., 1997).

Construct

To make pCAG-CBGr99-2A-mCherry, pCAG-CBGr99-2A-DTR-2A-mCherry (G.Küblbeck, DKFZ, Heidelberg) was cut with *Kpn I* to release the *DTR* gene and then self ligated to obtain the pCAG-CBGr99-2A-mCherry. Finally, pCAG-CBGr99-2A-mCherry was linearized with *PagI/XhoI* and resuspended into injection buffer prior to injection in oocystes.

Screening of founder mice

The 14 live offspring mice obtained after microinjection C57Bl/6 oocystes were tested for the presence of CBGr99 at 5 weeks of age by Southern blotting (see § 2.2.2.). The 2 positive founders were mated with C57B6/n mice. Unfortunately one died during mating. Presence of the transgene in the F1 generation was also checked by Southern blot and transfer of the transgene to the next generation was observed.

Characterization of CAG-CBGr99-2A-mCherry mice

To verify luciferase expression in this transgenic line, denoted CAG-L2Ach, we have performed *in vivo* BLI. The luminescence signal is very strong and leads to the saturation of the CCD camera with an exposure time of 1s [Fig. 38A]. The pattern of luciferase expression was estimated by imaging organs after dissection. All organs displayed luciferase expression with differences on the signal intensity. Thymus, lung, brain, heart, kidneys, skin, pancreas and lymph nodes emitted a very strong luminescence signal whereas liver and spleen signal emission is lower but still intense [Fig. 38B].
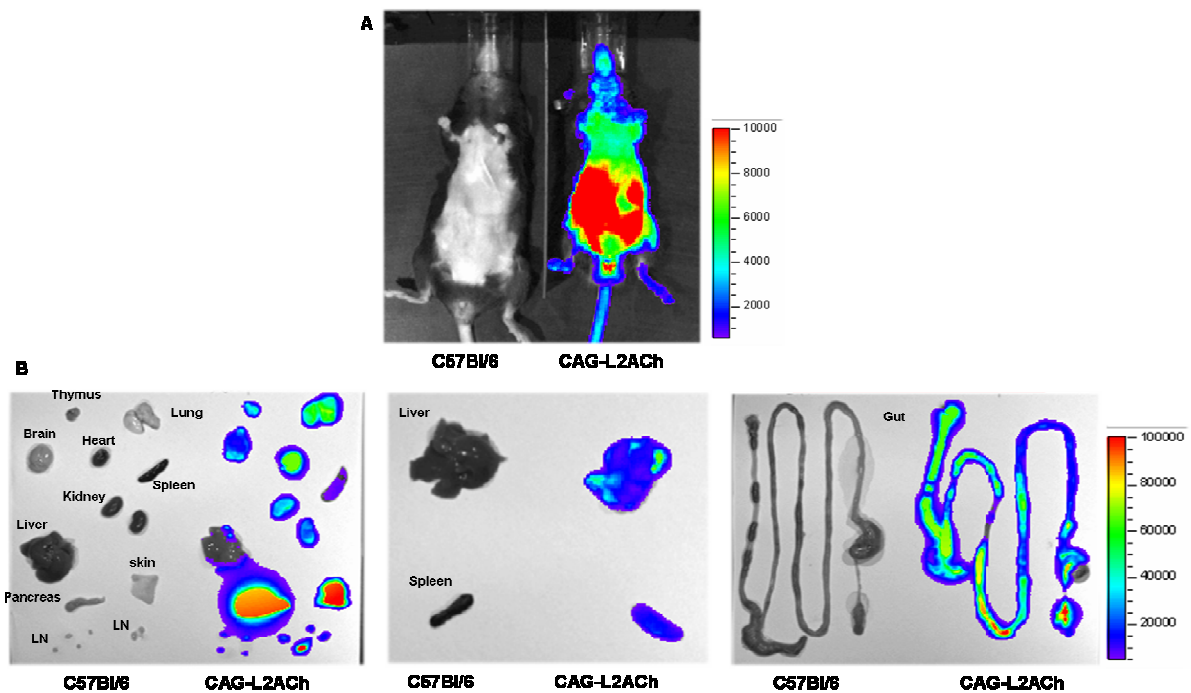
Figure 38 : **Luciferase expression of the CAG-L2ACh transgenic mice**

(A) BLI images of two transgenic lines, CAG-L2ACh. The mouse in the left is C57Bl/6, thereby does not luminesce, whereas the transgenic mouse in the right appears to luminesce from all areas of the body (B) Images of organs from C57Bl/6 and CAG-L2ACh mice. All organs from CAG-L2ACh mice luminesce.

Splenocytes were analyzed by FACS for the expression of the mCherry protein. Again, as it was previously described in the ßAc-G2A99 model, expression of the fluorescent reporter protein is not expressed in all cells. However in the CAG-L2ACh mouse model, approximately 60% of the splenocytes displayed mCherry expression [Fig. 39A], and therefore CBGr99, which is most likely sufficient to perform cell sorting of a defined cell population. We have stained splenocytes with a FITC labeled antibody directed against the T cells specific marker CD3 and showed that they all express mCherry [Fig. 39B].
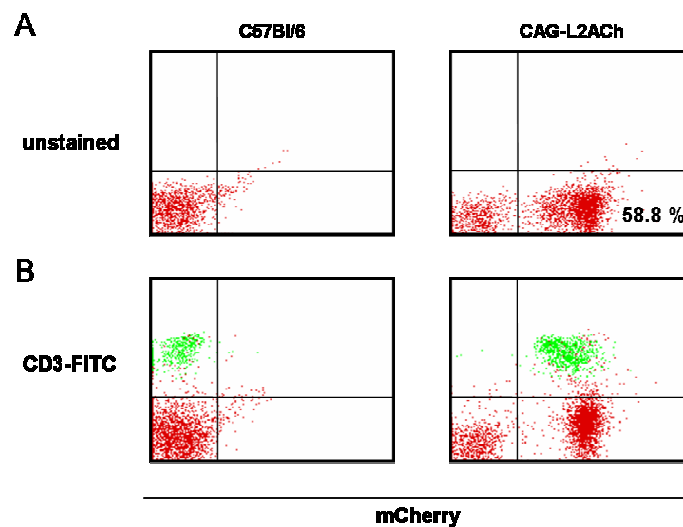
Figure 39 : mCherry expression of the CAG-L2ACh transgenic mice
(A) Flow cytometry analysis of total splenocytes from CAG-L2ACh mice. (B) Flow cytometry analysis of total splenocytes from CAG-L2ACh mice stained with CD3-FITC antibody.

After cell sorting, the CD3 positive cells were serially diluted and imaged to estimate the limit of detection *in vitro*. As shown in Figure 40A, between 2500 and 5000 cells are visible *in vitro*. We were also able to visualize cells *in vivo*. A luminescence signal was observed in the lung, liver and spleen after transfer of 1 x 10^6 CD3 positive cells in C57Bl/6 host [Fig. 40B]. These results indicate that most probably less than 1 x 10^6 T cells located at the same site are detectable by BLI. We conclude that the CAG-L2ACh mice can serve as an universal donor for cell transplantation.
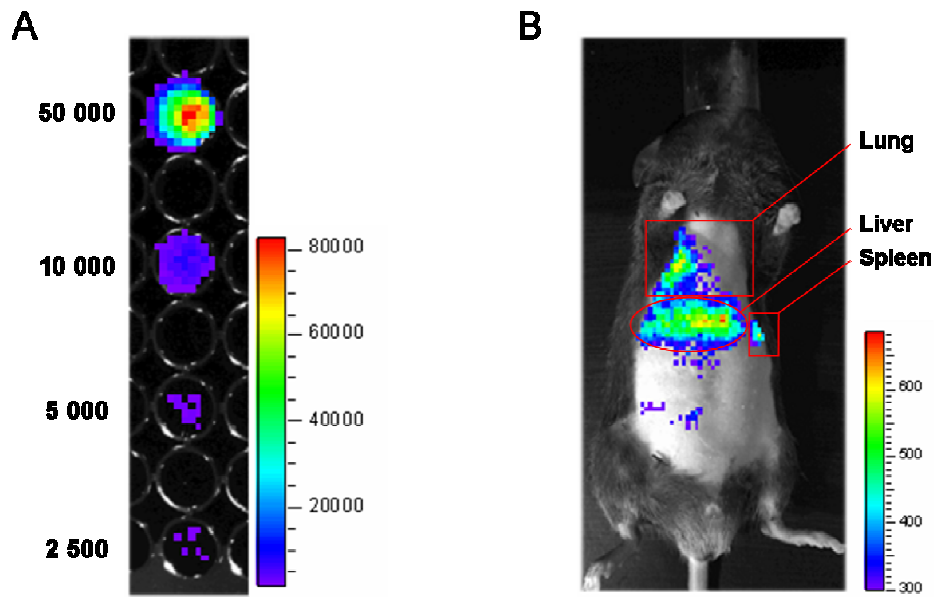
<u>Figure 40 :</u> Determination of BLI sensitivity of T cells from CAG-L2ACh

(A) T cells were diluted from 50 000 to 2500 cells, plated in black 96-well plate, and imaged for 1 minute after the addition of D-luciferin. (B) 1 x 10^6 T cells were intravenously injected in a C57Bl/6 mouse and imaged for 5 min after i.p. administration of D-luciferin.

D.   Discussion

Molecular imaging techniques aim at the visual identification, characterization and quantification of biological processes in a living organism. In contrary to "classical" diagnostic imaging it set for the *in vivo* monitoring of specific molecular and cellular processes such as gene expression, progression or regression of cancer, drug and gene therapy. Many traditional and clinically used imaging techniques, such as MRI, CT, US, PET and SPECT have been adapted in recent years for imaging of small laboratory animal models (Weissleder and Mahmood, 2001). All of these technologies differ in a variety of aspects: spatial and temporal resolution, depth of penetration, availability of the injectable probes and the detection threshold of probes for a given technology. However, the use of optical markers, such as bioluminescent or fluorescent markers, offer several advantages than can be used to refine and accelerate the study of mouse models of disease, cell migration and vector distribution. For example, when a reporter gene is introduced into a cell the gene is replicated with each cell division, therefore the signal is perpetuated over time. Moreover, the instrumentation used for optical imaging allows the imaging of several mice at the same time (up to 5), it is easy to use because specialized imaging technicians are not required and time for acquisition and analysis of the pictures is relatively short. In the field of optical imaging, there are several approaches including fluorescence imaging and bioluminescence imaging (BLI). Bioluminescent reporters include genetically expressed luciferase protein such as bacteria, firefly, red and green click beetle luciferases. Light emission is the result of a chemical reaction involving luciferase, luciferin, ATP and oxygen, therefore no light emission is required. Firefly and red click beetle are generally preferred due to their longer wavelengths which are less absorbed by tissues. Fluorescence reporter does not require luciferin, but instead require excitation light to excite the fluorescent protein. Fluorescent reporters include proteins such as green fluorescent protein (GFP), red fluorescent protein (RFP) and other variants. Luciferase is more representative probe to rapidly changing environmental conditions because these proteins mature rapidly following expression and are relatively short lived, whereas fluorescent protein can take up to several hours to become functional after which they may reside in the cell for many hours (Troy et al., 2004). Another limitation of fluorescence imaging is the higher background signal level due to autofluorescence of tissues compared with bioluminescence. Therefore, we have chosen to develop tools allowing the use of BLI for assessment of tumor growth, bacteria distribution and cell migration studies in mice. We first focus on the selection of the optimal luciferase to use for *in vivo* BLI.

1.   Selection of an optimal luciferase for BLI

BLI is a widely used method for non-invasive measurement of luciferase expression in small research animals. The sensitivity of detection is critical and depends on several factors such as the photon yield of the enzymatic reaction, absorption and scattering of the light by mammalian tissues, and the sensitivity of the detection system. *In vivo* the most important limitation is caused by absorption and scattering of light by tissues which reduce sensitivity and resolution. Whereas scattering of the light is mainly dependent on the tissue composition, absorption depends on the light emission spectrum. Therefore, we have compared various commercially available luciferases to define the most appropriate one for *in vivo* BLI studies. In tissues chromophores like hemoglobin will absorb light. Hemoglobin absorbs mainly in the green and blue part of the light spectrum, whereas less absorption occurs at wavelengths longer than 600 nm. Thus, the red component of the luciferase emission spectra is the most useful one for BLI. Several luciferases have been cloned and optimized for expression in mammalian cells. Fluc is the most commonly used luciferase for BLI. Light emission by Fluc includes a spectral content above 600 nm within a broad-band emission spectrum (530-640 nm) peaking at 612 nm at 37°C (Zhao et al., 2005). The click beetle luciferases, CBGr99, CBGr68 and CBRed, which were recently introduced also catalyze the degradation of D-luciferin allowing their comparison with Fluc. A comparative study of spectral imaging for Fluc and CBRed and CBGr68, has shown that the percentage of light above 600 nm relative to total light output was low for CBGr 68 (~ 15%) while the respective values were higher for CBRed and Fluc (80 % and 64%, respectively) (Zhao et al., 2005). These observations suggested that CBRed and Fluc are better candidates for BLI than CBGr68. However, a quantitative comparison of the total photons yield emitted at the various wavelengths of the spectra especially in the red wavelengths range has not been performed. We have, therefore, compared CBGr99, CBRed and Fluc. CBGr68 displays the same emission spectrum as CBGr99 (Promega), therefore it was not included into the comparative study.

For such studies it is critical that the cells used express equimolar amounts of the different luciferase. In order to achieve equimolar expression, CBGr99, CBRed and Fluc containing bicistronic plasmids were constructed in which CBGr99, CBRed and Fluc is linked to the eGFP sequence via a P2A sequence [Fig. 6]. The 2A peptide impairs the formation of a normal Gly-Pro peptide bound at the end of the 2A peptide consensus peptide without affecting translation of the second protein [Fig. 5] allowing the expression of the 2 proteins in

a stoichiometric manner (Holst et al., 2006). The transfection of MO4 cells with the respective constructs showed that the 2A cleavage is highly efficient (100 %) [Fig.7A]. To confirm that the cleavage leads to a stoichiometric co-expression of the 2 proteins, we have generated stable cells clones for each constructs. In a series of transfectants expressing increasing amounts of eGFP we have observed a strict correlation ($R \sim 0.9$) with the activity of the respective luciferase [Fig. 7B and C]. Altogether, these results show that eGFP and the respective luciferases are equimolary co-expressed. Thereby, eGFP can be use to standardize the expression of luciferases. The selection of stable clones exhibiting the same eGFP expression [Fig. 8] allowed us to compare identical amounts of the luciferases.

The comparison of light emission from the different clones demonstrated that the luciferases have a different kinetics regarding their enzymatic activity [Fig. 9A]. At early time points CBGr99 is clearly superior with regard to the total photon yield. However, the photons emitted in the red part of the emission spectrum (above 600 nm) are the critical photons for *in vivo* BLI as they can efficiently be transmitted through mammalian tissues. Therefore, we measured the red-orange component of the emission spectrum using a DsRed2-1 filter (pass band 575-650). These measurements indicate that in this part of the emission spectrum the photon yield of the enzymatic reaction catalyzed by CBGr99 is higher than that obtained with CBRed in the first 11 minutes and similar at later time points. Fluc clearly emits less photons [Fig. 9B].This observation indicates that despite an emission spectrum which is mainly in the green wavelengths, CBGr99 emits more photons above 600nm than Fluc or CBRed specially in the first minutes. Thus, CBGr99 is potentially useful for *in vivo* BLI.

In order to determine the sensitivity of detection of the respective luciferases *in vivo*, the cells clones expressing the different luciferase were inoculated in different locations, namely subcutaneous, in the peritoneal cavity, or in a highly vascularized organ such as the lung. In the subcutaneous model, CBGr99 produces a higher photon yield over time [Fig.10], which correlates with the *in vitro* results. The absorption of green light appears to be very low in the skin owing to superficial location of the cells as well as the weak presence of hemoglobin in the skin. In the intraperitoneal and in the lung model, cells are located deeper in the animals where the presence of organs and blood vessels lead to a high absorption of photons below 600 nm wavelengths. Consistent with the *in vitro* experiment, at early time points, detection of light emitted by CBGr99 is better [Fig. 11]; probably due a larger emission of red photons. At later time points, the sensitivity of CBGr99 and CBRed are similar; probably because CBRed is producing as many red photons as the CBGr99.

These results demonstrate that for BLI the click beetle luciferases are superior to Fluc which is the most frequently luciferase used for BLI. The comparison of the click beetle luciferases shows that CBGr99 has either a superior or a similar sensitivity *in vivo* as compared to CBRed, depending on the time point of the analysis. Despite the high attenuation of its signal *in vivo*, but owing to its high photon yield, the CBGr99 produces red photons in amounts that are comparable to CBRed. Together with its fast kinetic these properties characterize CBGr99 as a luciferase that is highly suitable for *in vivo* BLI.

CBGr99 is clearly the most sensitive luciferase for *in vivo* BLI. To validate the potential of CBGr99 as a reporter for tumor growth, it was applied to the measurement of growth of transplantation tumors by BLI. First, we have further characterized stable transfectants, denoted MO4/GL2A-10, expressing CBGr99 and Ovalbumin. As it was previously shown with Fluc (Craft et al., 2005), there is a linear correlation between cell number and the photons yield displayed by CBGr99 [Fig. 13B]. Notably, a low number of cells can be detected *in vitro* (100 cells) and *in vivo* (2500 cells subcutaneously) [Fig 13 A and C]. Even if the limit of detection is dependent on several factors including cell line, expression construct, gene copy number and luciferase concentration, these results demonstrate the high sensitivity that can be reached with BLI. Next, in the example of subcutaneous tumor growth of MO4/GL2A-10, we validated the use of CBGr99 as a reporter of tumor growth by direct comparisons of BLI with external caliper measurements [Fig. 15]. Again, high sensitivity of BLI was demonstrated in the subcutaneous tumors where tumors that were not measurable by calipers were quantifiable by photon emissions. BLI imaging of MO4/GL2A-10 injected intravenously has shown the ability to use these cells for the detection of metastasis formation [Fig. 16]. Altogether, we have proved here that, as it was already shown for Fluc (Jenkins et al., 2003), CBGr99 can also be used to assess non invasive tumor growth by BLI.

2.   Generation of autochthonous hepatocarcinoma model for BLI

We have previously shown that CBGr99 can be used to follow subcutaneous tumor development by BLI. However, transplantation tumors in rodents do not reflect the clinical situation. Therefore transgenic mouse models have been developed to closely mimic the sporadic cancer formation as it occurs in humans. In conventional transgenic mouse models tumors develop spontaneously within the targeted organ, but all cells have the capacity to transform. Once eliminated, e.g. by therapeutic intervention, the tumor cells are likely replaced by new transgene expressing cells. Therefore, Cre/loxP conditional mouse models

have been developed. In these models, the tumor growth is induced in a time and spatial dependent manner. This leads to the growth of tumors from few transformed cells within their physiologic environment. These models have proven most useful for furthering our understanding of *in vivo* tumor etiology (Jonkers et al., 2001; Marino et al., 2000). Despite such improved tools for modeling cancer, the often "non-visible" nature of tumorigenesis makes it difficult to follow tumor growth and therapeutic success. Furthermore, as autopsy is often the most effective way to evaluate therapeutic treatment efficacy, longitudinal studies examining the dynamics of tumor responses to treatment become problematic. Consequently, large cohorts of mice are required to generate statistically reliable results. Therefore, conditional tumor models have been adapted to enable noninvasive BLI of tumor development. The first model reported is a mouse model of pituitary cancer. In this model, somatic deletion of the gene encoding for the tumor suppressor protein RB results in the rapid development of a tumors in mice homozygous for a conditional Rb mutation (Vooijs et al., 1998). By crossing these mice with transgenic mouse line that conditionally expresses Fluc in the pituitary gland, the authors have generated a model where tumor development can by monitor by BLI (Vooijs et al., 2002). A similar and more general strategy was to generate a ubiquitously expressing conditional luciferase reporter mouse (LucRep) that can be used to render a wide range of Cre/loxP mouse tumor models suitable for BLI. To demonstrate that the LucRep mouse line could be used to image spontaneous tumor development *in vivo*, the authors have crossed the LucRep mouse with a conditional oncogenic K-ras2 transgenic mouse (Lyons et al., 2003). They have showed that LucRep mice could enable visualization of conditional Kras2-induced lung tumorigenesis by BLI.

In the present thesis, we have generated the first mouse line that conditionally expresses CBGr99 in the liver. By breeding them with a conditional transgenic line expressing the Tag oncogene we have generated a bitransgenic mouse line with which we have investigated the ability of CBGr99 to report hepatocarcinoma growth. An inducible hepatocarcinoma model, named AST, has been developed in the laboratory using the Cre/LoxP system (Stahl, in preparation). In this mouse model expression of the oncogene Tag is initiated by intravenous injection of an adenovirus encoding Cre recombinase. Dose dependent liver tumor formation is achieved by application of different adenovirus doses. In comparison to previous hepatocarcinoma models such as the Albumin-Tag in which tumor development is already observed four weeks after birth (Ryschich et al., 2006), the AST model is closer to the clinical situation of sporadic cancer formation. It allows investigation of different questions such as

the mechanisms of tumor development in the autochthonous environment and also the mechanisms of tolerance induction towards tumors. Moreover, it also constitutes a good model for the evaluation of therapeutic strategies. A major drawback of this model is that the tumor nodules are not directly visible by optical inspection of the mice because the tumors develop in the liver. Until now, the presence of tumors is estimated by the ALT level in the serum which reflects liver damage but does not allow to monitor tumor progression. To render the tumor visible by BLI, we have generated an Albumin-floxstop-CBGr99 (ASC) transgenic mouse line. In ASC mice, the induction of CBGr99 expression is also dependent on Cre recombinase. The albumin promoter results the specific expression of CBGr99 in hepatocytes. Breeding of ASC mice with the AST mice yielded in a double transgenic mouse line (ASCT), in which expression of both transgenes can be induced simultaneously by Adeno-Cre injection.

First we have looked for a potential leakage of the STOP cassette in unrecombined ASC mice. During construction of the AST mice in our laboratory, Dr. Sacher has observed that in some founder lines the STOP cassette is leaky, resulting in transcription of the transgene, albeit in very small amounts (Sacher, 2000). Willimsky *et al.* described also recently that a STOP cassette can be leaky. Briefly, these authors have generated transgenic mouse containing Tag in a silent form due to a STOP cassette separating a ubiquitously active promoter (chimeric ß-actin/ß-globin promoter) from the oncogene. However, this mouse line is able to develop sporadic tumors in the absence of Cre recombinase (Willimsky and Blankenstein, 2005). Hence, unrecombined AST mice displayed tolerance to the Tag antigen. In the particular AST mouse line used in this thesis for the crossing with ASC mice generated here, no leakage of STOP cassette was observed as judged by RT-PCR or by formation of tumor nodules in old unrecombined mice (Stahl, 2004). In the unrecombined ASC and ASCT mice describe here, a low luminescence signal from the liver was observed. Thus the STOP cassette in these mice appears to be leaky [Fig. 20]. BLI of old unrecombined ASCT mice (12 to 14 month old) show that this leakage does not increase with time and age does not lead to spontaneous tumor development. As this signal caused by the leaky cassette is very weak, it does not affect the visualization of tumor growth by BLI, because the signal emitted by tumors is at least 100 times stronger. It is also important to notice that, so far, the ASCT model is the first reported mouse line expressing CBGr99. The leaky STOP cassette is expected to result in tolerance to immunogenic antigens epitopes from the CBGr99 whereby an immune response CBGr99 may be avoided.

We show her that in ASCT mice injection of various doses of adenovirus encoding Cre leads to efficient recombination that can already be observed by BLI one day after virus injection [Fig. 21A]. The strength of the luminescence signal is dependent on dose of adenovirus which is injected. However, the signal intensity does not linearly correlate with viral doses [Fig. 21B]. The liver Kupffer have been shown to take up the adenoviral particles which reduce then the transgene delivery to the hepatocytes (Tao et al., 2001). Therefore, efficient transgene delivery to hepatocytes occurs when the liver Kupffer cells are saturated which could explain the highest luciferase expression per viral particles with high viral doses. Monitoring of induced mice over time shows that tumor growth can be noninvasively followed over time [Fig. 22]. A strong signal increase is observed 40 to 60 days after adenovirus injection [Fig. 23], at a time when hepatoma begin to grow rapidly in Cre induced mice. When in ASC recombination was induced with Cre, the signal intensity reached after recombination stayed constant over time because ASC mice lack the Tag antigen and, therefore do not develop tumors. In order to obtain a good correlation between signal evolution and hepatocarcinoma growth, it is important that the conditional gene, e.g CBGr99 and Tag, present in one hepatocyte are both switched on which results in cells that carry one or more oncogenic lesions together with an activated luciferase reporter. This criterion can be met under two circumstances. First, when CBGr99 is switched on more efficiently than the Tag oncogenes upon recombination. Second, when conditions are created in which all the conditional alleles switch on efficiently in the cell. In the first situation, luciferase will also be switch on in some cells in which no oncogenic lesions have been induced. Because these cells do not clonally expand, they will not provide an appreciable contribution to the signal and thereby tumor growth can still be monitored efficiently. The fact that a majority of ASCT mice (16/17) showed a good signal increase indicating tumor growth, suggests that in most of the hepatocytes both transgenes were simultaneously switched on. If Tag is switched on more efficiently than CBGr99 upon recombination, the luminescence signal will not properly report tumor growth, as it may have occurred in the 1 out of 17 mice [Fig. 24], which showed tumor growth but no increase of increase of the luminescence signal around day 40.

In conclusion, the ASCT model represents a physiological system for sporadic tumor formation in a tolerant environment, as it occurs in humans. In addition, the ASCT model has the advantage to allow monitoring of tumor growth by BLI. Thereby, it constitutes an attractive model to evaluate vaccination efficacy in mice without using a large cohort of animals.

3. Bioluminescence imaging of tumors in live animals with bacteria encoding luciferase and their usage in tumor therapy

The use of mouse models to understand bacterial infections and for testing efficacy of antibiotics has been well established. In addition, BLI has been use to follow the fate of bacteria in mice (Contag et al., 1995; Hamblin et al., 2002; Hamblin et al., 2003). The first report of monitoring disease progression in living mice using bioluminescence was conducted using infection by *Salmonella typhimurium* (Contag et al., 1995). The virulence of three different strain of *Salmonella typhimurium* expressing the lux operon was compared by *in vivo* BLI. A subsequent study has used *Vibrio cholerae*, *Salmonella typhimurium*, *Listeria monocytogenes* and *E.coli* DH5α carrying the lux operon to show that survival and replication of bacteria in a tumor could be localized and followed in real time by BLI (Yu et al., 2004). These observations were made in nude mice bearing human tumors. However, nude mice lack a functional immune system. Therefore, in the present thesis, we have investigated the ability to visualize by BLI *V.cholerae* tumor colonization in immunocompetent mice, which have a functional immune system and therefore the capacity to eliminate the bacteria.

To this end, C3H mice bearing subcutaneous tumors e.g. AG104A fibrosarcoma were injected intravenously with *V.cholerae.lux*. 20 minutes after injection, the bacteria were visible in the liver by BLI. After day 1, bacteria were found to be localized in the tumor where their growth could be visualized by an increase of light emission. The luminescence signal intensity reached a peak at about 1 week after injection and then decreases until it becomes non-visible around day 28 [Fig. 25]. In the experiments using nude mice bearing tumors, it has been estimated that one week after bacterial injection approximately 20% of the *V.Cholerae.lux* population retained the plasmid DNA *in vivo* (Yu et al., 2004). Even if the loss of luminescence signal seems to be due loss of the plasmid encoding the lux operon in the absence of antibiotic selection, we cannot exclude that bacterial clearance by the immune system occurs in immunocompetent mice. To address this issue, we have repeated the experiment using *E.coli Top10.lux* strain. This recombinant *E.coli* strain was generated by transposon-mediated integration of the luciferase operon into the bacterial chromosome in order to improve stability and to create a strain that remain bioluminescent in the absence of antibiotic selection. Moreover, in the *E.coli Top10.lux* strain, the luciferase expression is under the control of the inducible P_{BAD} promoter (Loessner et al., 2007b). The P_{BAD} promoter from the arabinose operon of *E.coli* can be activated by the sugar L-arabinose and is widely

108

used to positively control expression in bacterial cultures (Guzman et al., 1995). Together with Dr. Loessner, we were able to show that the inducible P_{BAD} promoter driving the expression of either Fluc or the lux operon in *Salmonella.lux* can be switched on *in vivo* by intraperitoneal injection of L-arabinose [Fig. 27] (Loessner et al., 2007b). 3 days after infection of CT26 tumor bearing mice with *Salmonella.lux*, we could show that intraperitoneal administration of L-arabinose leads to a strong induction of luciferase expression peaking 5 hours after induction.

To monitor the colonization of *Top10.lux* in C3H bearing subcutaneous tumors (AG104A), mice were injected intraperitoneally with L-arabinose and imaged 5 hours later. One day after intravenous injection of *Top10.lux* bacteria the luminescence signal was located in the tumor area and increased until day 6 followed by a decrease until being non-visible around day 14 [Fig. 28] suggesting that tumor colonization by bacteria is a transient phenomenon. Hence, it is likely that the kinetics of tumor colonization is dependent on the bacterial strain. Indeed, *V.cholerae.lux* was observable until day 28 whereas *Top10.lux* signal was already absent at day 14 in the same tumor model. The colonization of tumors by *Top10.lux* was also visualized in other subcutaneous tumor models such as B16 and RMA [Fig. 29]. However, neither *V.cholerae.lux* [Fig. 26] nor *Top10.lux* [Fig. 28C] has affected the growth of tumor in these experiments. Nonetheless, all subcutaneous tumor models that we have studied, so far, were efficiently targeted by bacteria. Therefore, we envisaged to use bacteria as a carrier of therapeutic genes to the tumor sites.

The ideal bacterial vector would be a vector that combines the following advantages (i) non-toxic to the host, (ii) the replication takes place only in the tumor (iii) they are slowly eliminated by the host. In other studies several recombinant strains of *Salmonella typhimurium* were engineered for DNA delivery of therapeutic genes like endostatin (Lee et al., 2004) and TSP-1 (encoding Thrombospondin-1) (Lee et al., 2005) or genes products expressed by the bacteria including HSV1-TK (Soghomonyan et al., 2005), cytosine deaminase (Cunningham and Nemunaitis, 2001; Dresselaers et al., 2003; King et al., 2002; Lee et al., 2001b; Nemunaitis et al., 2003). However, a main disadvantage of Salmonella is that they accumulate not only in tumor tissues but also in other organs such as liver and spleen (Pawelek et al., 1997). *Top10* has been shown to specifically target the tumor and to colonize tumors with the same efficiency than Salmonella (Stritzker et al., 2007) therefore it is an ideal vector for delivery of therapeutic genes.

To obtain an antitumoral effect several "therapeutic" genes may be considered, such as cytokines, pro-drug-converting enzymes, and agent toxic to tumor. Here, we have planned to elicit a specific immune response against the tumor. Therefore, we choose to express interleukins in bacteria for enhancement or induction of the immune responses at the tumor site. Interleukins are small proteins or glycoproteins that bind to cell surface receptors and regulate immune cell development, growth, survival, and function. As such, interleukins have been extensively studied as potential therapeutic agents to manipulate the immune response to malignantly transformed cells. Interleukin therapy thus aims at either augmenting the number of immune cells by stimulating growth and survival, or by activating cytotoxicity or interleukin production to boost immune reactivity. Among interleukins that were tested for immunotherapy, GM-CSF and IL-2 have shown to be promising in clinical studies (2002; Donohue et al., 1984; Dummer, 2001; Lafreniere and Rosenberg, 1985; Nemunaitis and Nemunaitis, 2003; Rosenberg et al., 1985; Tani et al., 2004). However, systemic toxicity is a serious issue that limits the application of interleukins in humans (White et al., 1994). A restriction of their expression to the tumor site may diminish their toxicity. It has been shown that both, GM-CSF and IL-2, are still biologically active in absence of glycosylation (DeLamarter et al., 1985; Sato et al., 1993). Therefore, these interleukins seems to be good candidates for expression in bacteria where glycosylation does not occur.

To avoid retention of the "therapeutic" proteins in bacterial inclusion bodies and, in order to maximize their secretion into the tumor milieu, we have used the Hemolysin A secretory system. In gram negative bacteria, recombinant proteins are often expressed in the intracellular compartment because the outer membrane is non-permeable. Therefore, the GM-CSF and IL-2 sequences were inserted into a plasmid encoding for the Hemolysin A secretory system [Fig. 30] which has been shown to be one of the most efficient for secretion of recombinant proteins (Gentschev et al., 1996). *Top10.lux* bacteria expressing the respective plasmids, pIHL-GM-CSF and pIHL-IL-2, were found here to efficiently secrete GM-CSF and IL-2 [Fig. 31]. The resulting *Top10.lux*.GM-CSF and *Top10.lux*.IL-2 recombinant bacteria strains conditionally express the lux operon and secrete GM-CSF and IL-2 through the outer membrane.

For reason of time, the *Top10.lux*.IL-2 bacterial strain has not been tested in the present study. *Top10.lux* bacteria secreting GM-CSF (*Top10.lux*.GM-CSF) were applied in a therapeutic vaccination setting to mice bearing subcutaneous AG104A tumors. Although tumor targeting by the *Top10.lux*.GM-CSF strain was visualized in all mice by BLI, there was no effect on tumor growth [Fig. 32A]. As GM-CSF is believed to enhance recruitment of dendritic cells to tumor site and subsequently increase antigen presentation (Timmerman and Levy, 1999), we have injected the *Top10.lux*.GM-CSF bacteria into mice bearing a tumor expressing a strong antigen, namely Tag (AG104A-Tag). By doing so, we thought to increase the probability for induction of an immune response against the tumor associated antigen. In a first experiment, a delay in tumor growth was visible in mice bearing AG104A-Tag tumors treated with *Top10.lux*.GM-CSF [Fig. 32B]. These data suggested that intravenous administration of *Top10.lux*.GM-CSF may affect the growth of a highly immunogenic tumor. However, in a second experiment the delay in tumor growth was observed in mice i.v. injected with *Top10.lux*.GM-CSF but also in animals receiving the control strain (*Top10.lux*) [Fig. 32C] suggesting that the bacteria by themselves could induce an antitumoral effect. Therefore, the vaccination with *Top10.lux*-GM-CSF has to be investigated in additional tumor models.

The advantage of subcutaneous tumor models is that they allow to perform studies in a relative short period of time but a major disadvantage is that they do not resemble tumorigenesis as it is observed in humans. Therefore, we have examined the tumor colonization by bacteria in spontaneous tumor models that more closely mimic cancer development (see § A.2.2.). The first spontaneous model to be examined was the Albumin-Tag model in which the expression of the oncogene Tag under the expression of the liver specific albumin promoter leads to the formation of several tumor nodules in the liver (Ryschich et al., 2006). When Albumin-Tag mice were injected with *V.cholerae.lux*, tumor colonization was visible by BLI only in 5 out of 9 mice. This is in contrast to the subcutaneous models described above where tumor colonization was observed in all mice (see table 3). Moreover, although Albumin-tag mice develop several tumor nodules in the liver, only few of them were targeted by *V.cholerae.lux* [Fig. 33A and B]. The fact that several Albumin-Tag mice with large hepatocellular carcinoma, remained negative even after several injection of *V.cholerae.lux* [Fig. 33C] indicates that the colonization of tumors in this model is independent on the tumor size. Therefore, the colonization of tumors may depend on the intrinsic properties of each tumor nodules, or depend on the accessibility of the tumor for bacteria. For example, a high local intrinsic pressure, as it is observed in tumors, may prevent

colonization. The second spontaneous model tested here is the RIP.Tag-5 insulinoma model in which expression of the Tag oncogene in the beta-islets of the pancreas leads to the development of solid insulinoma (Hanahan, 1985). None of the injected mice (3/3) displayed a luminescence signal 3 days after *V.cholerae.lux* inoculation [Fig. 34]. Thus V.cholerae probably does not colonize autochthonous insulinoma. Together with the observations made in the Albumin-Tag model, this data suggest that tumor targeting of *V.cholerae.lux* is less efficient in spontaneous tumor models. The third model investigated was the Her2/neu mammary tumor model in which mice develop Neu-overexpressing spontaneous mammary carcinomas in a stochastic manner (Guy et al., 1992). In these mice we investigated tumor colonization by *Top10.lux* bacteria. Tumor homing by the bacteria was observed only in 1 out of 7 injected mice. In this particular mouse, 3 out of 8 tumors displayed a luminescence signal [Fig. 35] indicating that each tumor has a different sensitivity to colonization. Upon reinjection, the remaining 6 Her-2/neu mice bearing advanced tumors remained negative. Thus, colonization of tumors in the Her-2/neu mice appears to be very inefficient.

From the observations made in the different spontaneous tumor models, it is questionable if bacterial vectors would be useful tumor vaccines against cancer. A critical issue is to understand the mechanisms of tumor colonization by bacteria and to improve tumor colonization, e.g. by manipulation of the tumor environment.

4. Generation and characterization of ß-actin-fstop-eGFP-2a-CBGr99 mouse line

The migration of lymphocyte population through the lymphoid organs and tissue targets remains elusive. Some progresses have been made by applying BLI to the study of lymphocyte trafficking *in vivo*. The labeling of effector lymphocytes *in vitro* permits these cells to be imaged by BLI in animals. For example, localization of T cells could be observed by BLI when T cells were transduced with a luciferase reporter gene and injected into mice intraperitoneally or intravenously (Costa et al., 2001; Nakajima et al., 2001). A critical issue in these studies is the introduction of the reporter gene into the cell of interest. Although multiple methods have been used, efficient transduction of reporter genes appears to be most effective via a viral infection method (Kootstra and Verma, 2003). However, this method requires *ex vivo* manipulations that may alter the biological properties of the cells. Therefore, we thought to generate a transgenic mouse line that ubiquitously expresses eGFP and

CBGr99, thus serving as a universal donor for transplantation and trafficking studies. The presence of eGFP facilitates the isolation of the CBGr99 positive cells from the donor animal and can also be used as a marker in fluorescence microscopy or flow cytometry studies. As BLI could also be envisaged to monitor the expression of promoters, we first generated a reporter transgenic mouse line (ßAc-S-G2A99). In the ßAc-S-G2A99, the expression of an eGFP-2A-CBGr99, controlled by the ubiquitous ß-actin promoter and is inducible upon Cre recombination. No background expression of CBGr99 could be detected in ßAc-S-G2A99 mice [Fig. 36A] due to the stop sequence inserted between the reporter and the coding sequence. When the reporter mice was crossed to Cre deleter mice (Schwenk et al., 1995) expressing Cre constitutively in all tissues, the resulting bitransgenic mouse line, named ßAc-G2A99, displayed ubiquitous expression of CBGr99 [Fig. 36B] indicating an efficient excision of the flox STOP cassette. In comparison to the existing reporter line like ROSA26-LacZ (Soriano, 1999) or ßactin-eGFP (Kawamoto et al., 2000), cell staining and preparation of cell suspension, respectively, is not require to report promoter activity. The promoter activity can be estimated by the imaging of the mouse and confirmed by the imaging of the organs after dissection. Therefore, the ßAc-S-G2A99 mouse line is suitable reporter line for the fast screening of promoter activity *in vivo.*

The ubiquitous expression of CBGr99 in the ßAc-G2A99 mouse was transmitted to the following generation, resulting in ubiquitously expressing lines of mice that could be useful as a universal donor of T cells tagged with CBGr99. However, although the signal is strong enough to visualize luminescent organs the sensitivity of detection of splenocytes *in vitro* has been shown to be relatively weak [Fig. 37A]. The absence of luciferase signal in recipient mice that have been transferred with 10×10^6 splenocytes confirmed the low sensitivity of detection (data not shown). The low sensitivity of detection can be explained by the single copy of transgene which remains after Cre recombination but also by the low percentage of cells expressing eGFP and thereby CBGr99. Although the ß-actin promoter is supposed to be ubiquitously expressed only a small percentage of cells express eGFP (1.5 % in the spleen) [Fig. 37B]. Because the ßAc-G2A99 mice were not satisfying, we have envisaged the generation of another transgenic mouse line that could be used as a source of reporter T cells for transplantation. We generated a transgenic mouse line that expresses a CBGr99-2A-mCherry cassette under the control of the Chicken ß-actin promoter and the cytomegalovirus enhancer (CAG). In this mouse line, named CAG-L2ACh, the mCherry protein, a monomeric red fluorescent protein optimized for mammalian expression (Shaner et al., 2004), is a marker

that can be use in fluorescent microscopy and flow cytometry. The characterization of the CAG-L2ACh mouse line has shown that all organs displayed a CBGr99 expression [Fig. 38] mCherry is expressed in around 60 % of splenocytes and, interestingly, in 100 % of the T cells [Fig. 39]. The measurement of the sensitivity of detection of splenocytes has indicated that a minimum of 2500 cells can be detected *in vitro*, and at about 1.10^6 cells distributed in the lung, spleen and liver of recipient mice *in vivo* [Fig. 40]. Therefore, the CAG-L2Ach animals can be used as a source of T cells and other immune cells for their tracking in real time. Respective studies may yield new information about the physiological behavior of various lymphocytes populations in tumor immunology, infectious disease, autoimmunity, and transplantation biology.

E.Conclusion

In conclusion, in this thesis, I have established several tools for *in vivo* BLI for tumor immunology studies. First, the comparison of different commercially available luciferases has shown that the click beetle luciferase CBGr99 displayed the highest photon yield *in vitro* and exhibits a higher sensitivity *in vivo* than the most commonly used luciferase, namely firefly luciferase and another click beetle luciferase, CBRed. We conclude from our studies that CBGr99 is the most suitable luciferase for *in vivo* BLI. Moreover, CBGr99 light emission correlates with cell number and therefore allowed monitoring by BLI of transplantation tumor growth *in vivo*. Based on these studies, by using the Cre/loxP system, I have generated a conditional autochthonous hepatocarcinoma mouse model, designated ASCT, for BLI. In this tumor model, the Tag oncogene and CBGr99 expression are simultaneous switched on and allow monitoring of hepatocarcinoma growth via *in vivo* BLI of CBGr99 expression. The ASCT model will be useful for the testing of therapeutic approaches.

Another approach for visualization of tumor is the use of bacteria as they have been shown to colonize and survive in tumors, probably because the tumor microenvironment constitutes an immune privileged site for bacteria. For respective studies that are published in the literature, transplantation tumors have been employed. Using bacteria expressing bacterial luciferase, the lux operon, we could show that *E.coli Top10* and *V.cholerae* indeed efficiently colonize a number of transplantation tumors in immunocompetent mice, thereby allowing BLI visualization of these tumors. However, the efficiency of tumor colonization was found to be much less frequent in spontaneous mouse tumor model, such as the hepatoma model. Because spontaneous tumor model are closer to the clinical situation than transplantable tumors it is questionable whether bacteria vectors are indeed promising and easy approach for tumor targeting in patients.

For tumor immunological studies one would like to monitor not only the growth of tumors, as describe above, but also to follow the fate of tumor specific T cells by non-invasive techniques. Therefore, a transgenic mouse was generated in which CBGr99 and mCherry are ubiquitously expressed, thereby allowing visualization of transferred T cells by BLI. This mouse will be useful for the visualization by BLI of T cell proliferation, migration and infiltration in tumors.

F. References

Bachiller, D., and Ruther, U. (1990). Inducible expression of the proto-oncogene c-fos in transgenic mice. Archiv fur Geschwulstforschung *60*, 357-360.

Binet, R., Letoffe, S., Ghigo, J.M., Delepelaire, P., and Wandersman, C. (1997). Protein secretion by Gram-negative bacterial ABC exporters--a review. Gene *192*, 7-11.

Bjerknes, R., Neslein, I.L., Myhre, K., and Andersen, H.T. (1990). Impairment of rat polymorphonuclear neutrophilic granulocyte phagocytosis following repeated hypobaric hypoxia. Aviation, space, and environmental medicine *61*, 1007-1011.

Bradl, M., Klein-Szanto, A., Porter, S., and Mintz, B. (1991). Malignant melanoma in transgenic mice. Proceedings of the National Academy of Sciences of the United States of America *88*, 164-168.

Brasier, A.R., Tate, J.E., and Habener, J.F. (1989). Optimized use of the firefly luciferase assay as a reporter gene in mammalian cell lines. BioTechniques *7*, 1116-1122.

Brinster, R.L., Chen, H.Y., Messing, A., van Dyke, T., Levine, A.J., and Palmiter, R.D. (1984). Transgenic mice harboring SV40 T-antigen genes develop characteristic brain tumors. Cell *37*, 367-379.

Burns, S.M., Joh, D., Francis, K.P., Shortliffe, L.D., Gruber, C.A., Contag, P.R., and Contag, C.H. (2001). Revealing the spatiotemporal patterns of bacterial infectious diseases using bioluminescent pathogens and whole body imaging. Contributions to microbiology *9*, 71-88.

Coley, W.B. (1991). The treatment of malignant tumors by repeated inoculations of erysipelas. With a report of ten original cases. 1893. Clinical orthopaedics and related research, 3-11.

Contag, C.H., Contag, P.R., Mullins, J.I., Spilman, S.D., Stevenson, D.K., and Benaron, D.A. (1995). Photonic detection of bacterial pathogens in living hosts. Molecular microbiology *18*, 593-603.

Contag, C.H., Spilman, S.D., Contag, P.R., Oshiro, M., Eames, B., Dennery, P., Stevenson, D.K., and Benaron, D.A. (1997). Visualizing gene expression in living mammals using a bioluminescent reporter. Photochemistry and photobiology *66*, 523-531.

Conti, E., Franks, N.P., and Brick, P. (1996). Crystal structure of firefly luciferase throws light on a superfamily of adenylate-forming enzymes. Structure *4*, 287-298.

Cook, S.H., and Griffin, D.E. (2003). Luciferase imaging of a neurotropic viral infection in intact animals. Journal of virology *77*, 5333-5338.

Cormier, M.J., Prasher, D.C., Longiaru, M., and McCann, R.O. (1989). The enzymology and molecular biology of the Ca2+-activated photoprotein, aequorin. Photochemistry and photobiology *49*, 509-512.

Costa, G.L., Sandora, M.R., Nakajima, A., Nguyen, E.V., Taylor-Edwards, C., Slavin, A.J., Contag, C.H., Fathman, C.G., and Benson, J.M. (2001). Adoptive immunotherapy of experimental autoimmune encephalomyelitis via T cell delivery of the IL-12 p40 subunit. J Immunol *167*, 2379-2387.

Cunningham, C., and Nemunaitis, J. (2001). A phase I trial of genetically modified Salmonella typhimurium expressing cytosine deaminase (TAPET-CD, VNP20029) administered by intratumoral injection in combination with 5-fluorocytosine for patients with advanced or metastatic cancer. Protocol no: CL-017. Version: April 9, 2001. Human gene therapy *12*, 1594-1596.

Dang, L.H., Bettegowda, C., Huso, D.L., Kinzler, K.W., and Vogelstein, B. (2001). Combination bacteriolytic therapy for the treatment of experimental tumors. Proceedings of the National Academy of Sciences of the United States of America *98*, 15155-15160.

de Wet, J.R., Wood, K.V., DeLuca, M., Helinski, D.R., and Subramani, S. (1987). Firefly luciferase gene: structure and expression in mammalian cells. Mol Cell Biol *7*, 725-737.

DeLamarter, J.F., Mermod, J.J., Liang, C.M., Eliason, J.F., and Thatcher, D.R. (1985). Recombinant murine GM-CSF from E. coli has biological activity and is neutralized by a specific antiserum. The EMBO journal *4*, 2575-2581.

Dobbelstein, M., Arthur, A.K., Dehde, S., van Zee, K., Dickmanns, A., and Fanning, E. (1992). Intracistronic complementation reveals a new function of SV40 T antigen that co-operates with Rb and p53 binding to stimulate DNA synthesis in quiescent cells. Oncogene *7*, 837-847.

Donohue, J.H., Rosenstein, M., Chang, A.E., Lotze, M.T., Robb, R.J., and Rosenberg, S.A. (1984). The systemic administration of purified interleukin 2 enhances the ability of sensitized murine lymphocytes to cure a disseminated syngeneic lymphoma. J Immunol *132*, 2123-2128.

Doyle, T.C., Burns, S.M., and Contag, C.H. (2004). In vivo bioluminescence imaging for integrated studies of infection. Cellular microbiology *6*, 303-317.

Dranoff, G., Jaffee, E., Lazenby, A., Golumbek, P., Levitsky, H., Brose, K., Jackson, V., Hamada, H., Pardoll, D., and Mulligan, R.C. (1993). Vaccination with irradiated tumor cells engineered to secrete murine granulocyte-macrophage colony-stimulating factor stimulates potent, specific, and long-lasting anti-tumor immunity. Proceedings of the National Academy of Sciences of the United States of America *90*, 3539-3543.

Dresselaers, T., Theys, J., Nuyts, S., Wouters, B., de Bruijn, E., Anne, J., Lambin, P., Van Hecke, P., and Landuyt, W. (2003). Non-invasive 19F MR spectroscopy of 5-fluorocytosine to 5-fluorouracil conversion by recombinant Salmonella in tumours. British journal of cancer *89*, 1796-1801.

Edinger, M., Sweeney, T.J., Tucker, A.A., Olomu, A.B., Negrin, R.S., and Contag, C.H. (1999). Noninvasive assessment of tumor cell proliferation in animal models. Neoplasia (New York, NY *1*, 303-310.

Foster, F.S., Zhang, M.Y., Zhou, Y.Q., Liu, G., Mehi, J., Cherin, E., Harasiewicz, K.A., Starkoski, B.G., Zan, L., Knapik, D.A., *et al.* (2002). A new ultrasound instrument for in vivo microimaging of mice. Ultrasound in medicine & biology *28*, 1165-1172.

Furth, P.A., St Onge, L., Boger, H., Gruss, P., Gossen, M., Kistner, A., Bujard, H., and Hennighausen, L. (1994). Temporal control of gene expression in transgenic mice by a tetracycline-responsive promoter. Proceedings of the National Academy of Sciences of the United States of America *91*, 9302-9306.

Germann, U.A., Gottesman, M.M., and Pastan, I. (1989). Expression of a multidrug resistance-adenosine deaminase fusion gene. J Biol Chem *264*, 7418-7424.

Gould, S.J., and Subramani, S. (1988). Firefly luciferase as a tool in molecular and cell biology. Analytical biochemistry *175*, 5-13.

Greer, L.F., 3rd, and Szalay, A.A. (2002). Imaging of light emission from the expression of luciferases in living cells and organisms: a review. Luminescence *17*, 43-74.

Guy, C.T., Webster, M.A., Schaller, M., Parsons, T.J., Cardiff, R.D., and Muller, W.J. (1992). Expression of the neu protooncogene in the mammary epithelium of transgenic mice induces metastatic disease. Proceedings of the National Academy of Sciences of the United States of America *89*, 10578-10582.

Guzman, L.M., Belin, D., Carson, M.J., and Beckwith, J. (1995). Tight regulation, modulation, and high-level expression by vectors containing the arabinose PBAD promoter. Journal of bacteriology *177*, 4121-4130.

Hamblin, M.R., O'Donnell, D.A., Murthy, N., Contag, C.H., and Hasan, T. (2002). Rapid control of wound infections by targeted photodynamic therapy monitored by in vivo bioluminescence imaging. Photochemistry and photobiology *75*, 51-57.

Hamblin, M.R., Zahra, T., Contag, C.H., McManus, A.T., and Hasan, T. (2003). Optical monitoring and treatment of potentially lethal wound infections in vivo. The Journal of infectious diseases *187*, 1717-1725.

Hanahan, D. (1985). Heritable formation of pancreatic beta-cell tumours in transgenic mice expressing recombinant insulin/simian virus 40 oncogenes. Nature *315*, 115-122.

Henderson, I.R., Nataro, J.P., Kaper, J.B., Meyer, T.F., Farrand, S.K., Burns, D.L., Finlay, B.B., and St Geme, J.W., 3rd (2000). Renaming protein secretion in the gram-negative bacteria. Trends Microbiol *8*, 352.

Hess, J., Gentschev, I., Goebel, W., and Jarchau, T. (1990). Analysis of the haemolysin secretion system by PhoA-HlyA fusion proteins. Mol Gen Genet *224*, 201-208.

Holst, J., Vignali, K.M., Burton, A.R., and Vignali, D.A. (2006). Rapid analysis of T-cell selection in vivo using T cell-receptor retrogenic mice. Nature methods *3*, 191-197.

Jonkers, J., Meuwissen, R., van der Gulden, H., Peterse, H., van der Valk, M., and Berns, A. (2001). Synergistic tumor suppressor activity of BRCA2 and p53 in a conditional mouse model for breast cancer. Nature genetics *29*, 418-425.

Karttunen, J., Sanderson, S., and Shastri, N. (1992). Detection of rare antigen-presenting cells by the lacZ T-cell activation assay suggests an expression cloning strategy for T-cell antigens. Proceedings of the National Academy of Sciences of the United States of America *89*, 6020-6024.

Kim, Y.J., Dubey, P., Ray, P., Gambhir, S.S., and Witte, O.N. (2004). Multimodality imaging of lymphocytic migration using lentiviral-based transduction of a tri-fusion reporter gene. Mol Imaging Biol *6*, 331-340.

Kimura, N.T., Taniguchi, S., Aoki, K., and Baba, T. (1980). Selective localization and growth of Bifidobacterium bifidum in mouse tumors following intravenous administration. Cancer research *40*, 2061-2068.

King, I., Bermudes, D., Lin, S., Belcourt, M., Pike, J., Troy, K., Le, T., Ittensohn, M., Mao, J., Lang, W.*, et al.* (2002). Tumor-targeted Salmonella expressing cytosine deaminase as an anticancer agent. Human gene therapy *13*, 1225-1233.

Kohwi, Y., Imai, K., Tamura, Z., and Hashimoto, Y. (1978). Antitumor effect of Bifidobacterium infantis in mice. Gann = Gan *69*, 613-618.

Kootstra, N.A., and Verma, I.M. (2003). Gene therapy with viral vectors. Annual review of pharmacology and toxicology *43*, 413-439.

Lakso, M., Sauer, B., Mosinger, B., Jr., Lee, E.J., Manning, R.W., Yu, S.H., Mulder, K.L., and Westphal, H. (1992). Targeted oncogene activation by site-specific recombination in transgenic mice. Proceedings of the National Academy of Sciences of the United States of America *89*, 6232-6236.

Lee, C.G., Kinoshita, K., Arudchandran, A., Cerritelli, S.M., Crouch, R.J., and Honjo, T. (2001a). Quantitative regulation of class switch recombination by switch region transcription. J Exp Med *194*, 365-374.

Lee, C.H., Wu, C.L., and Shiau, A.L. (2004). Endostatin gene therapy delivered by Salmonella choleraesuis in murine tumor models. The journal of gene medicine *6*, 1382-1393.

Lee, C.H., Wu, C.L., and Shiau, A.L. (2005). Systemic administration of attenuated Salmonella choleraesuis carrying thrombospondin-1 gene leads to tumor-specific transgene expression, delayed tumor growth and prolonged survival in the murine melanoma model. Cancer gene therapy *12*, 175-184.

Lee, J.H., Heffernan, L., and Wilcox, G. (1980). Isolation of ara-lac gene fusions in Salmonella typhimurium LT2 by using transducing bacteriophage Mu d (Apr lac). Journal of bacteriology *143*, 1325-1331.

Lee, K.C., Zheng, L.M., Margitich, D., Almassian, B., and King, I. (2001b). Evaluation of the acute and subchronic toxic effects in mice, rats, and monkeys of the genetically engineered and Escherichia coli cytosine deaminase gene-incorporated Salmonella strain, TAPET-CD, being developed as an antitumor agent. International journal of toxicology *20*, 207-217.

Leeper-Woodford, S.K., and Mills, J.W. (1992). Phagocytosis and ATP levels in alveolar macrophages during acute hypoxia. American journal of respiratory cell and molecular biology *6*, 326-334.

Lemmon, M.J., van Zijl, P., Fox, M.E., Mauchline, M.L., Giaccia, A.J., Minton, N.P., and Brown, J.M. (1997). Anaerobic bacteria as a gene delivery system that is controlled by the tumor microenvironment. Gene therapy *4*, 791-796.

Lipford, G.B., Hoffman, M., Wagner, H., and Heeg, K. (1993). Primary in vivo responses to ovalbumin. Probing the predictive value of the Kb binding motif. J Immunol *150*, 1212-1222.

Lobell, R.B., and Schleif, R.F. (1990). DNA looping and unlooping by AraC protein. Science (New York, NY *250*, 528-532.

Loessner, H., Endmann, A., Leschner, S., Westphal, K., Rohde, M., Miloud, T., Hammerling, G., Neuhaus, K., and Weiss, S. (2007a). Remote control of tumour-targeted Salmonella enterica serovar Typhimurium by the use of l-arabinose as inducer of bacterial gene expression in vivo. Cell Microbiol.

Loessner, H., Endmann, A., Leschner, S., Westphal, K., Rohde, M., Miloud, T., Hammerling, G., Neuhaus, K., and Weiss, S. (2007b). Remote control of tumour-targeted Salmonella enterica serovar Typhimurium by the use of L-arabinose as inducer of bacterial gene expression in vivo. Cellular microbiology *9*, 1529-1537.

Lorenz, W.W., McCann, R.O., Longiaru, M., and Cormier, M.J. (1991). Isolation and expression of a cDNA encoding Renilla reniformis luciferase. Proc Natl Acad Sci U S A *88*, 4438-4442.

Lory, S. (1998). Secretion of proteins and assembly of bacterial surface organelles: shared pathways of extracellular protein targeting. Curr Opin Microbiol *1*, 27-35.

Luker, G.D., Bardill, J.P., Prior, J.L., Pica, C.M., Piwnica-Worms, D., and Leib, D.A. (2002). Noninvasive bioluminescence imaging of herpes simplex virus type 1 infection and therapy in living mice. J Virol *76*, 12149-12161.

Luo, X., Li, Z., Lin, S., Le, T., Ittensohn, M., Bermudes, D., Runyab, J.D., Shen, S.Y., Chen, J., King, I.C.*, et al.* (2001). Antitumor effect of VNP20009, an attenuated Salmonella, in murine tumor models. Oncology research *12*, 501-508.

Lyons, S.K., Meuwissen, R., Krimpenfort, P., and Berns, A. (2003). The generation of a conditional reporter that enables bioluminescence imaging of Cre/loxP-dependent tumorigenesis in mice. Cancer research *63*, 7042-7046.

Malmgren, R.A., and Flanigan, C.C. (1955). Localization of the vegetative form of Clostridium tetani in mouse tumors following intravenous spore administration. Cancer research *15*, 473-478.

Mandl, S., Schimmelpfennig, C., Edinger, M., Negrin, R.S., and Contag, C.H. (2002). Understanding immune cell trafficking patterns via in vivo bioluminescence imaging. Journal of cellular biochemistry *39*, 239-248.

Marino, S., Vooijs, M., van Der Gulden, H., Jonkers, J., and Berns, A. (2000). Induction of medulloblastomas in p53-null mutant mice by somatic inactivation of Rb in the external granular layer cells of the cerebellum. Genes & development *14*, 994-1004.

Marton, I., Johnson, S.E., Damjanov, I., Currier, K.S., Sundberg, J.P., and Knowles, B.B. (2000). Expression and immune recognition of SV40 Tag in transgenic mice that develop metastatic osteosarcomas. Transgenic research *9*, 115-125.

Massoud, T.F., and Gambhir, S.S. (2003). Molecular imaging in living subjects: seeing fundamental biological processes in a new light. Genes & development *17*, 545-580.

Masumori, N., Thomas, T.Z., Chaurand, P., Case, T., Paul, M., Kasper, S., Caprioli, R.M., Tsukamoto, T., Shappell, S.B., and Matusik, R.J. (2001). A probasin-large T antigen transgenic mouse line develops prostate adenocarcinoma and neuroendocrine carcinoma with metastatic potential. Cancer research *61*, 2239-2249.

Meighen, E.A. (1993). Bacterial bioluminescence: organization, regulation, and application of the lux genes. Faseb J *7*, 1016-1022.

Meighen, E.A., and Dunlap, P.V. (1993). Physiological, biochemical and genetic control of bacterial bioluminescence. Advances in microbial physiology *34*, 1-67.

Moese, J.R., and Moese, G. (1964). Oncolysis by Clostridia. I. Activity of Clostridium Butyricum (M-55) and Other Nonpathogenic Clostridia against the Ehrlich Carcinoma. Cancer research *24*, 212-216.

Morgan, D.A., Ruscetti, F.W., and Gallo, R. (1976). Selective in vitro growth of T lymphocytes from normal human bone marrows. Science (New York, NY *193*, 1007-1008.

Morgan, W.W., Richardson, A., Sharp, Z.D., and Walter, C.A. (1999). Application of exogenously regulatable promoter systems to transgenic models for the study of aging. The journals of gerontology *54*, B30-40; discussion B41-32.

Murdoch, C., Giannoudis, A., and Lewis, C.E. (2004). Mechanisms regulating the recruitment of macrophages into hypoxic areas of tumors and other ischemic tissues. Blood *104*, 2224-2234.

Nemunaitis, J., Cunningham, C., Senzer, N., Kuhn, J., Cramm, J., Litz, C., Cavagnolo, R., Cahill, A., Clairmont, C., and Sznol, M. (2003). Pilot trial of genetically modified, attenuated Salmonella expressing the E. coli cytosine deaminase gene in refractory cancer patients. Cancer gene therapy *10*, 737-744.

Nguyen, V.T., Morange, M., and Bensaude, O. (1988). Firefly luciferase luminescence assays using scintillation counters for quantitation in transfected mammalian cells. Analytical biochemistry *171*, 404-408.

Paul, D., Hohne, M., Pinkert, C., Piasecki, A., Ummelmann, E., and Brinster, R.L. (1988). Immortalized differentiated hepatocyte lines derived from transgenic mice harboring SV40 T-antigen genes. Experimental cell research *175*, 354-362.

Pawelek, J.M., Low, K.B., and Bermudes, D. (1997). Tumor-targeted Salmonella as a novel anticancer vector. Cancer research *57*, 4537-4544.

Ray, P., Pimenta, H., Paulmurugan, R., Berger, F., Phelps, M.E., Iyer, M., and Gambhir, S.S. (2002). Noninvasive quantitative imaging of protein-protein interactions in living subjects. Proceedings of the National Academy of Sciences of the United States of America *99*, 3105-3110.

Reader, A.J., and Zweit, J. (2001). Developments in whole-body molecular imaging of live subjects. Trends in pharmacological sciences *22*, 604-607.

Rice, B.W., Cable, M.D., and Nelson, M.B. (2001). In vivo imaging of light-emitting probes. Journal of biomedical optics *6*, 432-440.

Robbins, J.R., Lee, S.M., Filipovich, A.H., Szigligeti, P., Neumeier, L., Petrovic, M., and Conforti, L. (2005). Hypoxia modulates early events in T cell receptor-mediated activation in human T lymphocytes via Kv1.3 channels. The Journal of physiology *564*, 131-143.

Rosenberg, S.A., Mule, J.J., Spiess, P.J., Reichert, C.M., and Schwarz, S.L. (1985). Regression of established pulmonary metastases and subcutaneous tumor mediated by the systemic administration of high-dose recombinant interleukin 2. The Journal of experimental medicine *161*, 1169-1188.

Rotzschke, O., Falk, K., Stevanovic, S., Jung, G., Walden, P., and Rammensee, H.G. (1991). Exact prediction of a natural T cell epitope. European journal of immunology *21*, 2891-2894. Rudin, M., Beckmann, N., Porszasz, R., Reese, T., Bochelen, D., and Sauter, A. (1999). In vivo magnetic resonance methods in pharmaceutical research: current status and perspectives. NMR in biomedicine *12*, 69-97.

Ryschich, E., Lizdenis, P., Ittrich, C., Benner, A., Stahl, S., Hamann, A., Schmidt, J., Knolle, P., Arnold, B., Hammerling, G.J.*, et al.* (2006). Molecular fingerprinting and autocrine growth regulation of endothelial cells in a murine model of hepatocellular carcinoma. Cancer research *66*, 198-211.

Sacher, T. (2000). Die Rolle von Entzündungseaktionen bei Immunoreaktionen gegen gesundes und malignes Gewebe : etbalierung eines autochthonen Tumormodels.

Sadowski, P.D. (1993). Site-specific genetic recombination: hops, flips, and flops. Faseb J *7*, 760-767.

Sampson, J.H., Archer, G.E., Ashley, D.M., Fuchs, H.E., Hale, L.P., Dranoff, G., and Bigner, D.D. (1996). Subcutaneous vaccination with irradiated, cytokine-producing tumor cells stimulates CD8+ cell-mediated immunity against tumors located in the "immunologically privileged" central nervous system. Proceedings of the National Academy of Sciences of the United States of America *93*, 10399-10404.

Sato, J., Hamaguchi, N., Doken, K., Gotoh, K., Ootsu, K., Iwasa, S., Ogawa, Y., and Toguchi, H. (1993). Enhancement of anti-tumor activity of recombinant interleukin-2 (rIL-2) by immunocomplexing with a monoclonal antibody against rIL-2. Biotherapy (Dordrecht, Netherlands) *6*, 225-231.

Sauer, B. (1998). Inducible gene targeting in mice using the Cre/lox system. Methods (San Diego, Calif *14*, 381-392.

Schwenk, F., Baron, U., and Rajewsky, K. (1995). A cre-transgenic mouse strain for the ubiquitous deletion of loxP-flanked gene segments including deletion in germ cells. Nucleic acids research *23*, 5080-5081.

Shaner, N.C., Campbell, R.E., Steinbach, P.A., Giepmans, B.N., Palmer, A.E., and Tsien, R.Y. (2004). Improved monomeric red, orange and yellow fluorescent proteins derived from Discosoma sp. red fluorescent protein. Nature biotechnology *22*, 1567-1572.

Shibata, H., Toyama, K., Shioya, H., Ito, M., Hirota, M., Hasegawa, S., Matsumoto, H., Takano, H., Akiyama, T., Toyoshima, K.*, et al.* (1997). Rapid colorectal adenoma formation initiated by conditional targeting of the Apc gene. Science (New York, NY *278*, 120-123.

Siegert, A., Denkert, C., Leclere, A., and Hauptmann, S. (1999). Suppression of the reactive oxygen intermediates production of human macrophages by colorectal adenocarcinoma cell lines. Immunology *98*, 551-556.

Smith, K.A. (1988). Interleukin-2: inception, impact, and implications. Science (New York, NY *240*, 1169-1176.

Soghomonyan, S.A., Doubrovin, M., Pike, J., Luo, X., Ittensohn, M., Runyan, J.D., Balatoni, J., Finn, R., Tjuvajev, J.G., Blasberg, R.*, et al.* (2005). Positron emission tomography (PET) imaging of tumor-localized Salmonella expressing HSV1-TK. Cancer gene therapy *12*, 101-108.

Soiffer, R., Lynch, T., Mihm, M., Jung, K., Rhuda, C., Schmollinger, J.C., Hodi, F.S., Liebster, L., Lam, P., Mentzer, S.*, et al.* (1998). Vaccination with irradiated autologous melanoma cells engineered to secrete human granulocyte-macrophage colony-stimulating factor generates potent antitumor immunity in patients with metastatic melanoma. Proceedings of the National Academy of Sciences of the United States of America *95*, 13141-13146.

Soriano, P. (1999). Generalized lacZ expression with the ROSA26 Cre reporter strain. Nature genetics *21*, 70-71.

Stahl, S. (2004). Establishment of an inducible mouse model for the development of autochthonous hepatocarcinoma. PhD thesis.

Stahl, S., Sacher, T. , Bechtold. A., Protzer, U., Ganss, R., Hämmerling, G.J., Arnold, B., Garbi, N. (in preparation). Tumor against peptides elicit CTL responses and break tolerance in a novel model of autchthonous hepatoma.

Stritzker, J., Weibel, S., Hill, P.J., Oelschlaeger, T.A., Goebel, W., and Szalay, A.A. (2007). Tumor-specific colonization, tissue distribution, and gene induction by probiotic Escherichia coli Nissle 1917 in live mice. Int J Med Microbiol *297*, 151-162.

Sweeney, T.J., Mailander, V., Tucker, A.A., Olomu, A.B., Zhang, W., Cao, Y., Negrin, R.S., and Contag, C.H. (1999). Visualizing the kinetics of tumor-cell clearance in living animals. Proceedings of the National Academy of Sciences of the United States of America *96*, 12044-12049.

Szittner, R., and Meighen, E. (1990). Nucleotide sequence, expression, and properties of luciferase coded by lux genes from a terrestrial bacterium. The Journal of biological chemistry *265*, 16581-16587.

Szymczak, A.L., Workman, C.J., Wang, Y., Vignali, K.M., Dilioglou, S., Vanin, E.F., and Vignali, D.A. (2004). Correction of multi-gene deficiency in vivo using a single 'self-cleaving' 2A peptide-based retroviral vector. Nat Biotechnol *22*, 589-594.

Tao, N., Gao, G.P., Parr, M., Johnston, J., Baradet, T., Wilson, J.M., Barsoum, J., and Fawell, S.E. (2001). Sequestration of adenoviral vector by Kupffer cells leads to a nonlinear dose response of transduction in liver. Mol Ther *3*, 28-35.

Timmerman, J.M., and Levy, R. (1999). Dendritic cell vaccines for cancer immunotherapy. Annual review of medicine *50*, 507-529.

Troy, T., Jekic-McMullen, D., Sambucetti, L., and Rice, B. (2004). Quantitative comparison of the sensitivity of detection of fluorescent and bioluminescent reporters in animal models. Mol Imaging *3*, 9-23.

Vogel, M., Hess, J., Then, I., Juarez, A., and Goebel, W. (1988). Characterization of a sequence (hlyR) which enhances synthesis and secretion of hemolysin in Escherichia coli. Mol Gen Genet *212*, 76-84.

Vooijs, M., Jonkers, J., Lyons, S., and Berns, A. (2002). Noninvasive imaging of spontaneous retinoblastoma pathway-dependent tumors in mice. Cancer research *62*, 1862-1867.

Vooijs, M., van der Valk, M., te Riele, H., and Berns, A. (1998). Flp-mediated tissue-specific inactivation of the retinoblastoma tumor suppressor gene in the mouse. Oncogene *17*, 1-12.

Weissleder, R., and Mahmood, U. (2001). Molecular imaging. Radiology *219*, 316-333.

White, R.L., Jr., Schwartzentruber, D.J., Guleria, A., MacFarlane, M.P., White, D.E., Tucker, E., and Rosenberg, S.A. (1994). Cardiopulmonary toxicity of treatment with high dose interleukin-2 in 199 consecutive patients with metastatic melanoma or renal cell carcinoma. Cancer *74*, 3212-3222.

Willimsky, G., and Blankenstein, T. (2005). Sporadic immunogenic tumours avoid destruction by inducing T-cell tolerance. Nature *437*, 141-146.

Wilmanns, C., Fan, D., O'Brian, C.A., Bucana, C.D., and Fidler, I.J. (1992). Orthotopic and ectopic organ environments differentially influence the sensitivity of murine colon carcinoma cells to doxorubicin and 5-fluorouracil. International journal of cancer *52*, 98-104.

Xu, X., Wagner, K.U., Larson, D., Weaver, Z., Li, C., Ried, T., Hennighausen, L., Wynshaw-Boris, A., and Deng, C.X. (1999). Conditional mutation of Brca1 in mammary epithelial cells results in blunted ductal morphogenesis and tumour formation. Nature genetics *22*, 37-43.

Yazawa, K., Fujimori, M., Amano, J., Kano, Y., and Taniguchi, S. (2000). Bifidobacterium longum as a delivery system for cancer gene therapy: selective localization and growth in hypoxic tumors. Cancer gene therapy *7*, 269-274.

Yu, J.S., Burwick, J.A., Dranoff, G., and Breakefield, X.O. (1997). Gene therapy for metastatic brain tumors by vaccination with granulocyte-macrophage colony-stimulating factor-transduced tumor cells. Human gene therapy *8*, 1065-1072.

Yu, Y.A., Shabahang, S., Timiryasova, T.M., Zhang, Q., Beltz, R., Gentschev, I., Goebel, W., and Szalay, A.A. (2004). Visualization of tumors and metastases in live animals with bacteria and vaccinia virus encoding light-emitting proteins. Nature biotechnology *22*, 313-320.

Zhao, H., Doyle, T.C., Coquoz, O., Kalish, F., Rice, B.W., and Contag, C.H. (2005). Emission spectra of bioluminescent reporters and interaction with mammalian tissue determine the sensitivity of detection in vivo. Journal of biomedical optics *10*, 41210.

Zinn, K.R., Chaudhuri, T.R., Buchsbaum, D.J., Mountz, J.M., and Rogers, B.E. (2001). Detection and measurement of in vitro gene transfer by gamma camera imaging. Gene therapy *8*, 291-299.

Abbreviation list:

Alb	Albumin
ALT	Alanine aminotransferase
AMP	Adenosine monophosphate
Amp	Ampicillin
APC	Antigen presenting cells
APS	Ammonium peroxodisulfat
ASC	Albumin-floxstop-CBGr99
AST	Albumin-floxstop-TAg
ATP	Adenosine triphosphate
BAC	Bacterial artificial chromosome
BLI	Bioluminescence imaging
bp	Base pair
BSA	Bovine Serum Albumin
CAG	CMV/Chicken ß-actin promoter
CBGr99	Click beetle green 99
CBluc	Click beetle luciferase
CBRed	Click beetle red
CCD	Cooled camera device
cDNA	Complementary DNA
Chlr	Chloramphenicol
CIAP	Calf intestine alkaline phosphatase
cm	Centimeter
Cre	Cause recombination
CT	Computed tomography
CTL	Cytotoxic T cells
Dig	Digoxygenin
DMEM	Dulbecco´s Modified Eagle Serum
DMSO	Dimethylsulfoxid
DNA	Deoxyribunucleic Acid
dNTPs	Deoxyribonucleotide-5´-triphosphate
D-PBS	Dulbecco´s modified PBS
E.coli	Escherichia Coli

EDTA	Ethylene diamine tetraacetic acid
eGFP	Enhanced Green fluorescent protein
FACS	Fluorescence activated cell sorter
FCS	Foetal calf serum
Fig	Figure
Fluc	Firefly luciferase
g	Gram
GM-CSF	Granulocyte macrophage colony stimulating factor
h	Hour
HCC	Hepatocellular carcinoma
HRP	horseradish peroxidase
i.f.u	Inclusion forming units
i.p.	Intraperitoneally
i.v.	Intravenously
IL-2	Interleukin-2
IRES	Internal ribosome entry sequence
Kan	Kanamycin
Kbp	Kilo base pair
L	Liter
LB	Luria bertani
M	Molar
mA	Milli-Ampere
MFI	Mea fluorescence intensity
Mg	Milligram
MHz	Mega Hertz
min	Minute
ml	Milliliter
MRI	Magnetic resonance imaging
mRNA	Messenger RNA
nm	Nanometer
NP-40	Nonidet P40
OD	Optical density
OVA	Ovalbumin
PAA	Polyacrylamide

PBL	Peripheral blood lymphocyte
PBS	Phosphate buffer saline
PCR	Polymerase chain reaction
PET	Positron emission tomography
PPi	Pyrophosphate
PVDF	Polyvynildene fluoride
RIP	Rat insulin promoter
RLU	Relative light unit
Rluc	Renilla luciferase
RNA	Ribonucleic Acid
ROI	Region of interest
Rpm	Rotation per minute
s.c	Subcutaneously
SDS	Sodiumdodecylsulfate
SPECT	Single photon emission computed tomography
TAE	Tris-acetate-EDTA
TAg	Simian virus 40 large T-antigen
TE	Tris-EDTA
TEMED	N,N,N',N'-Tetramethylethylendiamin
US	Ultrasound
UV	Ultraviolet
V	Volt
v/v	Volume per volume
vol	Volume
w/v	Weight per volume
Zeo	Zeocin

Acknowledgements

First and foremost, I would like to express my sincerest gratitude to my advisor, Prof. Dr. Hämmerling, for his knowledge and guidance during my Ph.D study. He offered me key ideas, inspiration and encouragement in tackling with my thesis problems, which I deeply appreciate. His critical reading and sharp comments have made this dissertation more rigorous.

My warm thanks to the other committee members, Prof. Johanna Chluba, Prof. Alain Pugin and Dr. Apprahamian for their careful reading and valuable comments on this dissertation. I also extend my thanks to Dr. Ulrike Protzer who kindly accepted to review my thesis.

I am very much grateful to Dr. Weiss and Dr. Loessner, Helmotz Center for Infection Research, for their contributions to the work with bacteria.

I am thankful to Dr. Natalio Garbi and Dr. Thomas Schüler for stimulating discussions, exchange of knowledge, and for valid advice throughout my PhD.

I especially want to thank Carmen Henrich and Günter Küblbeck for their nice contribution to my work as well as their friendly discussion.

I would like to express my gratitude to previous and present individuals from my lab (too many to name) for the good working environment.

Finally, I thank my family, my girlfriend and my friends for their endless and unselfish support. Particularly, I am grateful for the love and concern of my parents, my sisters and my brothers. Completing the PhD would have been impossible without their love and encouragement.